AD-A189 118 EXPLORATORY EVALUATION OF ALUMINA CERAMIC CYLINDRICAL HOUSINGS FOR DEEP S..(U) NAVAL OCEAN SYSTEMS CENTER SAN DIEGO CA J D STACHIW ET AL. SEP 87 NOSC/TR-1176 1/1

UNCLASSIFIED F/G 13/9 NL

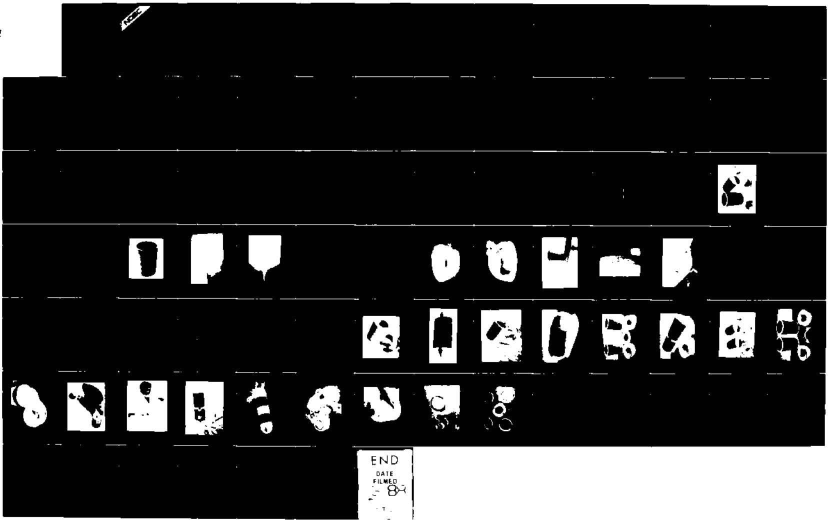

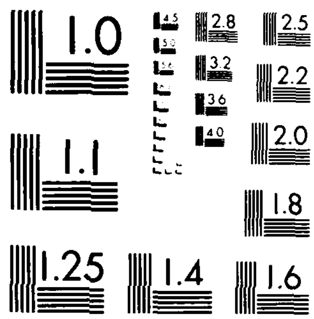

MICROCOPY RESOLUTION TEST CHART
NATIONAL BUREAU OF STANDARDS 1963 A

NOSC TR 1176

(4)

NOSC TR 1176

NOSC

NAVAL OCEAN SYSTEMS CENTER San Diego, California 92152-5000

Technical Report 1176
September 1987

Exploratory Evaluation of Alumina Ceramic Cylindrical Housings for Deep Submergence Service: The Second Generation NOSC Ceramic Housings

AD-A189 118

J. D. Stachiw
J. L. Held

UNITED STATES NAVY
NAVAL OCEAN SYSTEMS CENTER

Approved for public release, distribution is unlimited.

UNCLASSIFIED
SECURITY CLASSIFICATION OF THIS PAGE

REPORT DOCUMENTATION PAGE

1a REPORT SECURITY CLASSIFICATION UNCLASSIFIED	1b RESTRICTIVE MARKINGS
2a SECURITY CLASSIFICATION AUTHORITY	3 DISTRIBUTION AVAILABILITY OF REPORT Approved for public release; distribution is unlimited.
2b DECLASSIFICATION DOWNGRADING SCHEDULE	
4 PERFORMING ORGANIZATION REPORT NUMBER(S) NOSC TR 1176	5 MONITORING ORGANIZATION REPORT NUMBER(S)
6a NAME OF PERFORMING ORGANIZATION Naval Ocean Systems Center 6b OFFICE SYMBOL (if applicable) Code 9402	7a NAME OF MONITORING ORGANIZATION
6c ADDRESS (City State and ZIP Code) San Diego, CA 92152-5000	7b ADDRESS (City State and ZIP Code)
8a NAME OF FUNDING SPONSORING ORGANIZATION Naval Material Command 8b OFFICE SYMBOL (if applicable)	9 PROCUREMENT INSTRUMENT IDENTIFICATION NUMBER
8c ADDRESS (City State and ZIP Code) Washington, DC 20360	10 SOURCE OF FUNDING NUMBERS PROGRAM ELEMENT NO: 62936N PROJECT NO: ZE36100 TASK NO: ZE56 AGENCY ACCESSION NO: DN

11 TITLE (include Security Classification)

Exploratory Evaluation of Alumina Ceramic Cylindrical Housings for Deep Submergence Service: The Second Generation NOSC Ceramic Housings

12 PERSONAL AUTHOR(S)

J.D. Stachiw and J.L. Held

13a TYPE OF REPORT	13b TIME COVERED	14 DATE OF REPORT (Year Month Day)	15 PAGE COUNT
Final	FROM Jun 86 TO Jun 87	September 1987	91

16 SUPPLEMENTARY NOTATION

17 COSATI CODES			18 SUBJECT TERMS (Continue on reverse if necessary and identify by block number)
FIELD	GROUP	SUB GROUP	Ceramic Alumina housing Pressure housing Deep submergence hull Submersible Buoy

19 ABSTRACT (Continue on reverse if necessary and identify by block number)

Scale model ceramic pressure housing assemblies have been designed ~~by NOSC~~, fabricated ~~by Coors~~ Ceramics, and pressure-cycled 2,000 times to the 9,000-psi external design pressure without failure. The Model 1 cylinder, fabricated from 99.5-percent alumina ceramic, is 9 inches long and has an inside diameter of 5.624 inches and an outside diameter of 6.00 inches. The Model 2 cylinder, fabricated from 94-percent alumina ceramic, is the same as Model 1 in length and inside diameter, but its outside diameter is 6.037 inches. Each housing assembly was either a single cylinder or two cylinders of the same model joined together. The single cylinder housing assembly consisted of a cylinder and two titanium spherical end closures with a 5.624-inch inside diameter and a 0.136-inch thickness, that provided radial support for the ends of the cylinder. The two-cylinder assemblies were radially supported and joined together by a titanium T-ring in the center, and by titanium spherical end closures at either end of the lengthened cylinder. Fretting of the bearing surfaces on the ends of ceramic cylinders was eliminated by fitting the ends of the cylinders with U-shaped titanium rings held in place by epoxy adhesive. The weight-to-displacement ratio of the pressure housing assembly was 0.57.

At 9,000-psi design pressure the maximum recorded stresses were -98,601-psi axial stress on the interior surface of titanium hemispheres near the equatorial flange, 148,000- to 145,000-psi hoop stresses on the interior surface of the Model 1 and Model 2 cylinders at midbay, and -25,000-psi hoop stress on the interior of the joint ring supporting the cylinders. Based on the magnitude of the recorded stresses at design depth, the effective safety factors for the titanium and alumina ceramic materials exceed the specified 1.25 and 2.0 safety factors for material failure, respectively. The depth capability of the second generation NOSC pressure housing assembly is limited by plastic buckling of the titanium hemispheres that have been experimentally determined to occur at 11,500 psi (or approximately 25,000-foot depth).

20 DISTRIBUTION AVAILABILITY OF ABSTRACT	21 ABSTRACT SECURITY CLASSIFICATION
☐ UNCLASSIFIED UNLIMITED ☒ SAME AS RPT ☐ DTIC USERS	UNCLASSIFIED

22a NAME OF RESPONSIBLE INDIVIDUAL	22b TELEPHONE (include Area Code)	22c OFFICE SYMBOL
J.D. Stachiw	619-225-7812	Code 9402

DD FORM 1473, 84 JAN

83 APR EDITION MAY BE USED UNTIL EXHAUSTED
ALL OTHER EDITIONS ARE OBSOLETE

UNCLASSIFIED
SECURITY CLASSIFICATION OF THIS PAGE

EXECUTIVE SUMMARY

OBJECTIVE

Develop an external pressure resistant housing for the electronic components of deep submergence remotely operated vehicles (ROVs) that will not only protect them from contact with sea water, but will also provide the vehicle with positive buoyancy. A weight-to-displacement ratio *less* than or equal to 0.5 has been found by experience to be mandatory for the pressure housing assembly so that it may provide the vehicle with adequate buoyancy for its propulsion, guidance, and work systems. Pressure housing assemblies with a weight-to-displacement ratio *greater* than 0.5 provide inadequate buoyancy that must be augmented at great expense and increase in the vehicle's displacement by, for example, addition of syntactic foam blocks to the vehicle's structure.

APPROACH

Ceramic materials appear to possess the required structural properties for construction of external pressure housings with the 0.5 weight-to-displacement ratio and a design depth of 20,000 feet. To arrive at an operationally usable external pressure housing of ceramic material, several fabrication and design problems needed to be solved that have in the past worked against the acceptance of such housings by the ocean engineering community. These problems were economical fabrication of large ceramic cylinders, reliable mechanical joining of several ceramic cylinders into a cylindrical pressure housing of desired length, and elimination of stress risers on the ceramic bearing surfaces between individual housing assembly components.

RESULTS

Several 6-inch diameter scale model pressure housing assemblies have been designed, fabricated, and tested to 10,000 psi. The cylinders were made either from 99.5- or 94.0-percent alumina ceramic, while the joint rings, end caps, and end closures were fabricated of Ti-6Al-4V alloy. The following problems were attacked in this study and solved:

1. Large ceramic cylinders can be economically fabricated by brazing together many small rings or ring segments whose bearing surfaces have been precision ground beforehand, metalized with moly manganese, and nickel plated. The solder between mating surfaces provides a structural bond, seals them, and acts as a compliant bearing gasket.
2. Long cylindrical pressure housings can be assembled from several short ceramic cylinders and titanium end closures, using titanium joint rings between individual cylinders. The joint rings provide radial support to capped cylinder ends and, with the aid of O-rings, seal the mating bearing surfaces.

3. Stress risers on the axial and radial bearing surfaces of cylinder ends can be avoided by bonding circular, U-shaped titanium end caps to the cylinder ends with epoxy adhesive. The close fit between the caps and the cylinder prevents extrusion of adhesive from the annular spaces during application of high bearing stresses at design depth.

4. The elastic stability of monocoque ceramic cylinders can be raised to the desired critical pressure by supporting the capped ends of the cylinders with close fitting but removable titanium joint rings with adequate elastic stability. The pressure housing design, validated by testing 6-inch diameter scale models to 10,000-psi proof pressure, has an experimentally proven cyclic fatigue life in excess of 1,000 pressurizations to 9,000 psi. The weight-to-displacement ratio of the tested scale model housing is 0.57.

RECOMMENDATIONS

There are two major recommendations as a result of the second generation NOSC ceramic pressure housing testing program.

1. The concept of 20,000-foot design depth (9,000-psi) ceramic pressure housings, validated experimentally during the second generation NOSC ceramic housing test series by 6-inch OD scale models, should be extrapolated to larger, operationally useful sizes for further testing.

2. The third generation NOSC alumina ceramic pressure housings should incorporate cylinders and hemispheres with an outside diameter of 12 inches. The fabrication of 12-inch OD ceramic pressure housing components will provide valuable information on the technical difficulties associated with scaling up the fabrication processes, while testing these components will generate quantitative data for describing the effect of structural size on alumina ceramic external pressure housings.

CONTENTS

INTRODUCTION

GENERAL

Purpose

This report has two purposes. The first and general purpose is to suggest that ceramics must be considered as appropriate materials for the potential fabrication of ceramic-hulled submersibles and remotely operated vehicles (ROVs) to be used in deep submergence applications. The second and more specific purpose is to present the results of the design, fabrication, testing, and evaluation of NOSC's second generation ceramic housing assemblies.

Scope

The materials discussion is presented in sufficient detail to enable the reader to understand the reasons for examining the use of alumina ceramics for deep submergence applications. The history of NOSC's *second* generation ceramic housing assemblies (all ceramic components were fabricated by Coors Ceramics of Golden, Colorado) is presented in enough detail to substantiate the evaluations of those assemblies. The fabrication information and pressure data is presented along with conclusions and recommendations.

Organization

This report has three sections.

1. INTRODUCTION—This section introduces the report and reviews the materials being considered for deep submergence application, especially alumina ceramics.
2. BACKGROUND—This section briefly examines premium construction materials that are candidates for deep submergence housings, the most effective housing designs and fabrication methods, and the experimental evaluation results obtained during tests of NOSC's *first* generation ceramic housing assemblies.
3. NOSC'S SECOND GENERATION CERAMIC HOUSING ASSEMBLIES—This section summarizes the design, fabrication, testing, and evaluation of NOSC's *second* generation ceramic housing assemblies that had a 9,000-psi design pressure (or 20,000-foot operational depth).

WHY CERAMICS ARE GOOD CANDIDATE MATERIALS FOR DEEP SUBMERGENCE APPLICATIONS

The Navy, among other organizations and institutions, is very interested in acquiring the most effective and efficient manned submersibles and remotely operated vehicles (ROVs) for deep

submergence operations. Three factors determine if such submersibles or vehicles meet mission standards: payload, operational range, and speed. Each of these factors is a direct function of the system's buoyancy.

It is clear then that buoyancy is the critical issue. Optimally, buoyancy is provided by a well-designed pressure hull. However, if the buoyancy provided by the pressure hull is inadequate, there are palliative measures, but these usually reduce the effectiveness of the submersible in fulfilling its mission task. For instance, additional buoyancy can be provided by attaching blocks of syntactic foam or soft-shell tanks filled with lighter-than-water fluids to the pressure hull. This approach has an overall negative impact on system cost and effectiveness.

Thus, the design and materials used in fabricating pressure hulls are of critical concern. The optimization of shape and the use of premium material in the construction of the hull is required to obtain a pressure hull with low weight-to-displacement ratio (a large positive buoyancy). The reason for seeking the low weight-to-displacement ratio is to maximize payload, while maintaining optimum range and speed. For instance, assume a given payload volume bound by the interior of a pressure hull. For a higher weight material a weightier hull would perhaps require additional exterior buoyancy thus changing the design shape and propulsion, speed, and range capabilities. A lower weight, high strength hull material, however, could permit the same payload volume and maintain optimum range and speed. The choice of materials is more limited than the optimization of shape options as only a few materials are light in weight, corrosion resistant, and strong in compression. The characteristics of premium structural materials for external pressure housings are shown in Table 1, and housing assembly material characteristics in terms of design pressure and of weight-to-displacement ratio are presented in Figure 1.*

A weight-to-displacement ratio *less* than or equal to 0.5 has been found by experience to be mandatory for the pressure housing assembly so that it may provide the vehicle with adequate buoyancy for its propulsion, guidance, and work systems. Pressure housing assemblies with a weight-to-displacement ratio *greater* than 0.5 provide inadequate buoyancy that must be augmented at great expense and increase in vehicle's displacement.

Now a quick glance at the numbers is sufficient for recognizing that high strength steel does not meet the rigid requirements. Stated simply, the poor weight-to-strength ratio will sink deep submergence vehicles constructed from steel.

While graphite fiber-reinforced plastic (GFRP) is certainly an acceptable material for use by ocean engineering programs for economic and technical reasons, it is still above the weight-to-displacement ratio desired for lightweight pressure hull materials.

Ceramic materials, on the other hand, appear to possess the required structural properties for construction of external pressure housings with the 0.5 weight-to-displacement ratio and a design depth of 20,000 feet. To arrive at an operationally usable external pressure housing of ceramic material, several fabrication and design problems needed to be solved that have in the past worked against the acceptance of such housings by the ocean engineering community. These problems were economical fabrication of large ceramic cylinders, reliable mechanical joining of several ceramic cylinders into a cylindrical pressure housing of desired length, and elimination of stress risers on the ceramic bearing surfaces between individual housing assembly components.

NOSC set out to demonstrate, during its evaluation of the second generation ceramic housing assemblies, that the problems of economics, cylinder joining techniques, and the elimination of stress

*While *tables* are placed immediately after their citation in the text, *all* the report's *figures* (1 through 62) follow the complete text of the report.

Table 1. Premium structural materials for external pressure housings.

MATERIAL	WEIGHT (lbs/in^3)	COMPRESSIVE STRENGTH (kpsi)	STRENGTH / WEIGHT	SAFETY FACTOR
STEEL (HY80)	0.283	80	280	1.25
STEEL (HY130)	0.283	130	460	1.25
ALUMINUM (7075–T6)	0.10	73	730	1.25
TITANIUM (6AL–4V)	0.16	125	780	1.25
GLASS (PYREX)	0.08	100	1250	2
GLASS COMPOSITE	0.075	100	1330	2
GRAPHITE COMPOSITE	0.057	100	1750	2
BERYLLIA CERAMIC 96%	0.104	225	2160	2
ALUMINA CERAMIC 94%	0.130	300	2310	2
GLASS CERAMIC (PYROCERAM 9606)	0.093	350	3760	2

risers were addressed and solved to varying degrees. These solutions were instrumental in the recommendation that NOSC's *third* generation ceramic housing "should be extrapolated to larger, operationally useful sizes for further testing."

BACKGROUND

PREMIUM CONSTRUCTION MATERIALS

Extensive research efforts have been undertaken to determine the strengths and weaknesses of various materials for deep submergence service and to develop suitable designs for external pressure housings. Lightweight, high strength materials are required for the fabrication of external pressure vessels for deep submergence service. However, the operational performance requirements for buoyant deep submergence structures calling for < 0.5 weight-to-displacement ratios exceed the capabilities of most conventional metallic materials (Figures 1 through 6).

Some of the most impressive results obtained to date by using nonconventional materials can be found in studies involving alumina ceramic and PYROCERAM 9606. In 1964, the Van Karman Center of Aerojet General issued a report (Reference 1) on design concepts for deep submersibles. This early study focused on the properties of alumina (Table 1). It was reported that 99.5-percent alumina was used in polylithic monocoque cylinders and a minimum allowable compressive stress level of −175,000-psi was attained. To appreciate the strength of alumina ceramic, one has to compare it to other materials. The 300,000-psi ultimate compressive strength of alumina ceramic is equivalent to a strength-to-weight ratio of 2,310,000. By comparison, HY 130 steel has an approximate strength-to-weight ratio of only 460,000. The strength-to-weight ratios of titanium alloy 6A-4V and aluminum alloy 7075-T6 are somewhat higher than the ratio of HY 130 steel (780,000 and 730,000, respectively), but these materials still cannot provide a 0.5 weight-to-displacement ratio for cylindrical pressure housings with a 9,000-psi design depth.

PYROCERAM® is a product of the Corning Glass Works, while CERVIT® is manufactured by Owens Illinois. They represent a class of materials converted into crystalline ceramic from an original glassy state by the use of nucleating agents and heat treatment. Tests have shown that glass ceramic has an ultimate compressive strength of 300,000 to 350,000-psi. Thus, its strength-to-density ratio of 3,700,000 surpasses even that of alumina. Early evaluations of this material for external pressure hulls by the Ordnance Research Laboratory of the University of Pennsylvania (Reference 2) and the Naval Civil Engineering Laboratory (Reference 3) concluded that the compressive strength-to-weight ratio of glass ceramics is unexcelled and that, combined with their intrinsic high moduli of elasticity and ease of fabrication in large shapes, these materials are obvious choices as structural materials for mass production of oceanographic capsules and vehicles.

Another ceramic material that has received favorable consideration is beryllia. Because of its low density (0.1 lb/in^3) and high compressive strength (−225,000-psi), the strength-to-density ratio of beryllia is 2,250,000. Little experimentation has been done to date with beryllia as a structural material for external pressure housings because of its high intrinsic cost, which surpasses by an order of magnitude the cost of alumina or glass ceramics. There is no doubt, however, that because of its outstanding heat conductivity, it will experience wide application in small, nonmagnetic pressure housings for electronic components requiring low ambient temperatures for their successful operation. NOSC's first generation scale model ceramic housings were fabricated from this material (Reference 4).

HOUSING DESIGN AND FABRICATION

Once the choice of materials is made, the matter of design must be considered. The collapse resistance of any housing is dependent upon the shape of the shell. The two most common shapes used in oceanographic research are the sphere and cylinder. Spheres are used in applications where the hydrodynamic drag of the structure moving through the water is not important. However, if it is desirable that the submersible move quickly through the hydrospace, such as in a free-diving oceanographic instrumentation capsule, or remotely operated vehicle (ROV), a cylindrical shape is more appropriate.

The simplest type of cylindrical shell is the *monocoque cylinder* capped at the ends. For deep submergence, where thick walls are required not only by the cylinder's low elastic stability, but also by high stress loading of the cylinder wall, the monocoque cylinder provides an inexpensive shell design with a fair weight-to-buoyancy ratio. It is used when some structural efficiency can be sacrificed for decreased cost in fabrication.

To make a cylindrical housing elastically more stable for abyssal depths without increasing its wall thickness, it is necessary to incorporate radial supports (Figure 7). Five basic cylinder designs exist:

1. A monocoque shell
2. A monocoque shell with integral end stiffeners
3. A monocoque shell with integral stiffeners on the ends and one in the middle
4. A monocoque shell with a series of integral stiffeners in addition to those on the ends (References 2 and 3)
5. A monocoque shell supported radially at the ends by separate end stiffeners or metallic joint rings.

To fulfill the need for longer deep submergence housings, several cylindrical shell sections can be joined together by mechanically reliable and structurally strong metallic joints. It is vital that the joints be able to withstand hydrostatic pressure. It is also important that they be capable of withstanding the bending movements imposed on the cylindrical pressure housing during handling, launching, and retrieval from the ocean. Whenever feasible, the joint should also be flush with the exterior surface of the fairing enclosing the housing to decrease the vehicle's hydrodynamic drag.

Forming large diameter monolithic cylindrical housings is very definitely size limited. For alumina and beryllia ceramics, the size limit is imposed by the slumping of green ceramic in the firing kiln; while for glass ceramics, the limit is the nonuniformity of nucleation in thick sections.

However, an approach has been proposed and experimentally validated to increase economically the diameter of the cylindrical housing (References 1 and 4). This approach relies on forming large cylindrical housings by assembling many prefired small ceramic structural modules (Figure 8). The structural variables of these cylindrical modules are height and arc length. The size of the module can be chosen by the designer to minimize the surface area of their bearing surfaces and thereby minimize grinding cost. For cylinders of small (12 to 24 inches) and medium (24 to 48 inches) diameters, the modules may take the form of *complete rings* with parallel, plane bearing surfaces that can be stacked upon each other to form cylindrical sections. For cylinders of large (48 to 60 inches) and very large (60 to 120 inches) diameters, the individual modules may take the shape of *cylindrical segments*.

The key's, however, to construction of housings using this modular is, in either case, a reliable, inexpensive, bonded joint with the following characteristics:

1. Transfers high compressive axial stresses without squeezing out the bonding agent
2. Is watertight
3. Has good tensile strength
4. Deforms sufficiently to eliminate point loadings between adjacent ceramic bearing surfaces.

Two approaches appear promising for joining the modules: bonding with specially formulated adhesive or brazing with specially formulated metallic solder. Neither joining technique has been adequately evaluated to allow formulation of conclusive findings.

FIRST GENERATION NOSC CERAMIC HOUSINGS

Because neither of the joining techniques had received adequate evaluation, both techniques were selected by NOSC in 1982 for construction of the first generation ceramic scale models with a 20,000-foot design depth. (Reference 4 addresses NOSC's first generation beryllia ceramic housing efforts and should be consulted for more detailed information.) In these models, the monocoque cylindrical shells were assembled from beryllia ceramic rings joined together with either *epoxy adhesive* or *metallic brazing alloy*. It was hoped that by employing both joining techniques in structurally identical cylinders, it could be shown which technique was superior. Both were found to provide structural integrity for the beryllia ceramic cylinders at design depth. These cylinders, however, were not pressure-cycled long enough to establish experimentally the fatigue lives of either the adhesive or metallic brazed joints. There were, however, some indications that the brazed joints are structurally superior to adhesive bonded joints; the brazed joints have a *lesser tendency to extrude* or to delaminate under high bearing stresses, and, furthermore, their strength is not affected by immersion in sea water.

In addition, to minimize the weight, and at the same time to maximize the internal useful volume of the ceramic housing assembly, the elastic stability of the monocoque cylinder was raised by simple radial support provided to the ends of the monocoque cylinders by the titanium end closures, rather than by integral, circumferential ceramic end stiffeners (Figure 9). Radial support for ends of monocoque cylinders is not a new concept for metallic or plastic cylinders. As a matter of fact, it is considered to be the standard design approach for raising the elastic stability of monocoque cylinders. It has, however, never been tried before with glass or ceramic cylinders because it was considered very difficult to provide a simple, uniform, radial support to the ends of the cylinder without introducing point loadings to the ceramic radial and axial bearing surfaces on the ends of the cylinder.

The testing of NOSC's first generation beryllia ceramic monocoque cylinders supported radially at the ends with titanium end closures has shown conclusively that this is both a structurally acceptable, and, at the same time, a cost-effective approach to raising the elastic stability of thin monocoque ceramic cylinders for 9,000-psi external pressure service.

These tests, however, also disclosed that the radial and axial bearing stress risers resulting from the direct contact between the metallic end closures and the ends of the thin ceramic cylinders, Figure 10, resulted in an unacceptably short cyclic fatigue life (less than 100 dives to the design depth) of the ceramic surfaces. This shortcoming had to be eliminated if the concept of radially supported monocoque ceramic cylinders was to remain a structurally viable design approach.

The solution proposed by NOSC for elimination of fretting between the mating high points on the ceramic and metallic bearing surfaces at the ends of cylinders consists of enclosing the ends of the ceramic cylinders with U-shaped metallic rings bonded securely to the ceramic surfaces with

epoxy adhesive (Figure 11). Another proposed modification to NOSC's first generation ceramic pressure vessel housing consists of increasing its length by using two or more monocoque ceramic cylinders joined and radially supported at their ends by titanium stiffeners (Figure 12).

This report summarizes the design, fabrication, and testing of NOSC's second generation ceramic housing assemblies for 9,000-psi design pressure which incorporate the design improvements based on the findings and recommendations from the experimental evaluation of NOSC's first generation ceramic housing assemblies (Reference 4).

NOSC'S SECOND GENERATION CERAMIC HOUSING ASSEMBLIES

OBJECTIVE

The primary objective of the study was to evaluate for deep submergence service the cyclic fatigue life of *ceramic monocoque cylindrical housings* whose ends have been protected against chipping and fretting by specially designed metallic end caps.

The secondary objective of the study was to evaluate the structural performance of *metallic ring stiffeners* joining monocoque ceramic cylinders into an elongated pressure housing sealed at the ends with metallic hemispherical end closures.

APPROACH

The approach selected for this study was of an experimental nature. The structural components under investigation were evaluated by incorporating them into a ceramic external pressure housing that subsequently was subjected to repeated pressurizations in a pressure test facility. Since the second generation NOSC ceramic pressure housing design is identical to the previously tested first generation NOSC ceramic pressure housing design (Reference 4), any difference in structural performance would be the result of the two design modifications to the housing under investigation:

1. Protection of ceramic cylinder ends against fretting by enclosing them in titanium end caps filled with epoxy.
2. Increasing the length of the housing by joining several cylindrical sections with a titanium T-ring stiffener.

SCOPE

The study was limited to a single NOSC scale model pressure housing design consisting of two monocoque ceramic cylinders joined at the center with a titanium ring stiffener and sealed off at the ends with titanium hemispheres.

TEST SPECIMENS

Pressure housing assemblies made up from alumina ceramic monocoque cylinders, titanium hemispherical closures, titanium joint rings, and titanium cylinder end caps (Figure 13) served as the test specimens. The composition of the pressure housing assemblies varied from one test to another, depending on the purpose of the individual tests. All ceramic components were fabricated by Coors Ceramics, Golden, Colorado.

Cylinders

Table 2 presents the pertinent dimensions for the Model 1 and Model 2 cylinders. The Model 1 cylinders were fabricated from sintered 99.5-percent pure alumina ceramic (Figure 14). *Three* of the polylithic cylinders were fabricated by brazing together five 1.8-inch wide alumina ceramic rings (Figures 15 through 19). Prior to brazing, the ends of the ceramic rings were metallized by application and firing of moly manganese powder and plated with nickel to facilitate adhesion of the solder to the ceramic surfaces. Grinding the exterior and interior diameters of the brazed ring assemblies to specified tolerances completed the fabrication of these cylinders. *Two* additional Model 1 cylinders were ground to shape from *monolithic* alumina ceramic tubular castings. The monolithic cylinders were intended to serve as structural standards of comparison for the Model 1 brazed modular cylinders.

Table 2. Comparison of NOSC alumina ceramic monocoque cylinders Models 1 and 2.

Parameter	Model 1	Model 2
OD, inches	6.000	6.037
ID, inches	5.624	5.624
Length, inches	9.000	9.000
Hull thickness, inches	0.188	0.206

Two Model 2 cylinders were fabricated from sintered 94-percent pure alumina ceramic (Figure 20). These cylinders were ground to shape from monolithic alumina ceramic tubular castings. These monolithic cylinders were fabricated from the somewhat softer and weaker 94-percent alumina ceramic composition to assess the feasibility of substituting the less expensive and easier to sinter material for the more expensive and harder to sinter 99.5-percent alumina ceramic in the construction of full scale ceramic pressure housings.

All the cylinders were dimensioned to provide, at the design pressure of 9,000 psi, safety factors of approximately *2 based on compressive material failure* and *1.5 based on general elastic instability*, when radially supported at both ends with either the metallic end closures or the joint rings. Without radial supports at the ends the cylinders would elastically buckle at approximately 3,900 psi, well below the design depth of 9,000 psi.

To make the Model 1 cylinders elastically self supporting at 9,000 psi with a safety factor of 1.5 would require an increase in the wall thickness from 0.188 to 0.290 inches. The resulting weight increase of approximately 54 percent would make the cylinders too heavy (insufficient positive buoyancy) for their intended service as pressure housings in remotely controlled vehicles. It is for this reason that the Model 1 and 2 monocoque ceramic cylinders were not designed to be elastically self supporting at the design depth of 9,000 psi.

The wall thicknesses, diameters, and lengths of the 99.5-percent alumina ceramic Model 1 cylinders were identical to the cylinders in NOSC's *first* generation ceramic housing assemblies. The only difference consisted in using alumina (Table 3) instead of beryllia ceramic for reasons of economy and health hazards (50 million psi for beryllia versus 54 million psi modulus of elasticity for 99.5-percent alumina). The thickness of 94-percent alumina ceramic Model 2 cylinders was increased by 10 percent over that of Model 1 cylinders to make up for the difference in moduli of elasticity between those two alumina ceramic compositions (i.e., 54 million psi for 99.5-percent alumina ceramic versus 41 million psi for 94-percent alumina ceramic). Thus, the elastic stabilities of both Model 1 and Model 2 alumina ceramic cylinders under external hydrostatic pressure were made to be the same.

Table 3. Typical properties of alumina ceramics.

PROPERTIES*	UNITS	TEST	AD-85	AD-90 Nom 90% Al_2O_3	AD-94 Nom 94% Al_2O_3	AD-96 Nom 96% Al_2O_3	AD-995 Nom 99.5% Al_2O_3
SPECIFIC GRAVITY		ASTM-C20-70	3.41	3.60	3.62	3.72	3.89
HARDNESS ROCKWELL KNOOP	R45N GPa	ASTM E18-67 1000-g load	73 9.8	79 10.8	78 11.1	78 11.1	83 14.7
SURFACE FINISH AS-FIRED GROUND POLISHED	MICROMETRES (MICROINCHES)	PROFILOMETER (0.75mm cutoff)	1.6 (63) 1.0 (39) 0.2 (8.0)	1.6 (63) 0.5 (20) 0.1 (3.9)	1.6 (63) 1.3 (51) 0.3 (12)	1.6 (63) 1.3 (51) 0.3 (12)	0.9 (35) 0.5 (20) 0.1 (3.9)
CRYSTAL SIZE RANGE AVERAGE	MICROMETRES (MICROINCHES)		2-12 (79-473) 6 (236)	2-10 (79-394) 4 (158)	2-25 (79-985) 12 (473)	2-20 (79-788) 11 (433)	5-50 (197-1970) 16 (670)
WATER ABSORP.		ASTM C373-72	NONE	NONE	NONE	NONE	NONE
GAS PERM.**			NONE	NONE	NONE	NONE	NONE
COLOR			WHITE	WHITE	WHITE	WHITE	IVORY
COMPRESSIVE STRENGTH 25 C 1000 C	MPa (kpsi)	ASTM C773-74	1930 (280) — (—)	2482 (360) 517 (75)	2103 (305) 345 (50)	2068 (300) — (—)	2620 (380) — (—)
FLEXURAL STRENGTH TYP 25 C MIN 25 C*** TYP 1000 C MIN 1000 C***	MPa (kpsi)	ASTM F417-75T	296 (43) 269 (39) 172 (25) 138 (20)	338 (49) 303 (44) — (—) — (—)	352 (51) 317 (46) 138 (20) 117 (17)	358 (52) 324 (47) 172 (25) 138 (20)	379 (55) — (—) — (—) — (—)
TENSILE STRENGTH 25 C 1000 C	MPa (kpsi)	ACMA TEST 4	155 (22) — (—)	221 (32) 103 (15)	193 (28) 103 (15)	193 (28) 96 (14)	262 (38) — (—)
MOD. OF ELAST. SHEAR MODULUS BULK MODULUS TRANS. SONIC VEL. POISSON'S RATIO	GPa (10^6psi) GPa (10^6psi) GPa (10^6psi) m/sec (ft/sec)	ASTM C623-71	221 (32) 96 (14) 138 (20) 8.2 (27)' 10^3 0.22	276 (40) 117 (17) 158 (23) 8.8 (29)' 10^3 0.22	283 (41) 117 (17) 165 (24) 8.9 (29)' 10^3 0.21	303 (44) 124 (18) 172 (25) 9.1 (30)' 10^3 0.21	372 (54) 152 (22) 228 (33) 9.8 (32)' 10^3 0.22
MAX.-USE TEMP. (No-load conds.)	°C (°F)		1400 (2550)	1500 (2730)	1700 (3100)	1700 (3100)	1750 (3180)
COEFFICIENT OF LINEAR THERMAL EXPANSION 200-25 C 25-200 C 25-500 C 25-800 C 25-1000 C 25-1200 C	10^{-6}/°C (10^{-6}/°F)	ASTM C372-56	3.4 (1.9) 5.3 (3.0) 6.2 (3.5) 6.9 (3.9) 7.2 (4.0) 7.5 (4.2)	3.4 (1.9) 6.1 (3.4) 7.0 (3.9) 7.7 (4.3) 8.1 (4.5) 8.4 (4.7)	3.4 (1.9) 6.3 (3.5) 7.1 (4.0) 7.6 (4.3) 7.9 (4.4) 8.1 (4.5)	3.4 (1.9) 6.0 (3.4) 7.4 (4.1) 8.0 (4.5) 8.2 (4.6) 8.4 (4.7)	3.4 (1.9) 7.1 (4.0) 7.6 (4.3) 8.0 (4.5) 8.3 (4.6) —
THERMAL CONDUCTIVITY 20 C 100 C 400 C 800 C	W/m-K (g-cal/(sec)(cm²) (°C/cm))	ASTM C408-58	14.6 (0.035) 12.1 (0.029) 6.7 (0.016) 4.2 (0.010)	16.7 (0.040) 13.4 (0.032) 7.9 (0.017) 5.0 (0.010)	18.0 (0.043) 14.2 (0.035) 7.9 (0.017) 5.0 (0.010)	24.7 (0.059) 18.8 (0.045) 10.0 (0.024) 5.4 (0.013)	35.6 (0.085) 25.9 (0.062) 12.1 (0.028) 6.3 (0.015)
SPECIFIC HEAT 100 C	J/kg-K (cal/g/°C)	ASTM C351-61	920 (0.22)	920 (0.22)	880 (0.21)	880 (0.21)	880 (0.21)

NOTE: The ceramic compositions shown above are the commercial products of Coors Porcelain Co., Golden, Colorado 80401.

Hemispherical End Closures

The end closures consisted of hemispherical shells machined from Ti-6Al-4V alloy with 125,000-psi minimum yield point (Figure [illegible]). The hemispheres have an inside diameter of 5.624 inches and are 0.136 inch thick. At its equator each one has a flange for axial and radial support of the ceramic cylinder (Figures 22 through 24). In NOSC's first generation design of the ceramic pressure housing (Reference 4), the ends of the ceramic cylinder were in direct contact with the equatorial flanges on the hemispherical end closures. The differential radial movement between the ends of the ceramic cylinder and the flange on the titanium hemisphere produced fretting of the mating surfaces that, after 30 to 50 repeated pressurizations to the design depth of 9,000 psi, resulted in fracture of the ceramic cylinder (Figure 25).

In NOSC's second generation design,the ends of the Models 1 and 2 ceramic cylinders were protected from fretting by titanium U-shaped end caps bonded with epoxy adhesive to the ceramic bearing surfaces (Figure 15). The application of U-shaped titanium end caps eliminated any point contact between the ceramic bearing surfaces on the ends of the cylinder and the titanium bearing surfaces on the flange of the hemispherical end closure. Thus, fretting of the ceramic bearing surfaces was not initiated any more by the differential radial movement between the cylinder and the end closures. The fretting, if any, now took place between the titanium end cap and the titanium end closure where it could not initiate fracture in the tough metallic bearing surfaces (Figure 25).

The hemispherical end closures were in all respects identical to the end closures used in NOSC's first generation ceramic housing assemblies. The BOSOR 4B computer program was used in designing the end closures to minimize wall thickness without compromising the specified safety factors of 1.25 and 1.50 at design depth for material failure and buckling, respectively.

U-Shaped End Caps

U-shaped end cap rings, machined from Ti-6Al-4V alloy (Figures 26 through 28), were bonded with epoxy adhesive to the ends of the ceramic cylinders to serve as protectors for these surfaces. The walls of the rings were very thin in order to exert very little radial force on the ends of the ceramic cylinder due to difference in thermal expansion coefficients between these dissimilar materials. Because of small clearances between the external surfaces of the cylinder and the internal surfaces of the end caps the layer of adhesive bond was less than 0.010 inch thick. The reason for keeping the bond layer so thin was to prevent its extrusion under the high (i.e., 70,000 to 80,000 psi) axial and radial bearing stresses during repeated pressurizations of the cylinder to the design pressure of 9,000 psi.

Joint Rings

T-shaped rings machined from Ti-6Al-4V titanium alloy provided radial support and axial alignment to the ends of the cylinders and two hemispherical end closures. The flanges on the T-shaped rings were dimensioned for a close fit with the interior diameter of the U-shaped end caps on the cylinder ends. The tight fit (less than a 0.005-inch radial clearance) was to ensure good radial support for the end caps enclosing the ends of the ceramic cylinders. Loose fit between those components could result in buckling of the ceramic cylinder at lower pressure.

Three joint ring designs were used in the tests. Joint ring A (Figures 29 and 30) was designed to fail at approximately 50 percent below the design pressure, while joint rings B (Figures 31 and 32) and C (Figures 33 and 34) were designed to fail at 17 and 40 percent above the design pressure,

respectively, when supporting Models 1 or 2 alumina cylinders. The BOSOR 4B computer program was employed in the calculation of stresses in the joint rings and their elastic instability. In the above calculations it was assumed that the length of the pressure housing assembly was *infinite*, made up of a large number of cylindrical sections (more than 6 units long) joined together by many titanium joint stiffeners. The critical buckling pressures of the joint ring designs used in the second generation NOSC ceramic housings were: joint ring A, 4,900 psi; joint ring B, 10,500 psi; and joint ring C, 12,500 psi.

Needless to say that the critical pressure of the joint stiffeners will increase if the length of the housing assembly is shortened to only two cylindrical sections. Since in this test program the cylindrical pressure housing consisted of only two cylinders joined together by a single titanium joint stiffener, its critical pressure would be significantly higher than that calculated for an infinitely long cylinder. Thus, for example, the critical pressure of joint ring A increases from *4,900 psi* when joining Model 1 or Model 2 ceramic cylinders in an infinitely long cylindrical housing assembly to *7,700 psi* in a cylindrical assembly made up of just two Model 1 or Model 2 ceramic cylinders.

The reason for evaluating three different joint ring designs was to minimize the weight, increase internal diameter, and at the same time validate the computer program for this pressure housing configuration where the stiffeners were fabricated from a material with a totally dissimilar elastic response from the ceramic cylinder. It was hoped that, even if the computer program was significantly in error, the joint ring C design would stiffen the cylinder sufficiently to provide the housing assembly with a safety margin of at least 1.25 in buckling at the design pressure of 9,000 psi.

TEST ARRANGEMENT

Test Assemblies

The housing components were combined in several ways to arrive at seven different test assemblies.

Test Assembly I — A single *modular* alumina ceramic Model 1 cylinder equipped with titanium end caps and supported at both ends by titanium hemispherical end closures (Figures 35 and 36)

Test Assembly II — A single *monolithic* alumina ceramic Model 1 cylinder equipped with titanium end caps and supported at both ends by titanium hemispherical end closures (Figures 37 and 38)

Test Assembly III— Two *modular* alumina ceramic Model 1 cylinders equipped with titanium end caps, joined together and supported by the titanium *joint ring A* and supported at the other ends by titanium hemispherical end closures (Figures 39 and 40)

Test Assembly IV — Two *monolithic* alumina ceramic Model 1 cylinders equipped with titanium end caps, joined together and supported by the titanium *joint ring B* and supported at the other ends by titanium hemispherical end closures (Figure 41)

Test Assembly V — Two *monolithic* alumina ceramic Model 1 cylinders equipped with titanium end caps, joined together and supported by the titanium *joint ring C* and supported at the other end by titanium hemispherical end closures (Figure 42)

Test Assembly VI — A single *monolithic* alumina ceramic Model 2 cylinder equipped with titanium end caps and supported at both ends by titanium hemispherical end closures

Test Assembly VII — Two *monolithic* alumina ceramic Model 2 cylinders equipped with titanium end caps, joined and supported by the titanium *joint ring C* and supported at the other ends by titanium hemispherical end closures

Test Schedule

The test assemblies were to be subjected to test schedules shown in Table 4.

Test Procedure

Pressurization medium — 30 SAE oil served as the pressurization medium to prevent corrosion of the pressure vessel and high pressure pump.

Pressurization took place at a 1,000-psi/minute rate. Depressurization rate was not constant, but varied from a 10,000-psi/minute rate in the 9,000- to 1,000-psi range to a 50-psi/minute rate in the 1,000- to 0-psi range.

Pressure cycles were of constant duration. Each pressure cycle consisted of pressurizing to the specified maximum pressure, holding the specified maximum pressure for 30 minutes within a plus or minus 100-psi range, depressurizing to 0 pressure, and relaxing for 15 minutes at 0 pressure.

Test assemblies were prepared for testing by inserting into their interior loosely fitted solid plastic cylinders (Figure 43). The purpose for the use of these inserts was to decrease the implodable volume inside the pressure housing so that the implosion of a single pressure housing component in the test assembly would not necessarily result in the destruction of the other components.

Sealing of joints between the cylinder ends, end closures, and/or joint ring was accomplished by wrapping around the exterior of the assembly a continuous length of black vinyl electrical insulation tape (Figures 44 and 45). By overlapping the tape on adjacent wraps a watertight seal was achieved. The tape was also helpful in holding together the fragments of the ceramic cylinder after implosion took place.

Instrumentation of the test assemblies consisted of 0.25 inch electric resistance strain gages bonded to the ceramic and metallic surfaces (Figure 46). The number of gages was kept to a minimum since the magnitude and distribution of strains on many of the assembly components were already measured during the testing of the first generation NOSC ceramic housings (Reference 4). The instrumentation leads from the interior of the housing assembly were fed through custom-made, epoxy-filled penetrators threaded into the titanium end closures (Figure 47). Housing assemblies with strain gages only on their exterior surface did not require any penetrators in the titanium end closures; instead the wetted ends of the leads were embedded in the waterproofing compound covering each gage installation.

TEST OBSERVATIONS

Assembly I successfully withstood without failure the proof test to 10,000 psi and 1,000 pressure cycles to 9,000 psi. It failed after 150 pressure cycles to 10,000 psi. The failure originated at the apex of one of the titanium hemispherical end closures. The mechanism of failure was local plastic instability of the titanium end closure (Figures 48 through 50).

Table 4. Test schedule for alumina ceramic assemblies

Test Assembly	Phase 1	Phase 2	Phase 3
I	Proof test once to 10,000 psi	Pressure cycle 1,000 times from 0 to 9,000 psi	Pressure cycle to 10,000 psi until failure
II	Proof test once to 10,000 psi	Pressure cycle 1,000 times from 0 to 9,000 psi	Pressure cycle to 10,000 psi until failure
III	Proof test once to 10,000 psi	Pressure cycle 100 times from 0 to 9,000 psi	Pressure cycle 10 times to 10,000 psi
IV	Proof test once to 10,000 psi	Pressure cycle 100 times from 0 to 9,000 psi	Pressure cycle 10 times to 10,000 psi
V	Proof test once to 10,000 psi	Pressure cycle 100 times from 0 to 9,000 psi	Pressure cycle 10 times to 10,000 psi
VI	Proof test once to 10,000 psi	Pressure cycle 100 times from 0 to 9,000 psi	Pressure cycle 10 times to 10,000 psi
VII	Proof test once to 10,000 psi	Pressure cycle 100 times from 0 to 9,000 psi	Pressure cycle 10 times to 10,000 psi

Assembly II successfully withstood without failure the proof test to 10,000 psi and 1,000 pressure cycles to 9,000 psi. It failed after 98 pressure cycles to 10,000 psi. The failure originated at the apex of one of the titanium hemispherical end closures. The mechanism of failure was local plastic instability, similar to failure of the end closure in Assembly I.

Assembly III failed during the proof test at 7,400 psi. The failure originated in the titanium joint ring A joining two alumina ceramic Model 1 cylinders. The mechanism of failure was plastic instability of the joint ring (Figure 51).

Assembly IV successfully withstood the proof test to 10,000 psi, 100 pressure cycles to 9,000 psi and 10 subsequent pressure cycles to 10,000 psi. There were no visible signs of deformation or cracks in the components of the pressure housing assembly. Joint ring B deformed uniformly and elastically around its circumference, and the hoop strains on the rings matched those on the ends of the Model 1 ceramic cylinder (Figures 52 through 54). The stresses on the exterior surfaces of the assembly were below design values for both the ceramic and titanium (Figures 55 through 57).

Assembly V successfully withstood the proof test to 10,000 psi, 100 pressure cycles to 9,000 psi, and 10 subsequent pressure cycles to 10,000 psi. There were no visible signs of deformation or cracks in the components of the pressure housing assembly.

Assembly VI successfully withstood the proof test to 10,000 psi, 100 pressure cycles to 9,000 psi, and 10 subsequent pressure cycles to 10,000 psi. There were no visible signs of deformation or cracks in the components of the pressure housing assembly. The distribution of strains on the inside diameter and web of the H-shaped flange of joint ring C followed very much the values predicted by computer analysis (Figures 58 through 60). It is interesting to note that the magnitude of *compressive hoop strains* on the interior surface of the H-shaped flange at its center equals the magnitude of *tensile strains* in the axial direction at that location. Both the hoop and radial strains on the web of the flange were nonlinear with pressure indicating the presence of sideways displacement. The magnitude of stresses at proof test depth was less than 50 percent of the titanium yield strength (Figures 61 and 62).

Assembly VII successfully withstood the proof test to 10,000 psi, 100 pressure cycles to 9,000 psi, and 10 subsequent pressure cycles to 10,000 psi. There were no visible signs of deformation or cracks in the components of the pressure housing assembly.

FINDINGS

The pressure tests of the seven test asemblies resulted in the following findings:

1. The 99.5- percent Model 1 and 94-percent Model 2 alumina ceramic monocoque cylinders with titanium end caps perform satisfactorily at 10,000-psi proof test pressure when simply supported at the ends by titanium hemispherical end closures or titanium joint rings B or C.

2. The Model 1 and Model 2 alumina ceramic cylinders with titanium end caps have a cyclic fatigue life in excess of 1,000 cycles when the hoop and axial compressive stresses on the interior of the ceramic cylinder at midbay do not exceed 150,000 and 75,000 psi, respectively.

3. Both the modular and monolithic alumina ceramic cylinders of same composition, when protected at the ends with titanium end caps, performed equally well under several proof pressurizations to 10,000 psi and over 1,000 pressurizations to 9,000-psi working pressure.

This data suggests that the structural performance of modular alumina ceramic cylinders (fabricated by brazing of cylindrical modules with metallized bearing surfaces) under external pressure loading equals that of monolithic alumina ceramic cylinders with identical diameter, thickness, and overall length.

4. The adhesive-bonded titanium end caps adequately protect the radial and axial bearing surfaces on the ends of alumina ceramic cylinders against fretting due to relative movement between the ends of the cylinders and the titanium end closures and/or titanium joint rings during hydrostatic loading of the housing assembly. The 0.010-inch thick adhesive layer does not extrude from the annular space between the interior surfaces of the end cap and the exterior surface of the cylinder in the presence of bearing stresses in the 70,000- to 80,000-psi range.

5. The titanium hemispherical end closures have a short (<100 cycles) cyclic fatigue life at 10,000-psi proof test pressure and long (>1,000 cycles) cyclic fatigue life at 9,000-psi design pressure. This is the result of the high compressive stress found at the apex on the external surface. The presence of high compressive stress at this location causes the end closure to fail by local plastic instability after a low number of pressure cycles to 10,000-psi proof pressure. The magnitude of compressive stress at the apex of the hemisphere is 96,000 psi at 10,000-psi proof test pressure.

6. The BOSOR 4B computer program appears to predict well the distribution of stresses and the critical pressures of individual assembly components. For example, the calculated and experimentally measured critical pressures of joint ring A in Test Assembly I were 7,700 and 7,400 psi, respectively.

7. The titanium joint rings B and C are radially stiffer than the alumina ceramic cylinder. The simple radial support decreases the compressive hoop stress in the ceramic cylinder at the point of support.

8. The simple radial support by the joint ring also generates a bending moment in the ceramic shell which locally *increases the axial compressive stress on the exterior surface, and decreases it on the interior surface*. The maximum value of the axial compressive stress at design depth was measured to be 76,170 psi on the exterior ceramic surface just past the edge of the lip on joint ring B.

9. Joint ring C provides the Model 1 and 2 ceramic cylinders with higher resistance to buckling than joint ring B, even though its weight is approximately the same as that of joint ring B. For this reason joint ring C is considered structurally superior to joint ring B and should be used exclusively in future housing assemblies.

10. The magnitude of stresses in joint rings B and C at proof pressure is below the yield of the titanium alloy Ti-6Al-4V. The hoop and axial stresses on the exterior surface of joint ring B while supporting two Model 1 cylinders at 10,000 psi proof pressure were measured to be only −49,500 and −33,680 psi, respectively. On joint ring C the hoop and axial stresses on the interior diameter of the *lower flange* at proof pressure were −29,000 and +24,000 psi, respectively. The hoop and axial (radial) stresses measured on the surface of the *ring web* between the upper and lower flanges of ring C were lower than those measured on the lower flange.

11. The pressure housing Test Assemblies I, II, IV, V, VI, and VII appear to be properly designed for 9,000-psi working pressure and can safely withstand up to 10 proof tests to 10,000 psi without structural damage.

12. The pressure housing Test Assembly III is not adequately designed for 9,000-psi working pressure. The plastic buckling of titanium joint ring A at 7,400 psi lowers the *working pressure* of this assembly to approximately 4,500 psi. If joint ring A is replaced by joint rings B and C, the working pressure of the whole housing assembly can be raised to 9,000 psi.

13. Because joint ring A has *not proved adequate* for service in Model 1 or Model 2 ceramic housings with 9,000-psi design pressure, it should not be considered for service in those housings.

DISCUSSION

The test findings of this study validate the hypothesis postulated earlier at NOSC (Reference 4) that the elastic stability of monocoque ceramic cylinders can be raised to the desired critical pressure without increasing their thickness or the addition of integral ribs. This is accomplished by providing radial support to the cylinder ends with closely fitted titanium structural components that have the appropriate elastic stability. These structural components were bulkheads in the shape of hemispherical shells or joint rings with a T-shaped or H-shaped cross section.

Although the theoretical proof for this hypothesis had been developed a long time ago (References 5 and 6) and applied to the design of cylindrical steel pressure hulls for submarines, the peculiar physical properties of ceramics proved to be a formidable obstacle to practical implementation of this hypothesis to ceramic monocoque cylinders under external pressure. The physical properties of ceramics that made the design of a ceramic housing radially supported by metallic stiffeners such a challenge were low strength in tension or shear and lack of ductility.

To compensate for the above mentioned physical properties of ceramic cylinders, the design of the metallic housing components must meet the following criteria:

1. *Direct contact* between the mating surfaces of the ceramic cylinder and the metallic stiffeners must be avoided to eliminate any stress risers in the ceramic due to point contact between these surfaces.

   This was achieved by potting the ends of the cylinders in epoxy-filled U-shaped end caps. As a result a 0.010- to 0.015-inch thick layer of epoxy was interposed between the radial and axial bearing surfaces on the ceramic cylinder and the metallic surfaces of the end caps.

2. *The radial clearance* between the capped cylinder ends and the radial bearing surface of the stiffener must be kept to a minimum so that the cylinder does not have sufficient radial play to buckle before it mates with the circular bearing surface of the stiffener (or end closure, as it may be the case) all around its circumference.

   This was achieved by keeping the *radial* clearance between the capped cylinder ends and the mating cylindrical bearing surface of the stiffener (or end closure) to less than 0.003 inches.

3. *The shear stress* in the cylinder near its radial support must be kept below the shear strength of the ceramic to prevent fracturing the cylinder. To accomplish this, the

difference between the radial compliance of the ceramic cylinder and that of the metallic stiffener (or end closure) under external pressure loading must be minimized.

This was achieved by designing the stiffener (or end closure) in such a manner that its *radial deformation* was approximately 25 percent of the ceramic cylinder's radial deformation, while at the same time providing the additional elastic stability needed to raise the critical pressure of an *infinitely long* cylindrical assembly made of many individual cylindrical modules above 11,250 psi (9,000-psi design pressure times the 1.25 safety factor).

With the hypothesis proven by experimental evaluation of scale model alumina ceramic monocoque cylinders, no further obstacles remain on the path to successful construction of full scale monocoque cylindrical pressure housings radially supported by metallic ring stiffeners and end closures.

CONCLUSIONS

The following conclusions have been drawn regarding the second generation NOSC alumina ceramic cylinders as a consequence of the pressure testing conducted in this study.

1. Cylindrical external pressure housings of *any desired length* can be successfully assembled from many short cylindrical monocoque alumina ceramic modules joined and radially supported at the ends by flanged titanium rings with appropriate stiffness.

2. The cyclic fatigue life of the 99.5- or 94-percent alumina ceramic cylindrical shells circumferentially and axially stressed by external hydrostatic loading to −150,000 and −75,000 psi, respectively, is in excess of 1,000 pressure cycles.

3. A weight-to-displacement ratio of 0.57 has been achieved for the alumina ceramic cylindrical pressure housings with titanium hemispherical end closures and titanium joint rings designed for a 9,000-psi depth with a safety factor of 2 for the ceramic cylinder and 1.25 for the titanium components.

4. There is a significant reduction in fabrication costs and only a 5-percent weight penalty associated with the substitution of 94-percent alumina ceramic for the premium quality 99.5-percent alumina ceramic in monocoque cylindrical pressure housings with a 9,000-psi design pressure.

5. The fabrication cost of 6-inch diameter, 94-percent alumina ceramic monocoque cylinder Models 1 and 2 with a 9,000-psi design pressure ($2,000/cylinder) has been found to be at least 90 percent less than that of graphite fiber-reinforced plastic composite cylinders and 50 percent less than that of titanium cylinders of the same size and design depths.

6. The fabrication cost of 94-percent alumina ceramic monocoque cylinders with a 9,000-psi design pressure appears to increase linearly with the diameter of the cylinder in the 6- to 12-inch range.

RECOMMENDATIONS

There are two major recommendations as a result of the second generation NOSC ceramic pressure housing testing and evaluation program.

1. The concept of 20,000-foot design depth (9,000-psi) ceramic pressure housings, validated experimentally during the second generation NOSC ceramic housing test series by 6-inch OD scale models, should be extrapolated to larger, operationally useful sizes for further testing.

2. The third generation NOSC alumina ceramic pressure housings should incorporate cylinders and hemispheres with an OD of 12 inches. The fabrication of 12-inch OD ceramic pressure housing components will provide valuable information on the technical difficulties associated with scaling up the fabrication processes, while testing these components will generate quantitative data for describing the effect of structural size on alumina ceramic external pressure housings.

REFERENCES

1. Aero Jet General Corporation, Van Karman Center, Report TR-328:64-207, *Design Concepts Study For Deep Submersibles*, by R. D. Saunders, July 1964.

2. Pennsylvania State University Ordnance Research Laboratory, Report NO 63-0209-C-2, *Solid Glass and Ceramic External Pressure Vessels*, by J. D. Stachiw, 1964.

3. American Ceramic Society, Ceramic Bulletin Vol. 47, No. 2, "Hulls For Deep Submergence Capsules," by J. D. Stachiw, February 1968.

4. Naval Ocean Systems Center, Technical Report TR-951, *Exploratory Evaluation of Beryllia Ceramic Cylindrical Housing For Deep Submergence Service*, by J. D. Stachiw, January 1984.

5. Stodolas Festschrift, "Der Kritische Aussendruck Zylindrischer Roehre," by R. von Mises, 1929, pp. 418-430.

6. Naval Ship Research and Development Center, Report 309, *The Critical External Pressure of Cylindrical Tubes*, by R. von Mises, August 1931.

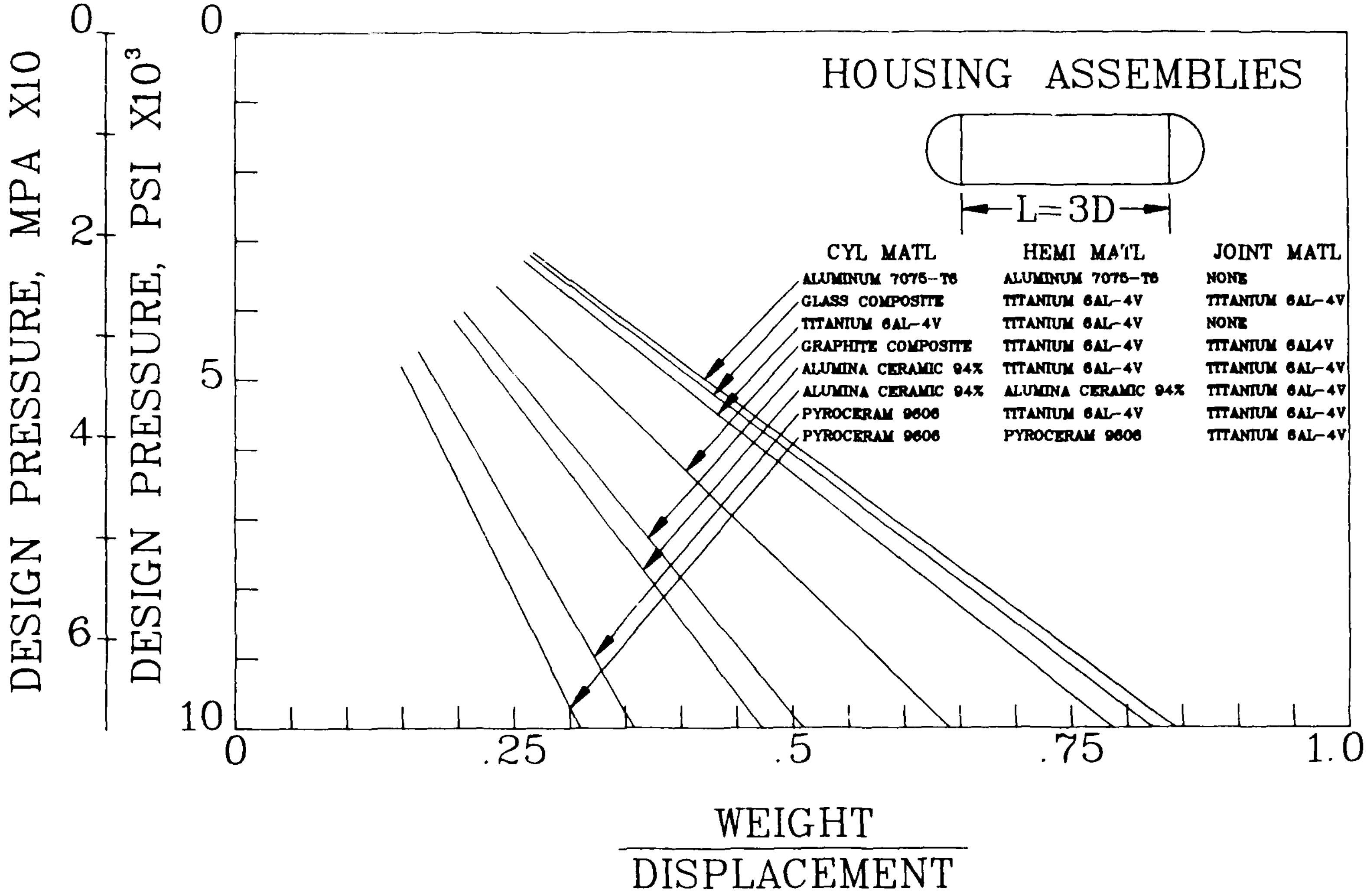

Figure 1. Design pressure versus weight-to-displacement ratio of external pressure housings assembled from components fabricated from different materials. Note that maximum buoyancy is provided by *glass ceramics* (i.e. PYROCERAM or CERVIT pressure housings).

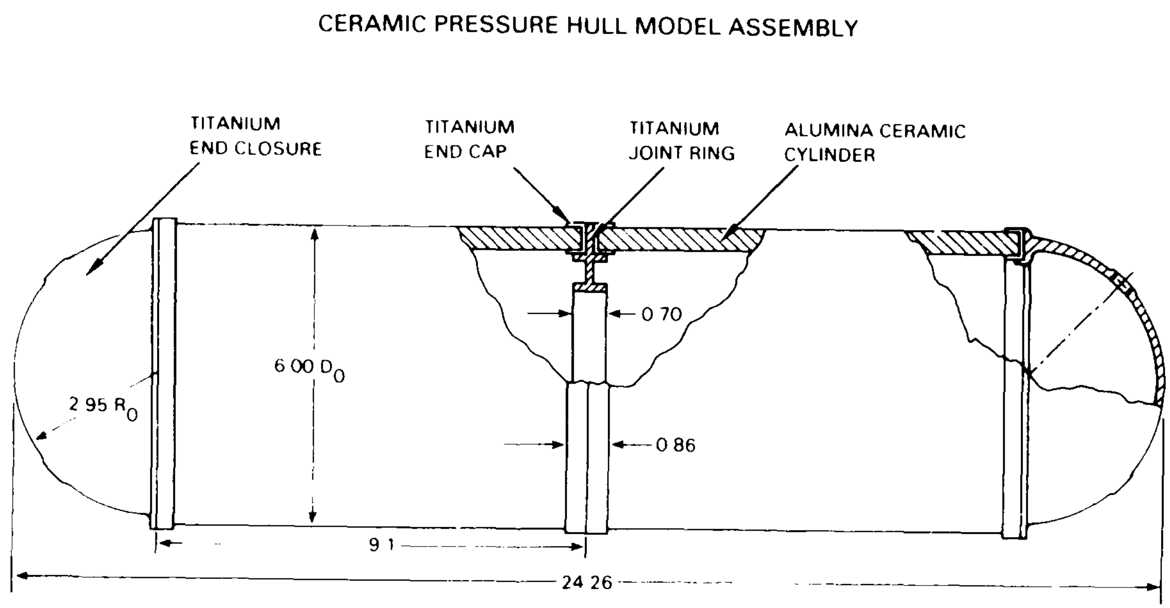

Figure 2. One of the ceramic pressure housing assemblies for 20,000-foot depth service that successfully withstood 1,000 simulated dives to design depth.

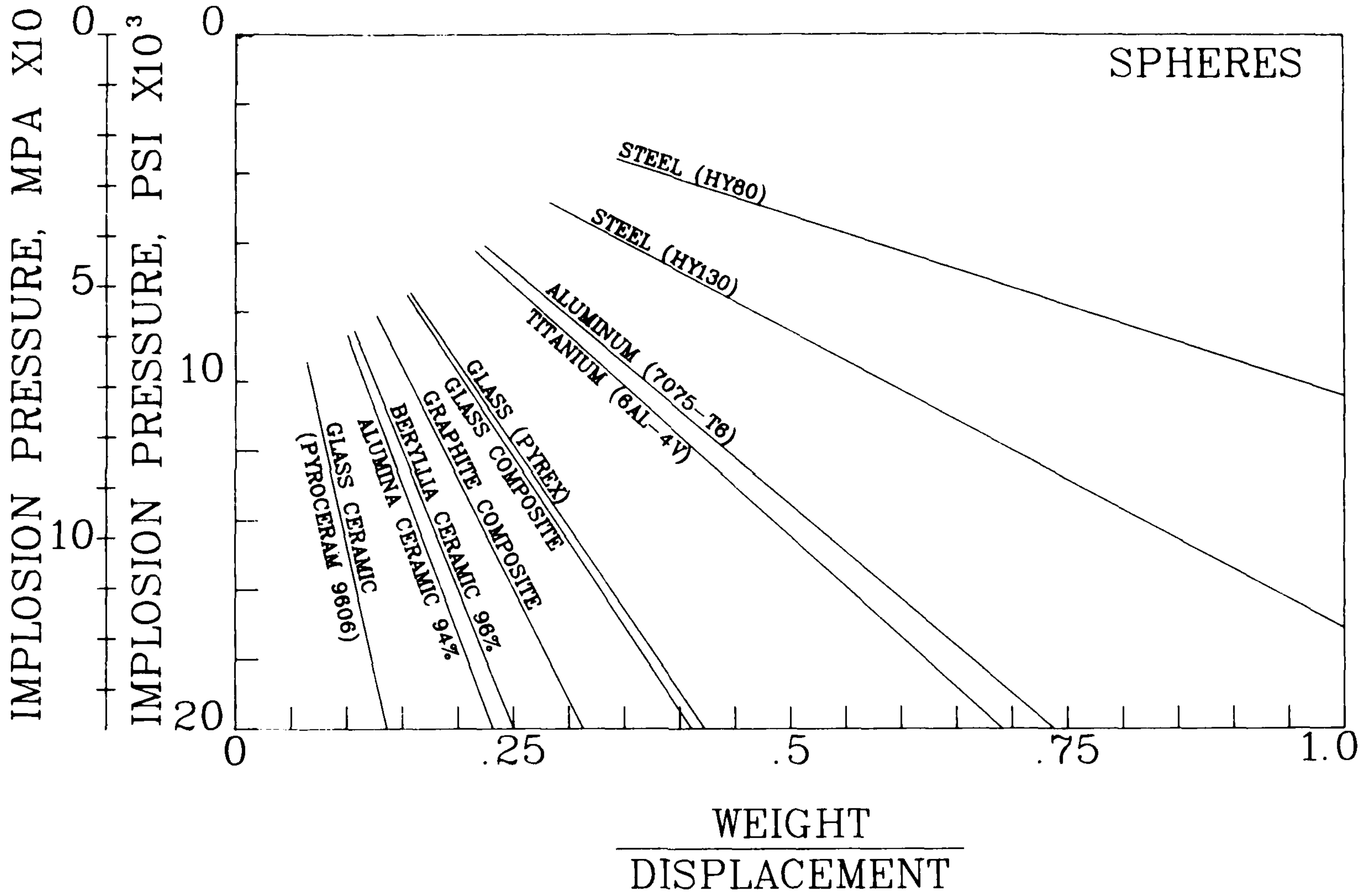

Figure 3. Implosion pressure versus weight-to-displacement ratio of spheres from different structural materials. Note that ceramics provide the lowest weight-to-displacement ratios.

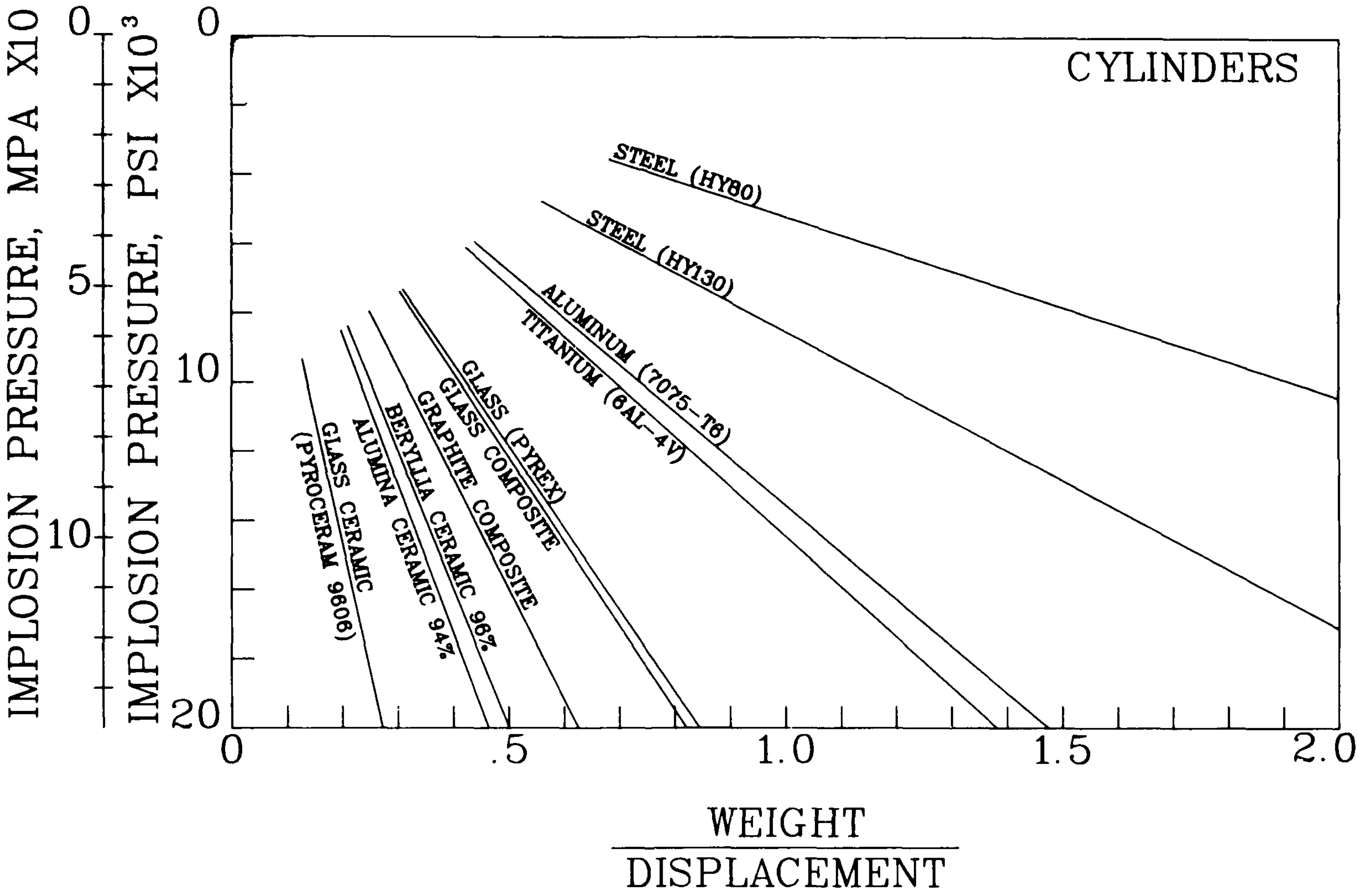

Figure 4. Implosion pressure versus weight-to-displacement ratio of cylinders from different structural materials. Note that ceramics provide the lowest weight-to-displacement ratios. The cylinders are designed to implode due to material failure and not by buckling.

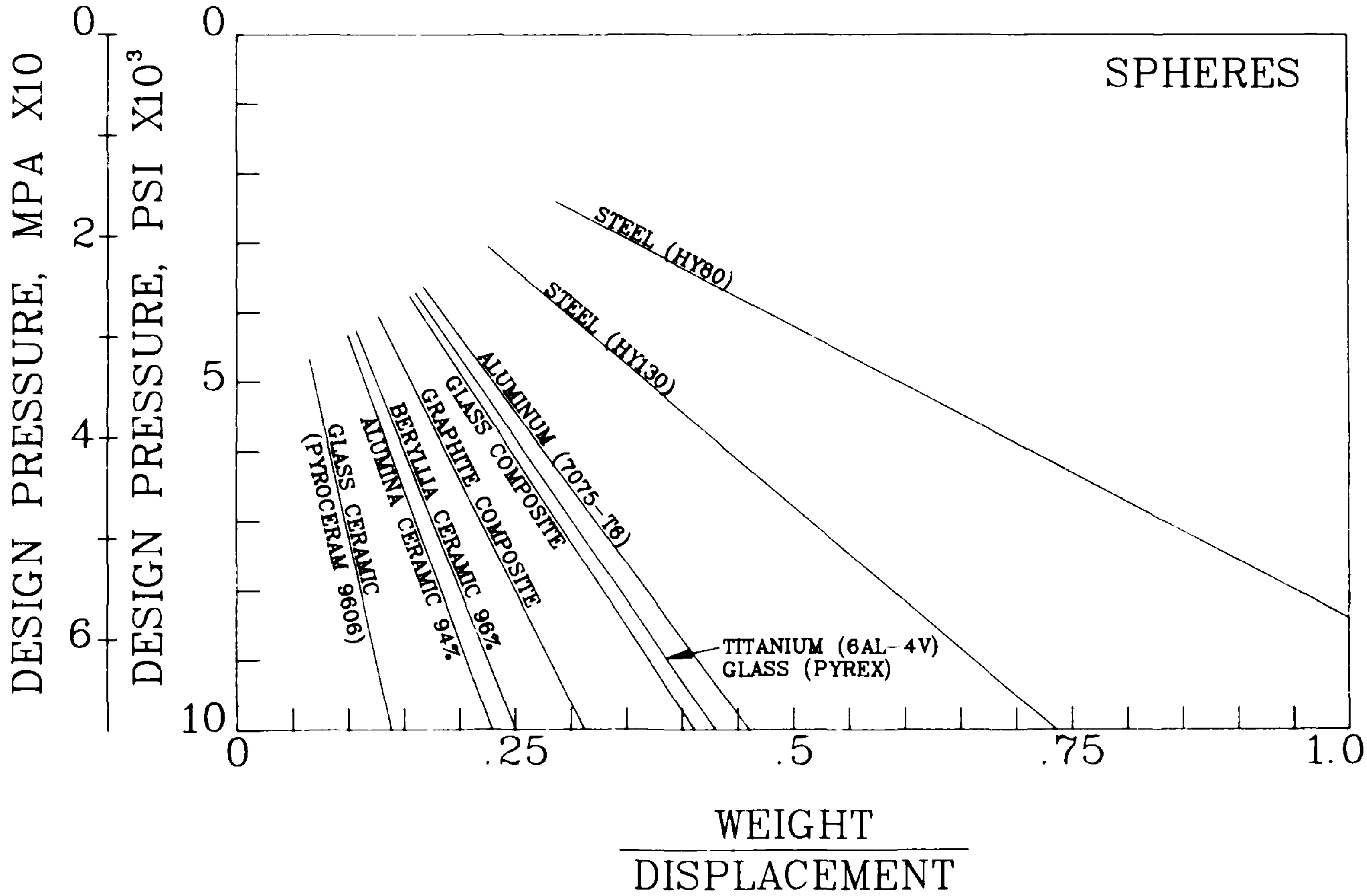

Figure 5. Design pressure versus weight-to-displacement ratio of spheres from different structural materials. Note that the weight-to-displacement ratios shown on this figure changed significantly from Figure 2 due to application of the safety factors presented in Table 1.

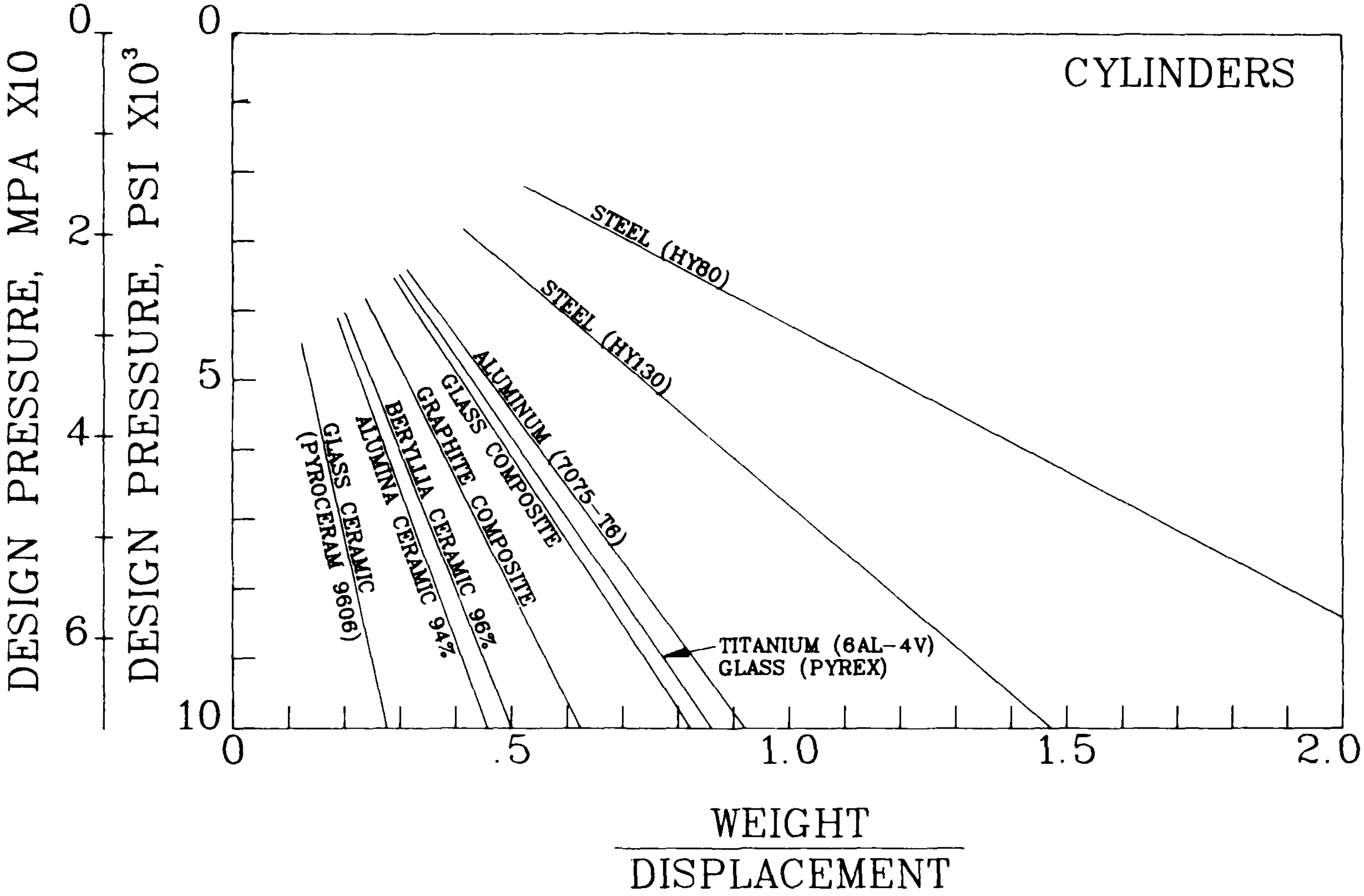

Figure 6. Design pressure versus weight-to-displacement ratio of cylinders from different structural materials. Note that the weight-to-displacement ratios shown on this figure changed significantly from Figure 3 due to application of the safety factors presented in Table 1.

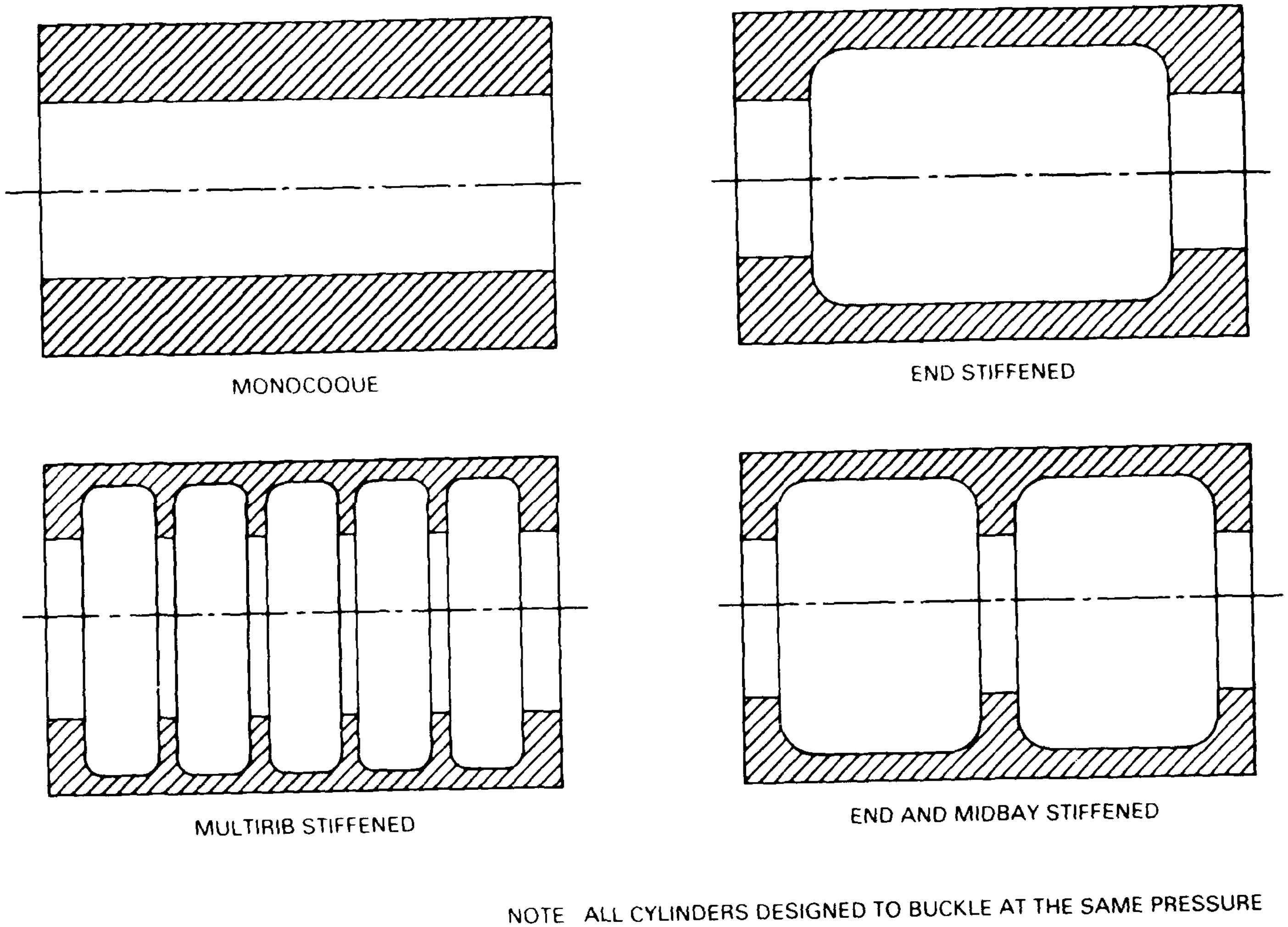

Figure 7. Different approaches to providing the required elastic stability for cylinders under external pressure loading. The monocoque cylinder is the *least* weight effective, while the cylinder with many integral ribs is the *most* weight effective design for ceramic cylinders.

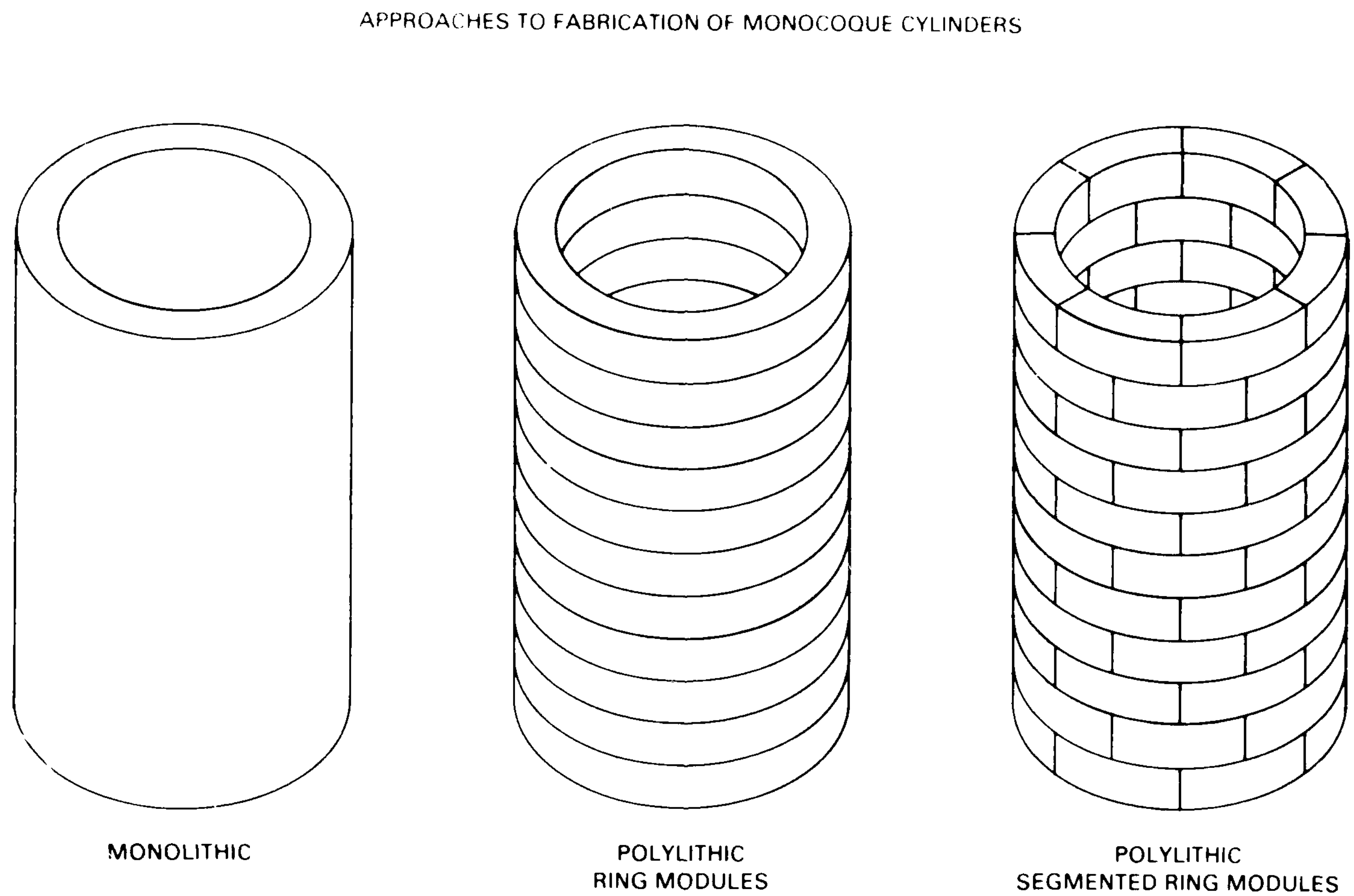

Figure 8. Techniques for fabrication of large diameter cerami. .linders from structural modules joined by brazing with metallic solder.

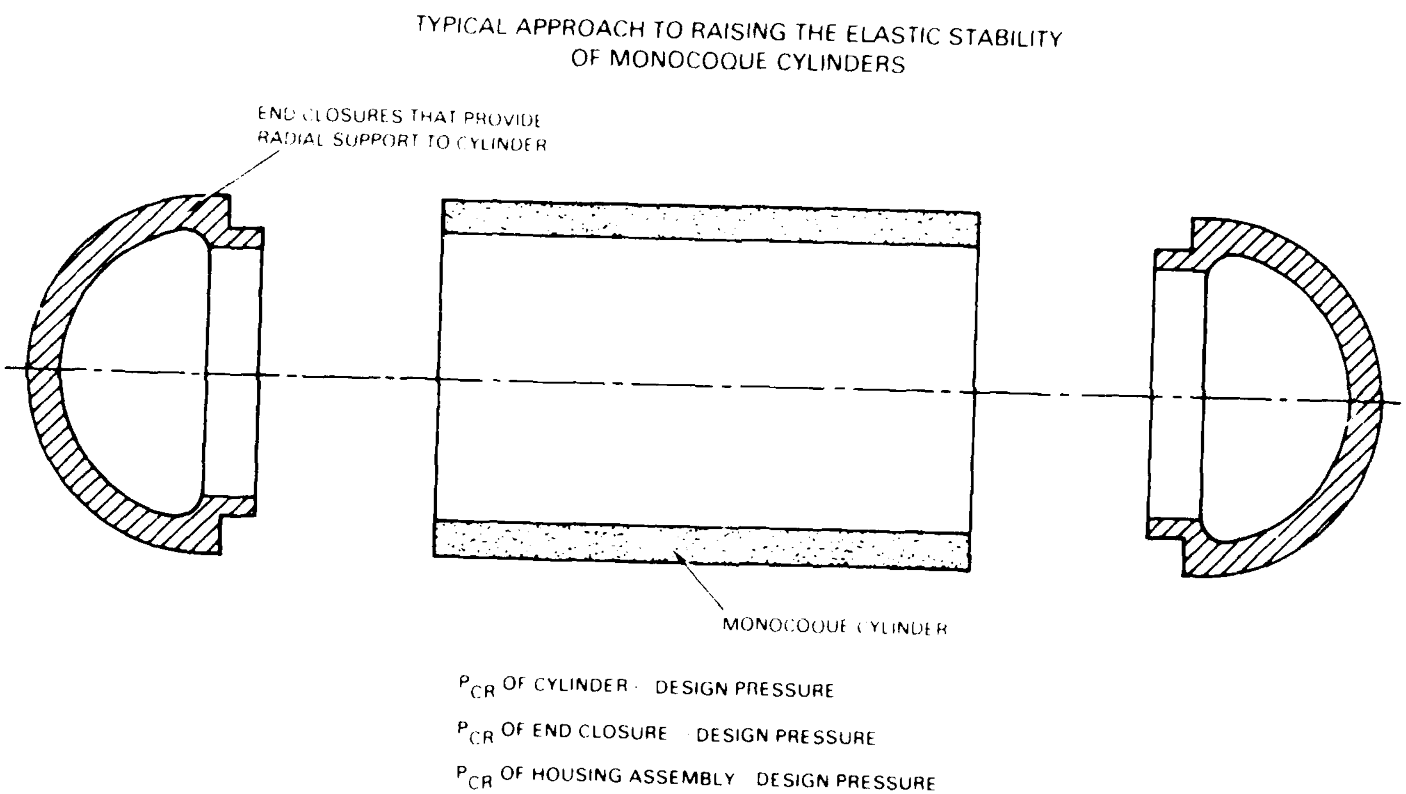

Figure 9. Simple radial support by metallic spherical end closures can raise the inadequate elastic stability of thin, monocoque, ceramic cylinders of high strength materials to the critical pressure of end closures

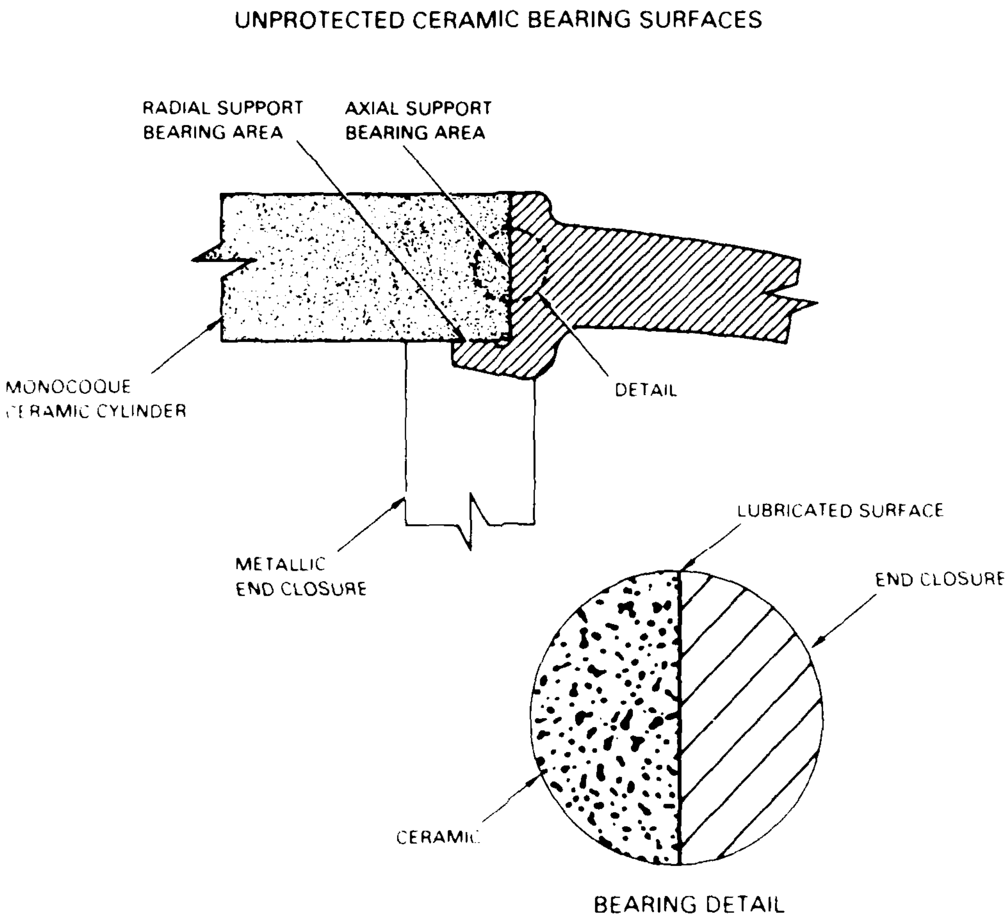

Figure 10. Direct radial support of the ceramic cylinder by the metallic end closure results in fretting of the ceramic bearing surfaces that leads ultimately to crack initiation.

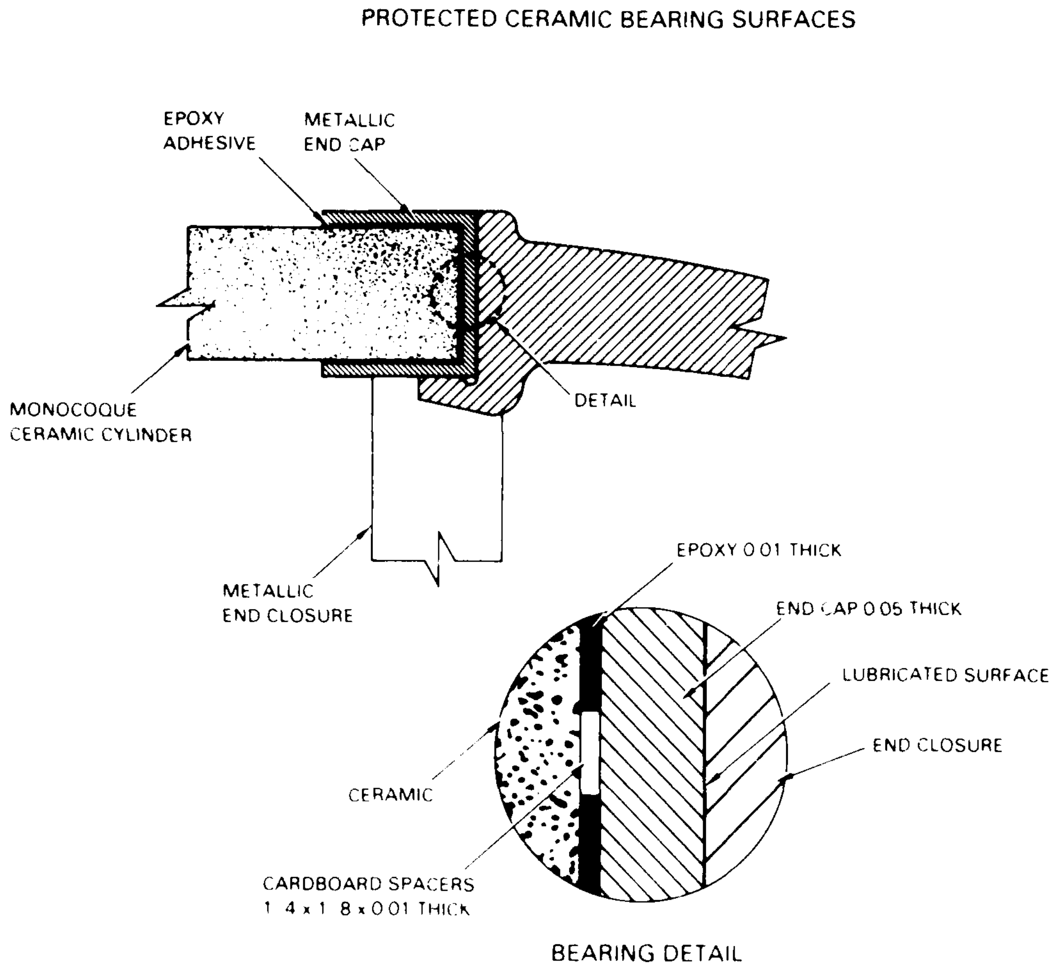

Figure 11 Circular, metallic caps bonded with epoxy to the ends of the cylinder protect the ceramic bearing surfaces from chafing and fretting during repeated pressurizations.

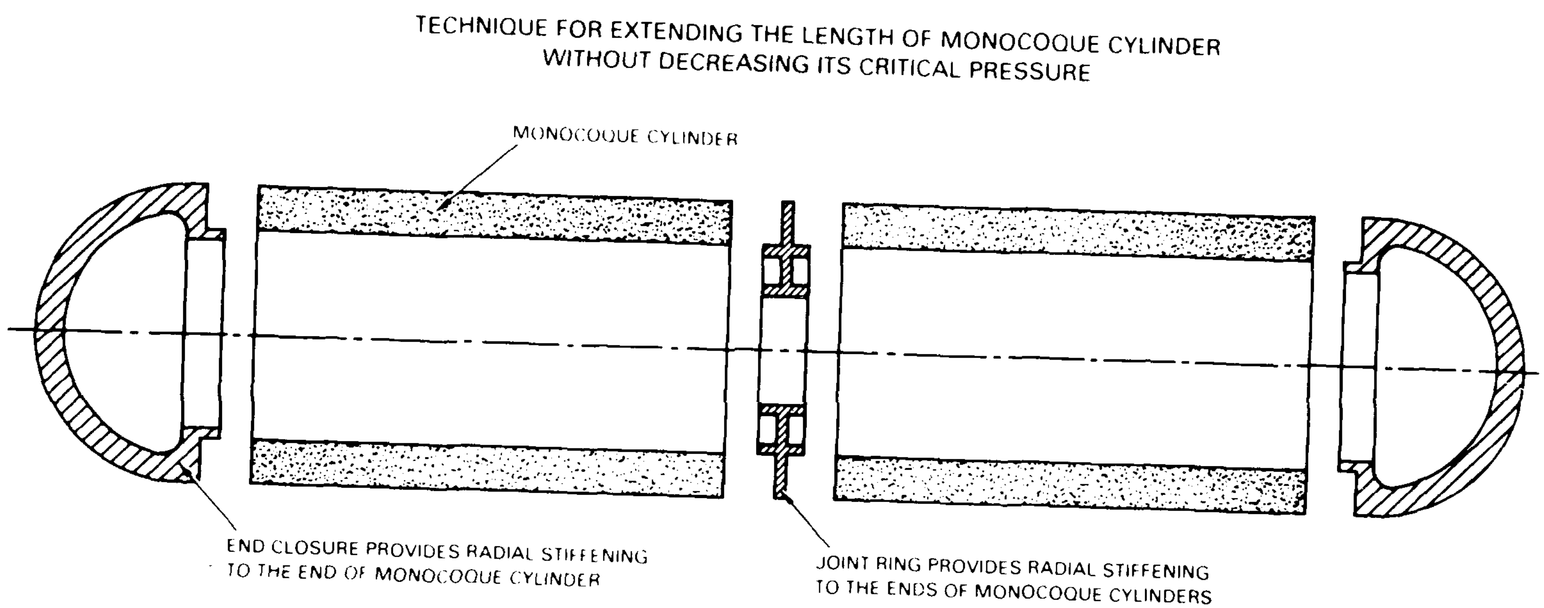

Figure 12. The length of a cylindrical pressure housing assembly consisting of a *single* monocoque cylinder supported radially at the ends by metallic end closures can be extended without decrease in critical pressure by adding more cylinders that are joined and radially supported at their ends by metallic joint rings.

Figure 13. Typical components of the 6-inch diameter scale model pressure housings used in this study.

Ceramic Pressure Hull Model 1

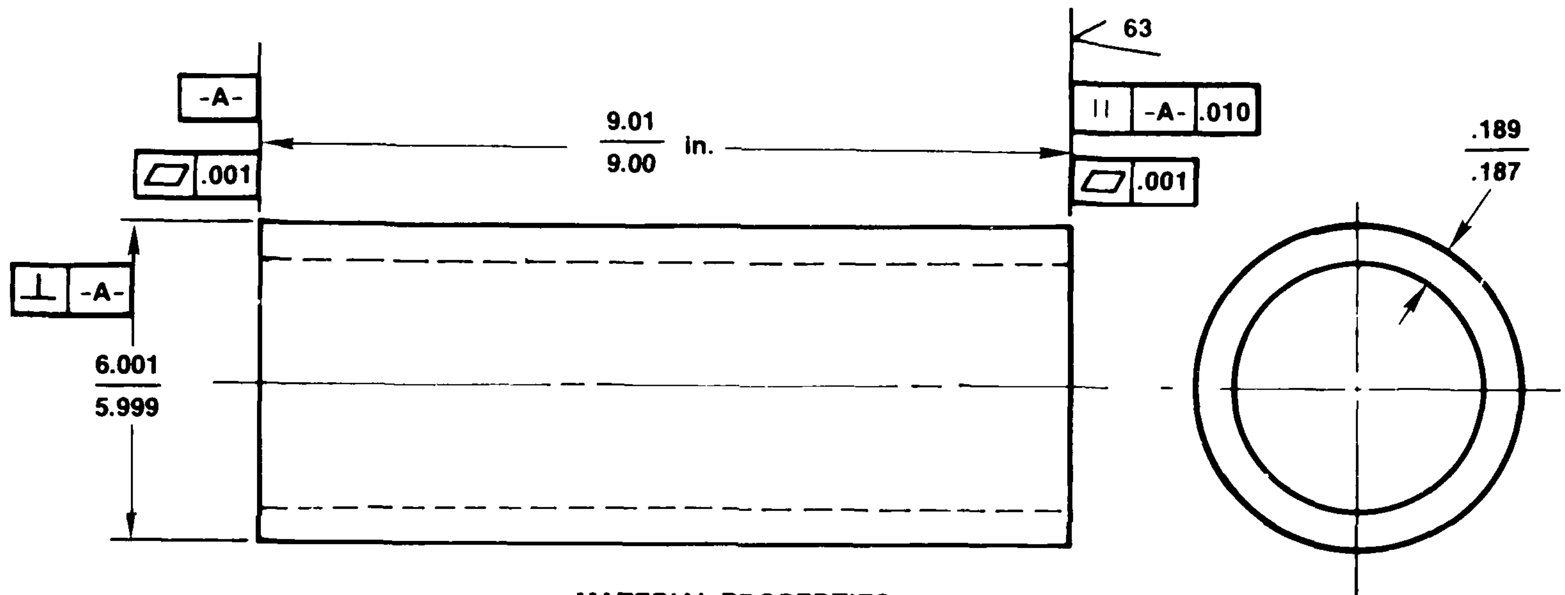

MATERIAL PROPERTIES

CERAMIC COMPOSITION	99.5% Al_2O_3
MODULUS OF ELASTICITY	54×10^6 psi
COMPRESSIVE STRENGTH	$>$ 300,000 psi
FLEXURAL STRENGTH	$>$ 50,000 psi
POISSON'S RATIO	0.22
SHEAR MODULUS	22×10^6
BULK MODULUS	33×10^6
SPECIFIC GRAVITY	3.89
COEFF OF THERMAL EXPANSION AT ROOM TEMP	2×10^{-6}/°F

Figure 14. Dimensions of ceramic cylinder Model 1 fabricated by Coor's Ceramics from AD 99.5 alumina compound. Weight of the cylinder with titanium end caps is 2,117 grams.

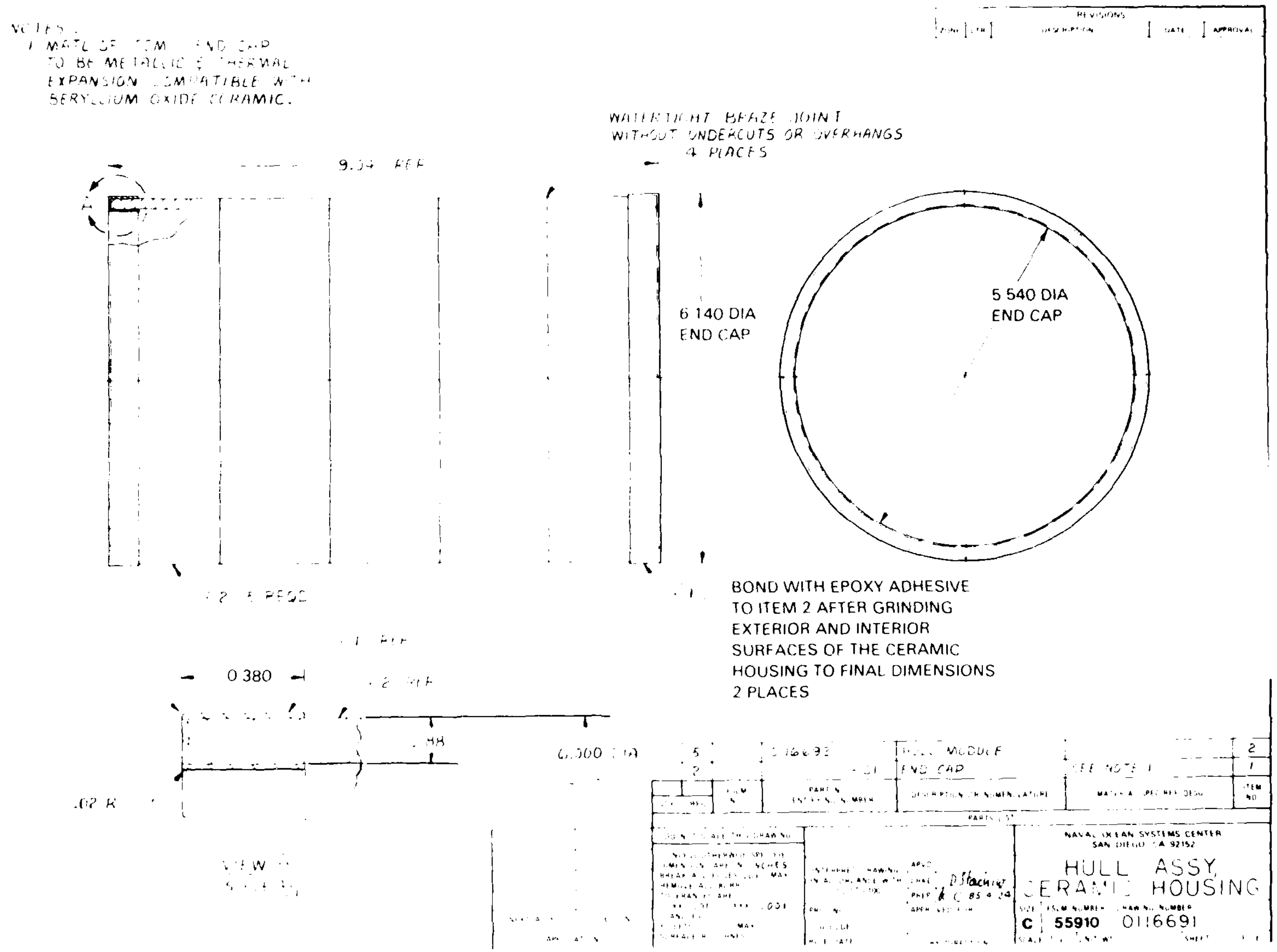

Figure 15. Polylithic (modular) approach to construction of the Model I ceramic cylinder by assembling it from five rings joined together by brazing with metallic solder

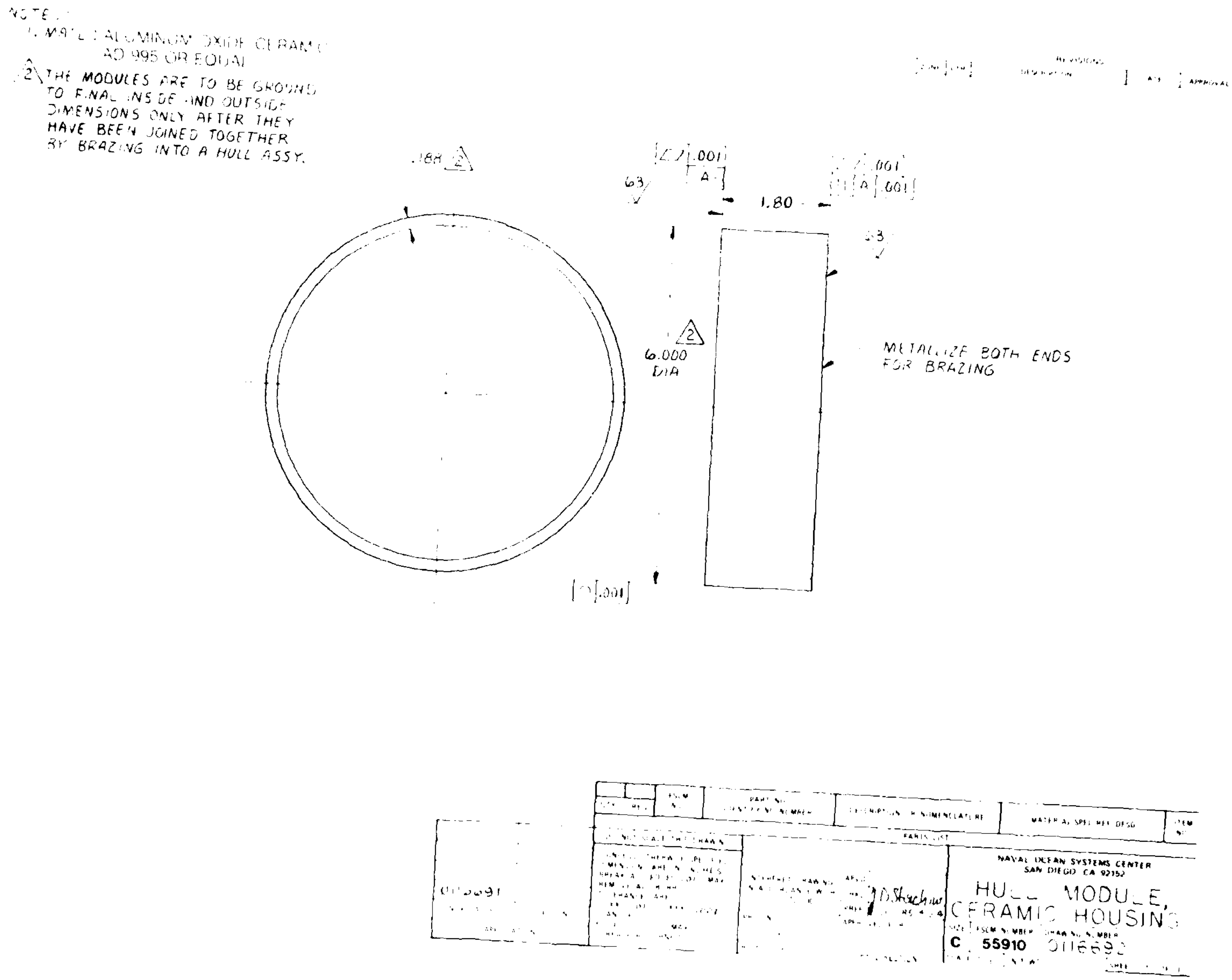

Figure 16. One of the ceramic rings used in the modular polylithic construction of the Model 1 cylinder.

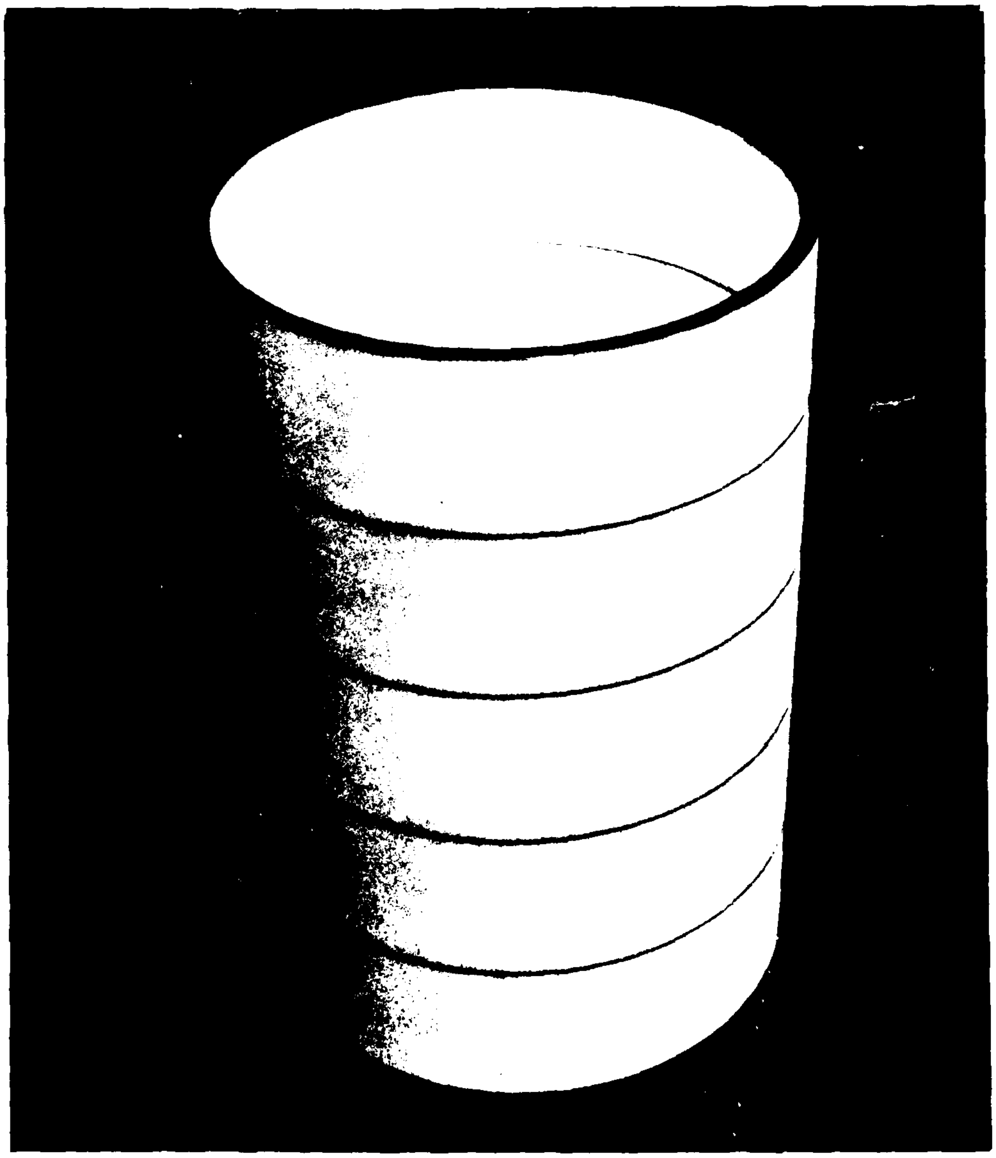

Figure 17. Model I cylinder of polylithic construction prior to the attachment of the metallic end caps.

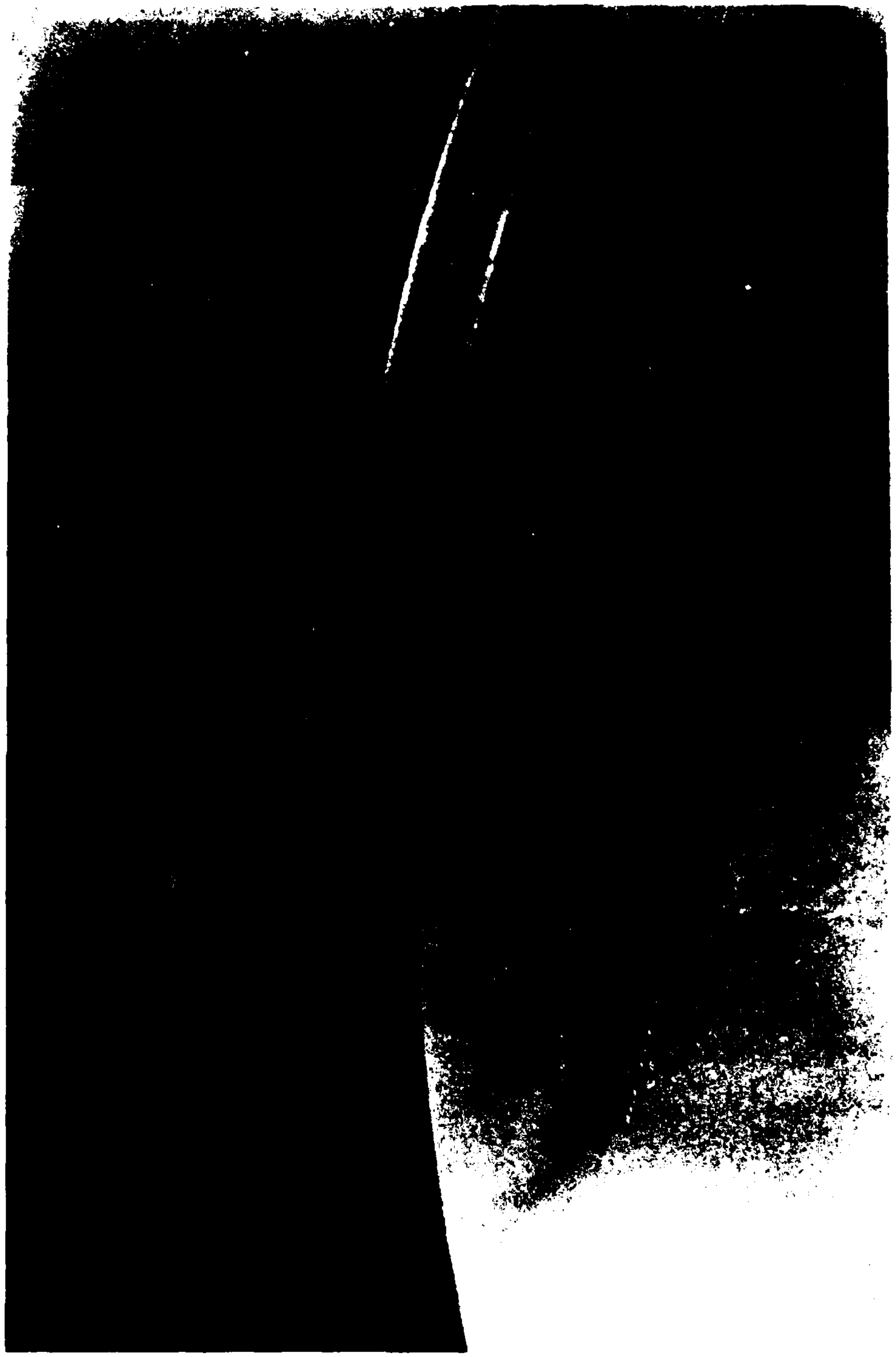

Figure 18. Closeup of the metal plated surface on the individual alumina ceramic ring.

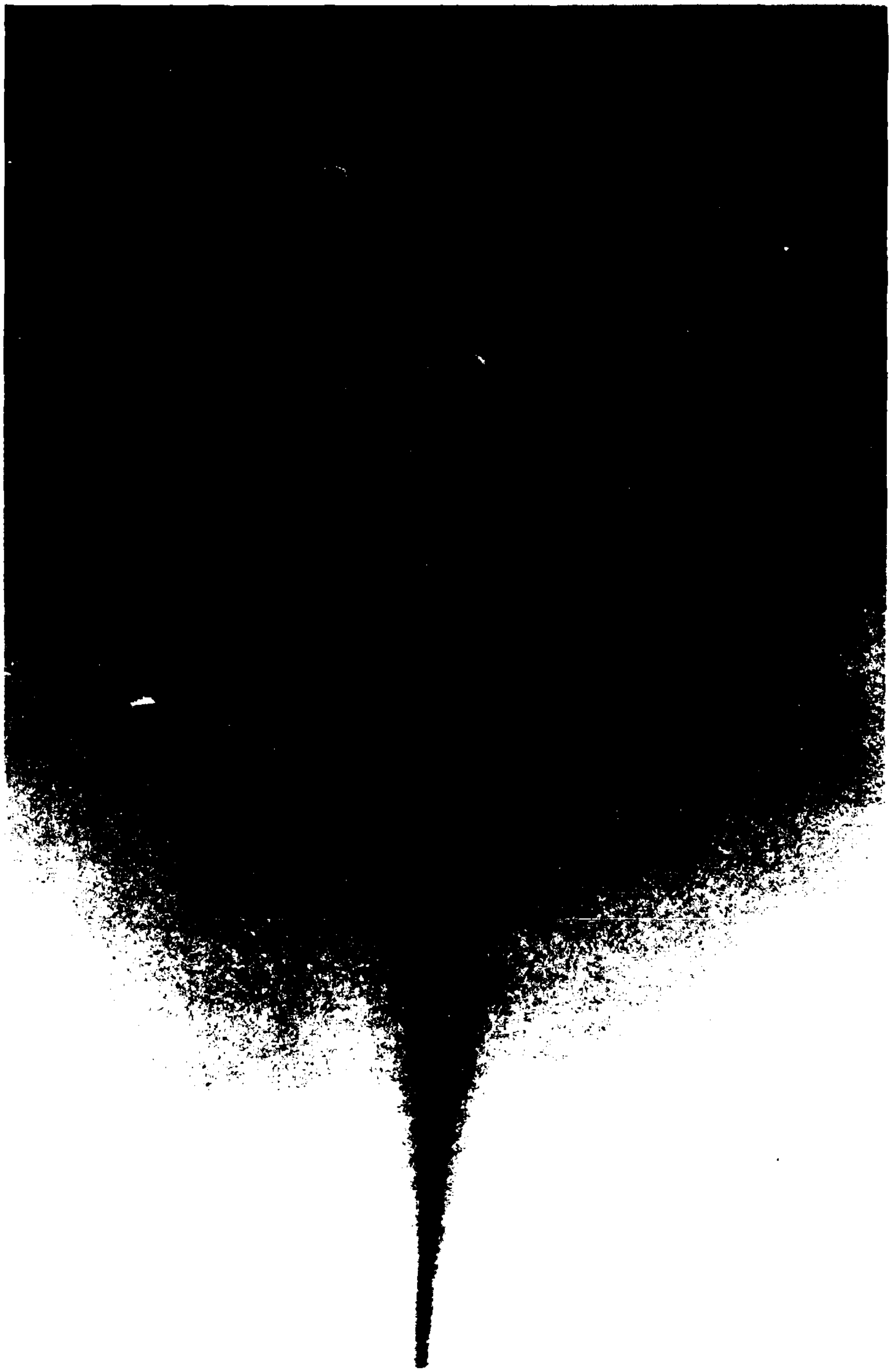

Figure 19. Closeup of the brazed joints between the individual ceramic rings.

Ceramic Pressure Hull Model 2

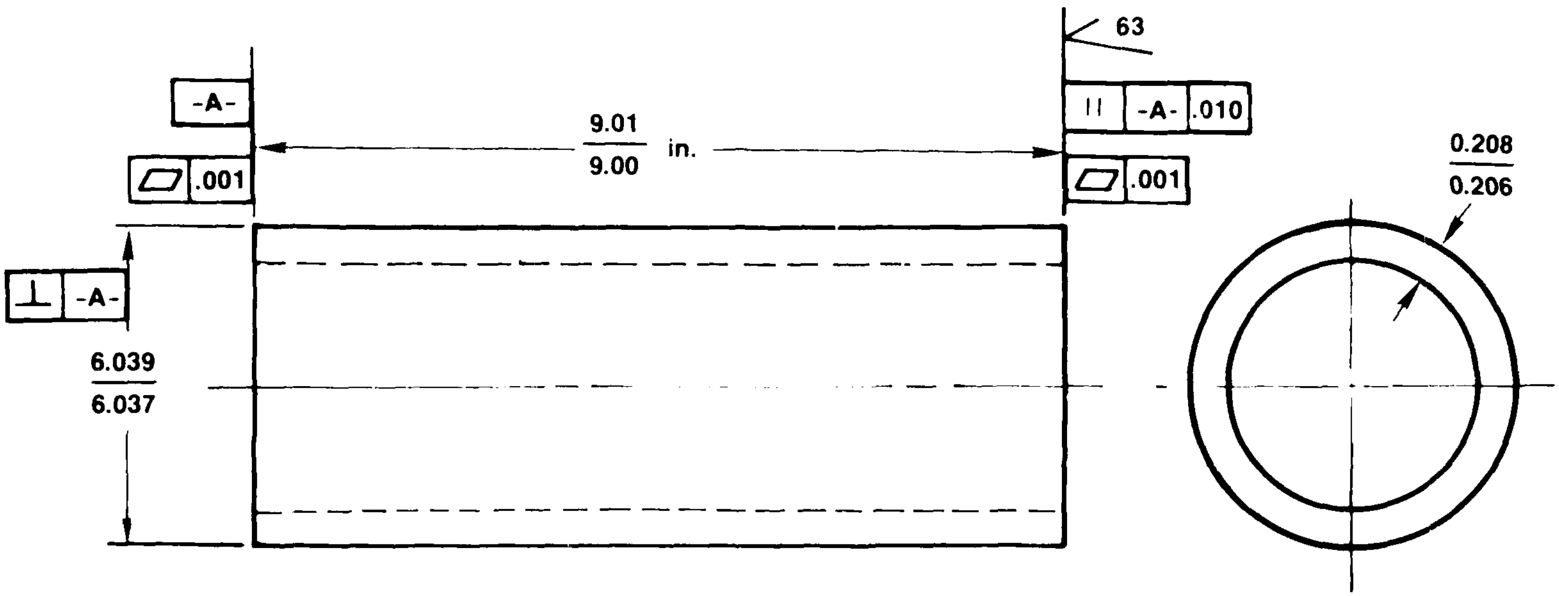

MATERIAL REQUIREMENTS:

CERAMIC COMPOSITION	94% Al_2O_3
MODULUS OF ELASTICITY	41×10^6 psi
COMPRESSIVE STRENGTH	≥ 300,000 psi
FLEXURAL STRENGTH	≥ 50,000 psi
POISSON'S RATIO	0.21
SHEAR MODULUS	17×10^6
BULK MODULUS	24×10^6
SPECIFIC GRAVITY	3.62
COEFF OF THERMAL EXPANSION AT ROOM TEMP	2×10^{-6}/°F

Figure 20. Dimensions of ceramic cylinder Model 2 fabricated by Coor's Ceramics from AD 94 alumina compound. Weight of the cylinder with titanium end caps is 2,176 grams.

Ceramic Pressure Hull Models 1 & 2
Titanium End Closure

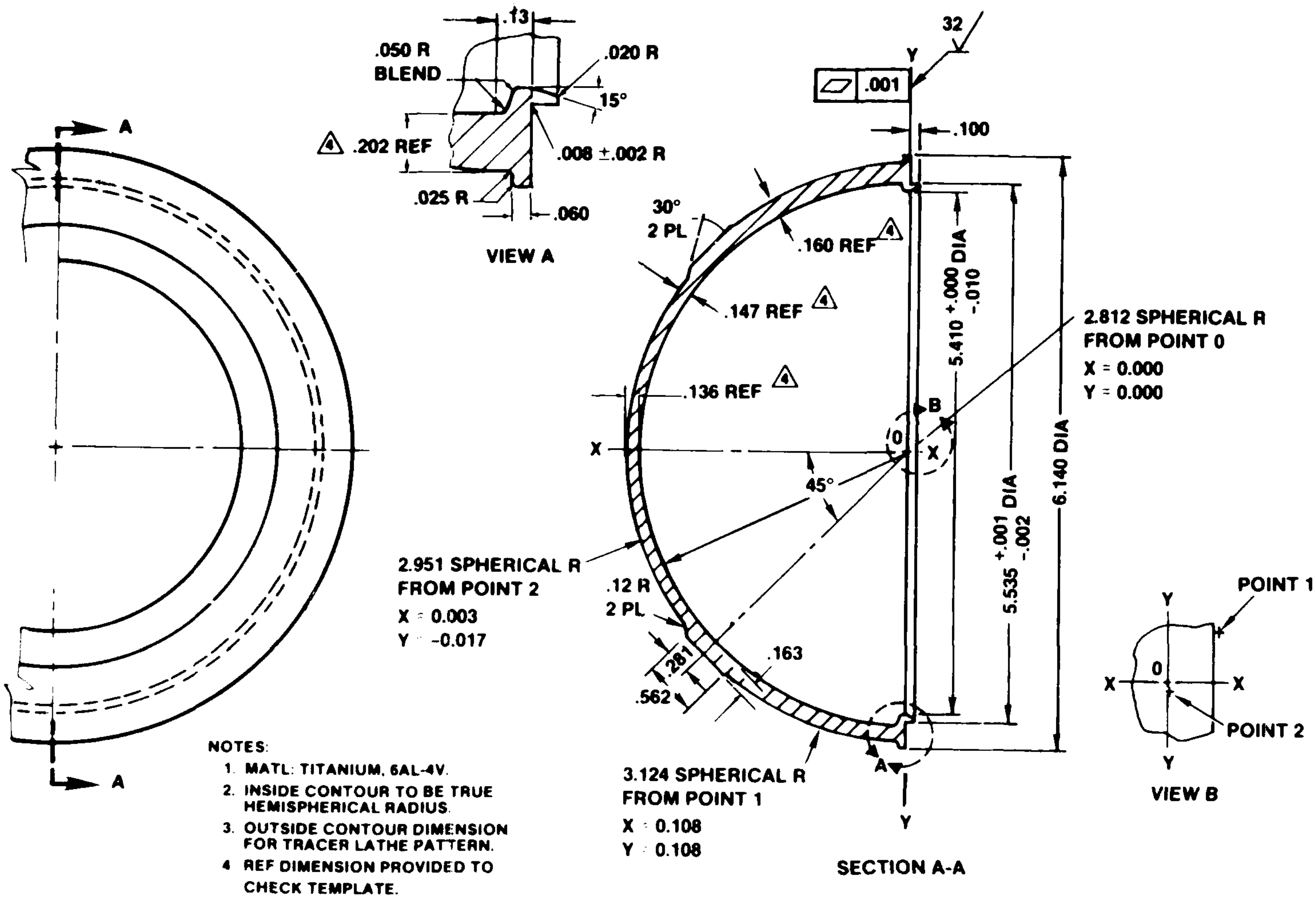

Figure 21. Dimensions of metallic end closures that provide radial support to cylinders Model 1 or Model 2. The weight of the individual end closures is 673 grams.

Figure 22. Interior view of end closure machined from Ti-6Al-4V alloy. Several of the end closures had penetrations machined in them to receive bulkhead penetrators for the instrumentation cables.

Figure 23. Exterior view of the end closure

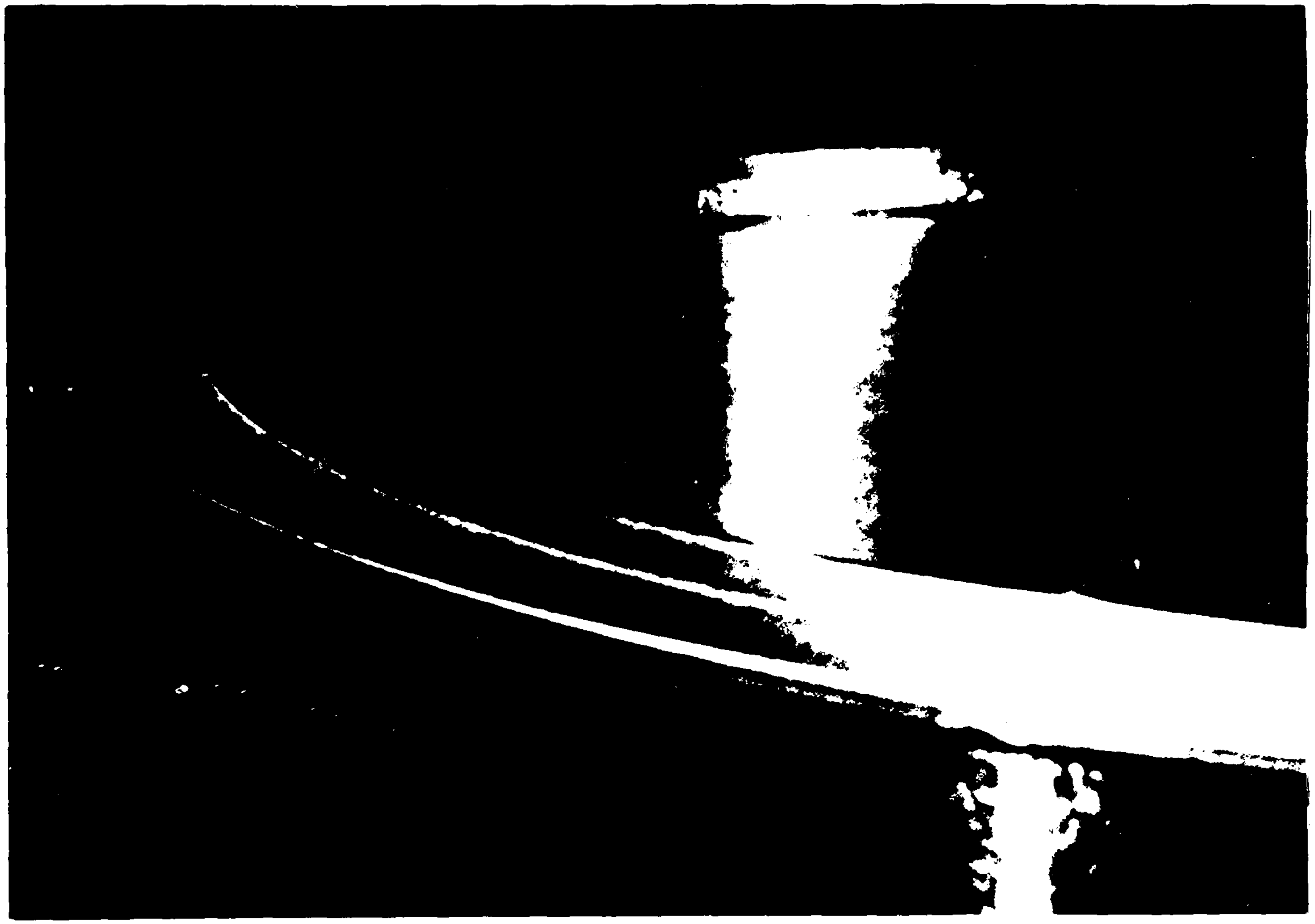

Figure 24. Closeup of the lip on the end closure's equatorial flange that provides *radial* support to the ceramic cylinder.

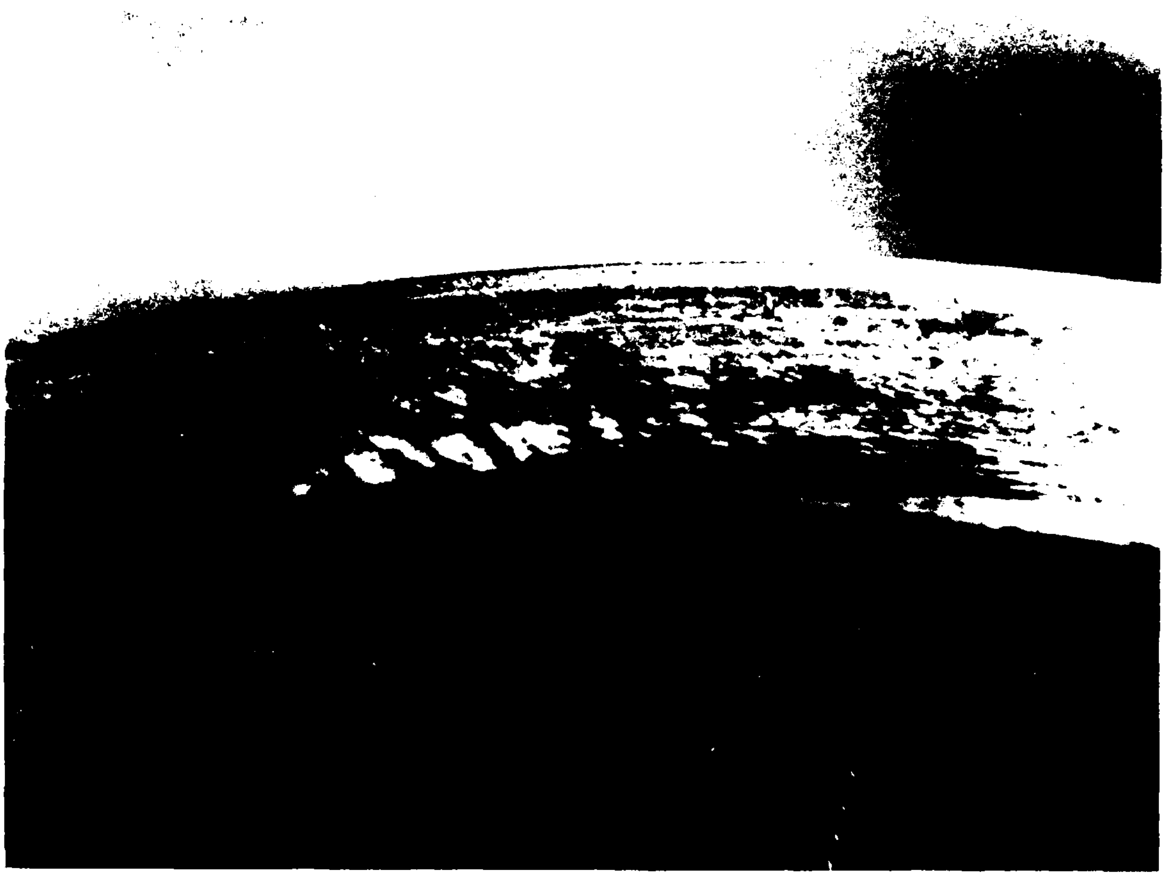

Figure 25. Closeup of the plane bearing surface on the end closure's equatorial flange that provides *axial* support to the ceramic cylinder. Note the scuff marks produced during hydrostatic loading by differential radial movement between the end closure and the metallic cap bonded to the ceramic cylinder.

Figure 26. Circular, U-shaped end cap, machined from Ti-6Al-4V alloy, interior view.

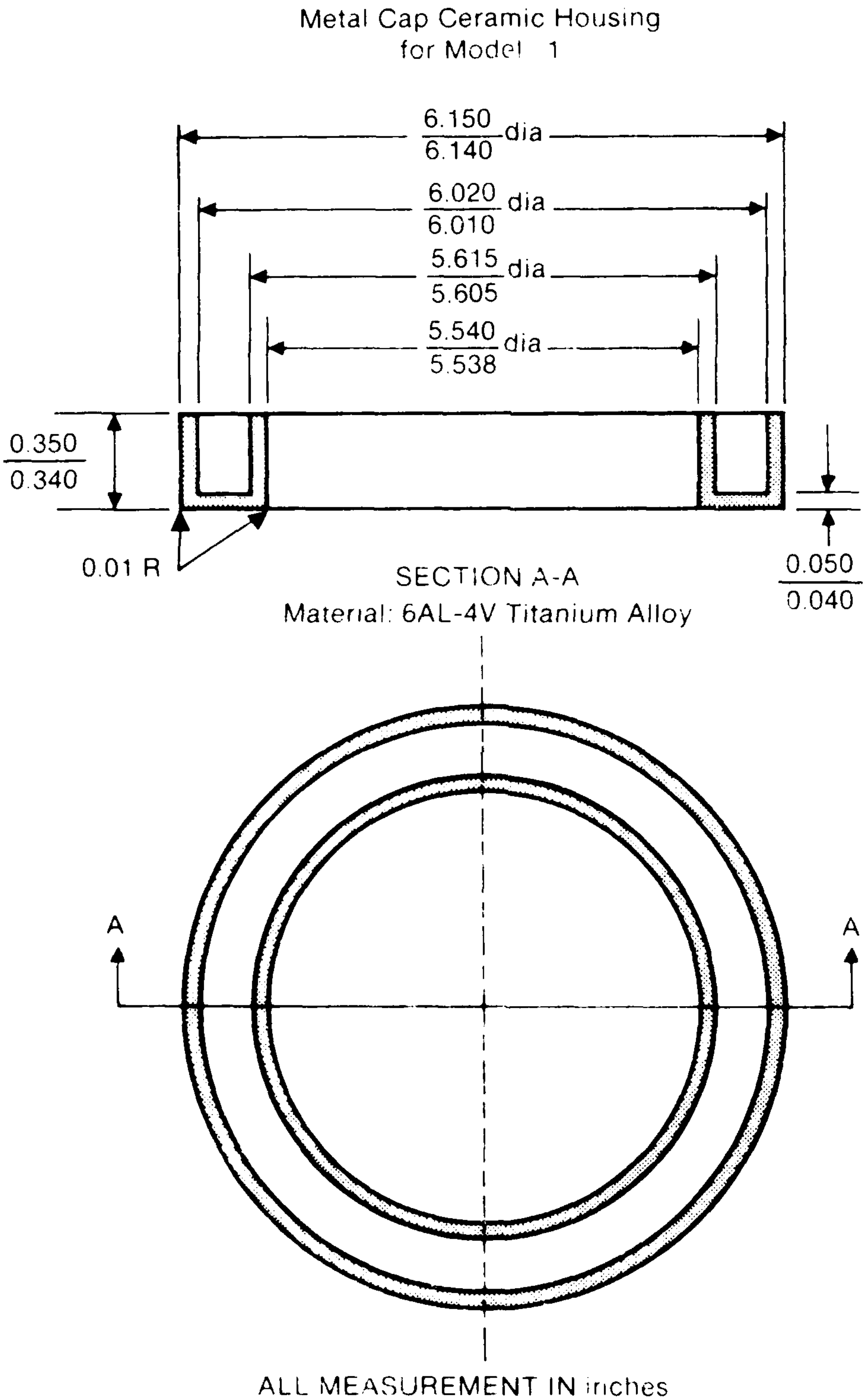

Figure [illegible]. Dimensions of the end cap for the Model 1 ceramic cylinder.

Metal Cap Ceramic Housing
for Model 2

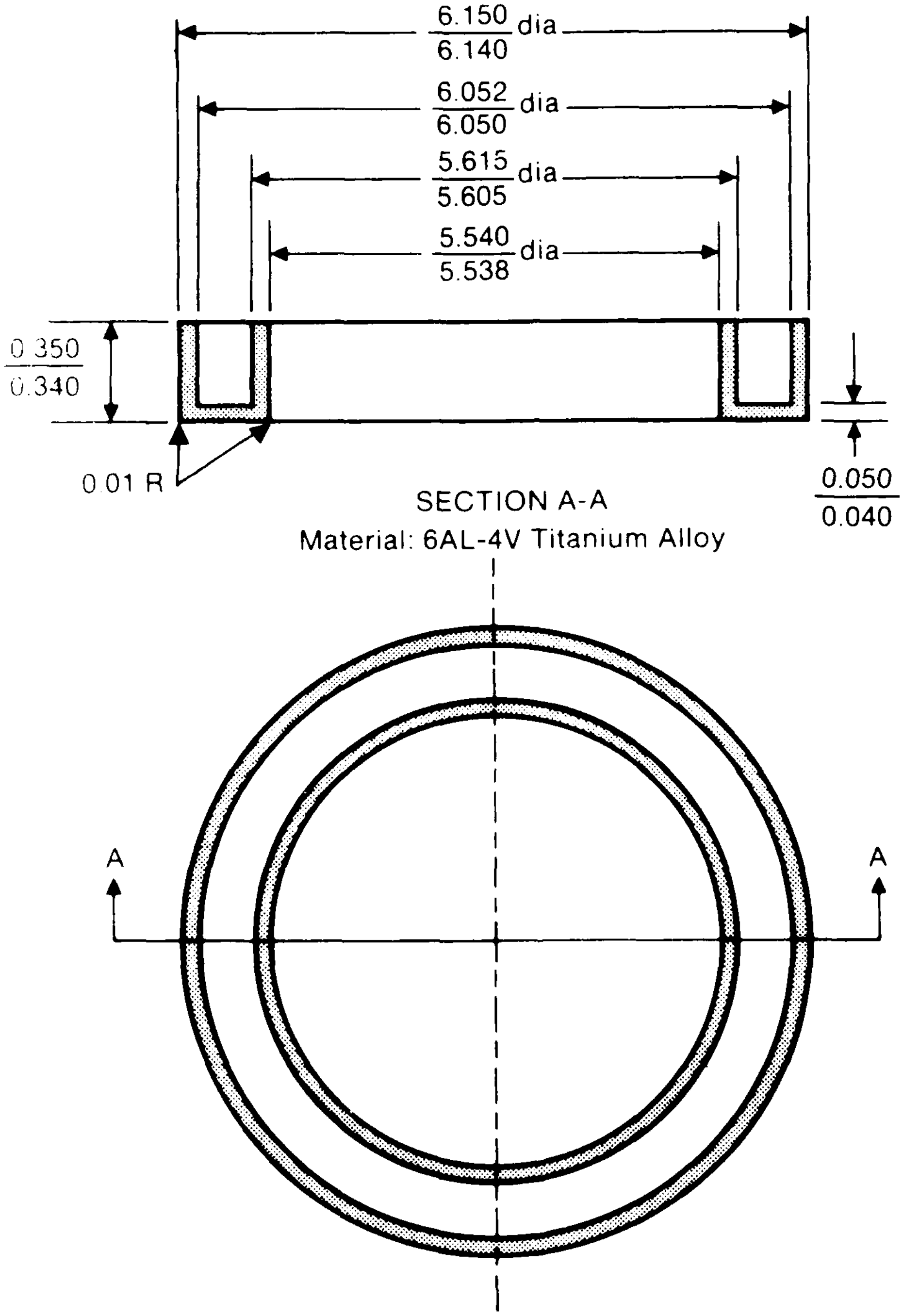

Figure 28. Dimensions of the end cap for the Model 2 ceramic cylinder.

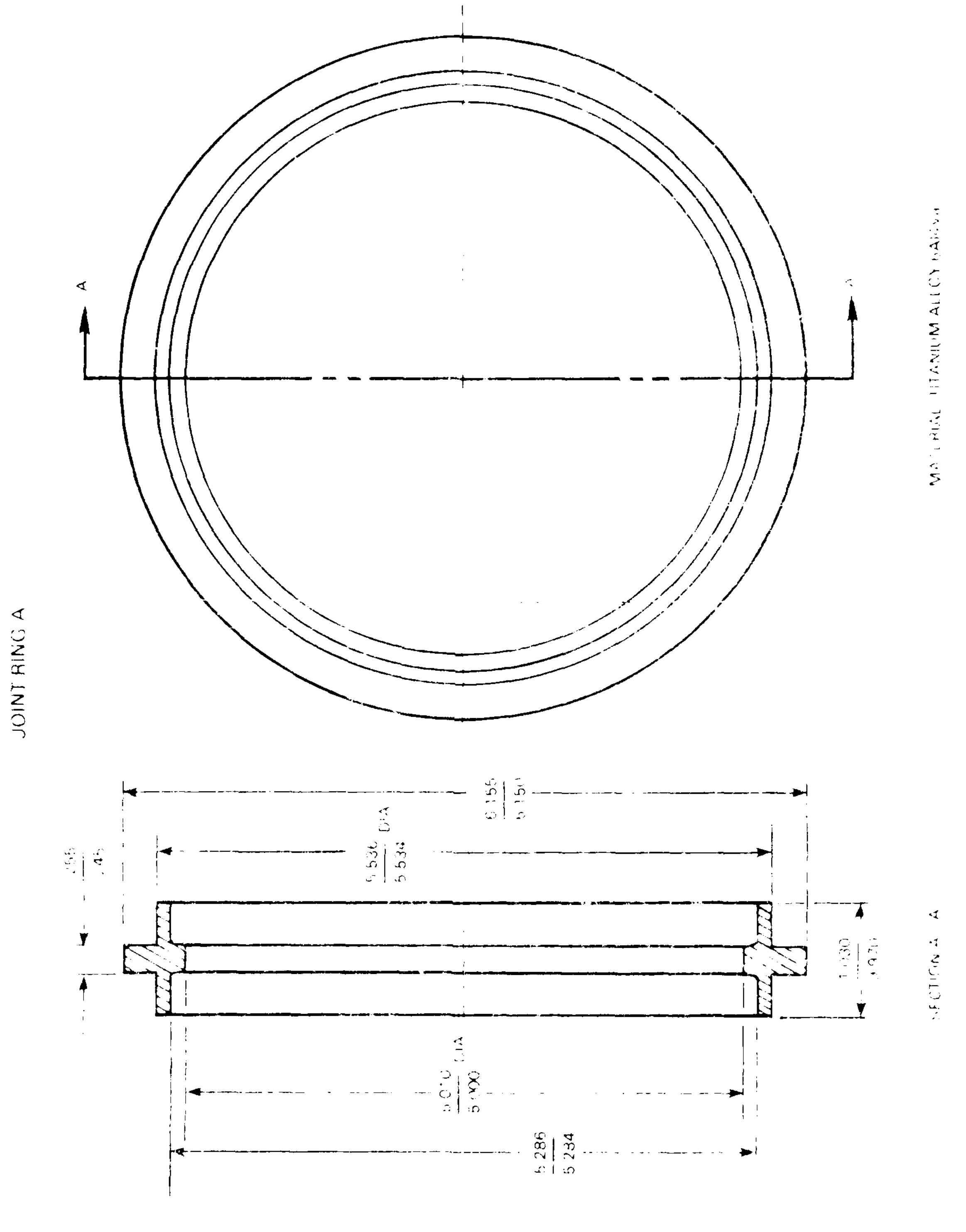

Figure 29 – Dimensions of joint ring A for Model 1 and Model 2 ceramic cylinders. Joint ring A weighs 306 grams

CYLINDER JOINT ASSEMBLY: JOINT RING A

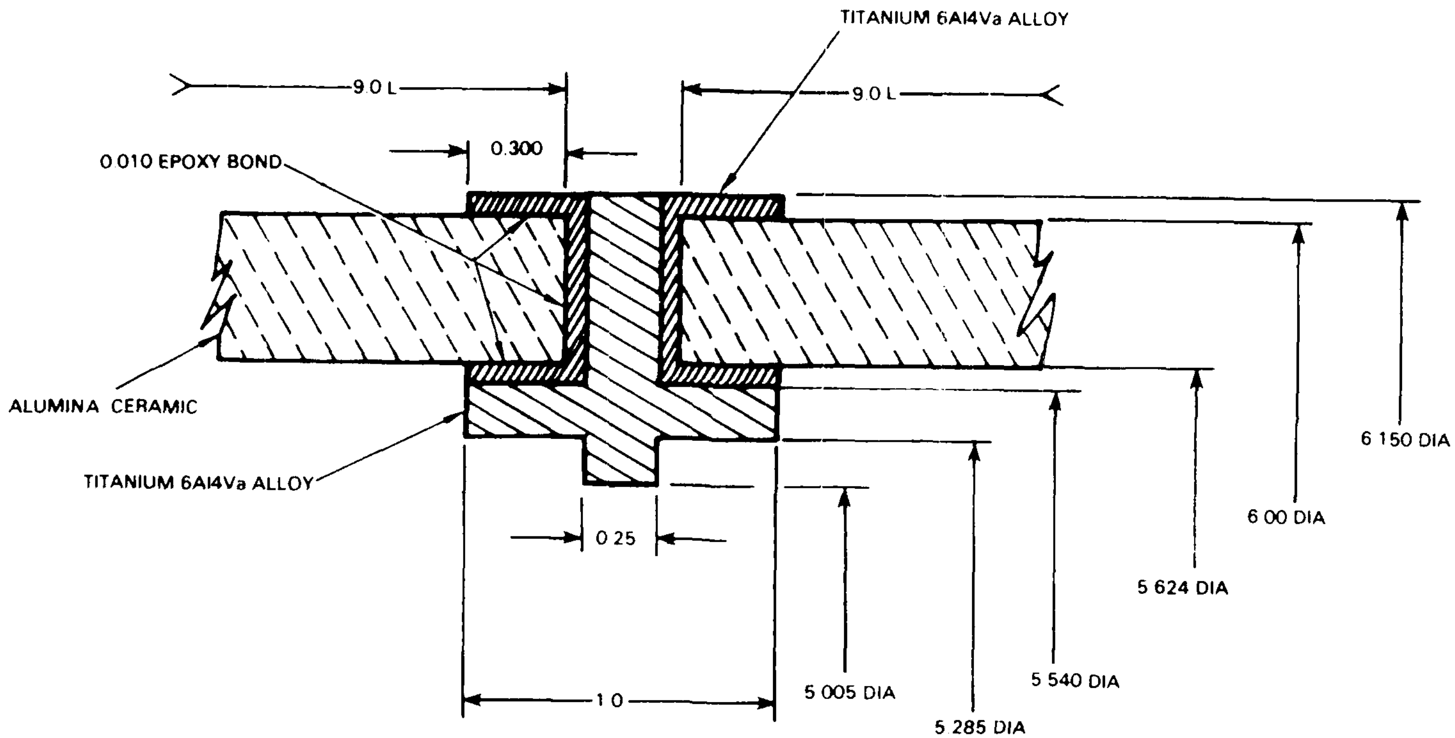

Figure 30. Two Model 1 cylinders joined by joint ring A. The joint ring A is calculated to fail under 7,700 psi external pressure when incorporated into a housing assembly made up of *only two* Model 1 or Model 2 ceramic cylinders and Figure 21 end closures. The same joint rings will fail under only 4,900 psi when incorporated into a housing assembly made up of *six, or more,* ceramic cylinders and Figure 21 end closures.

JOINT RING B

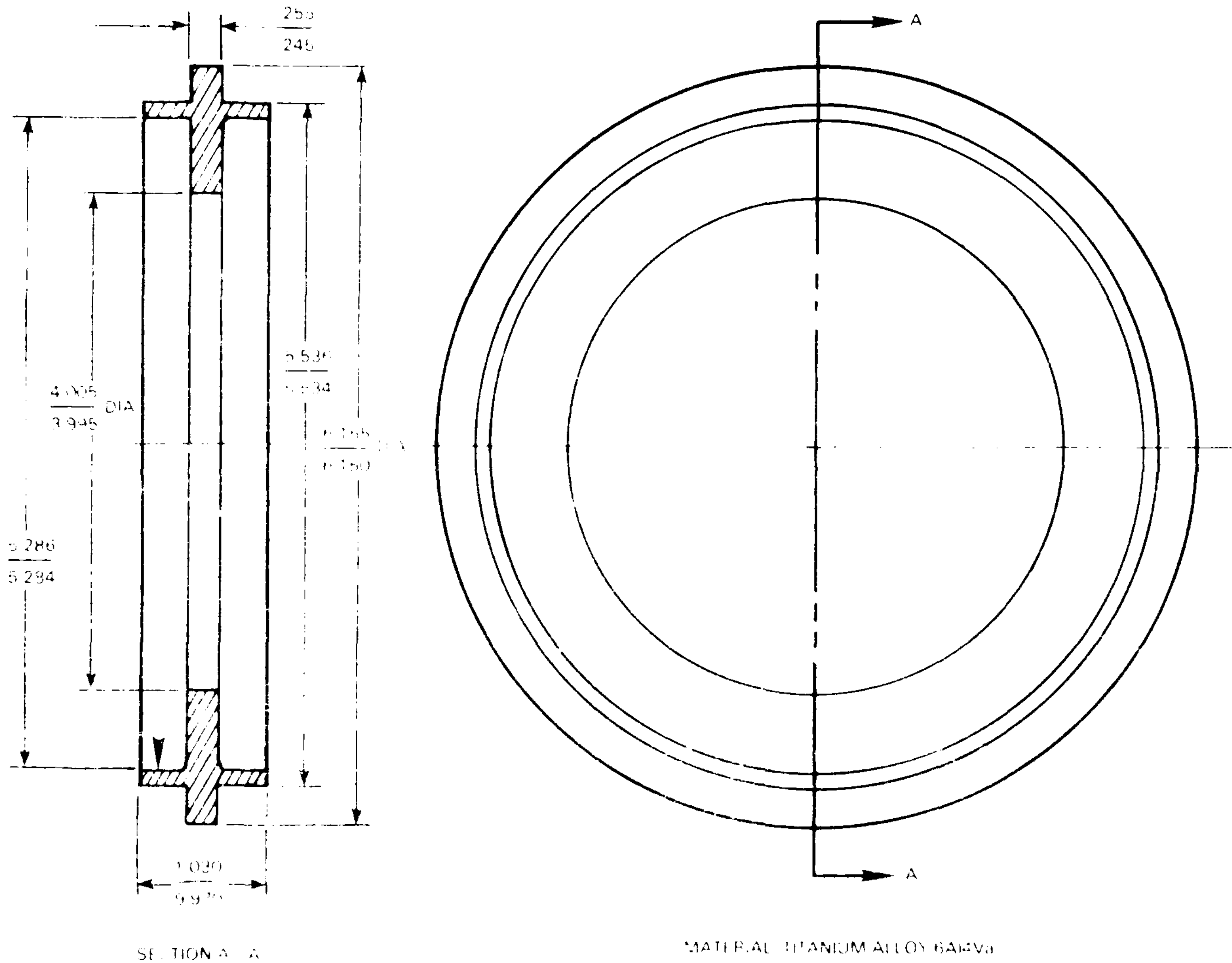

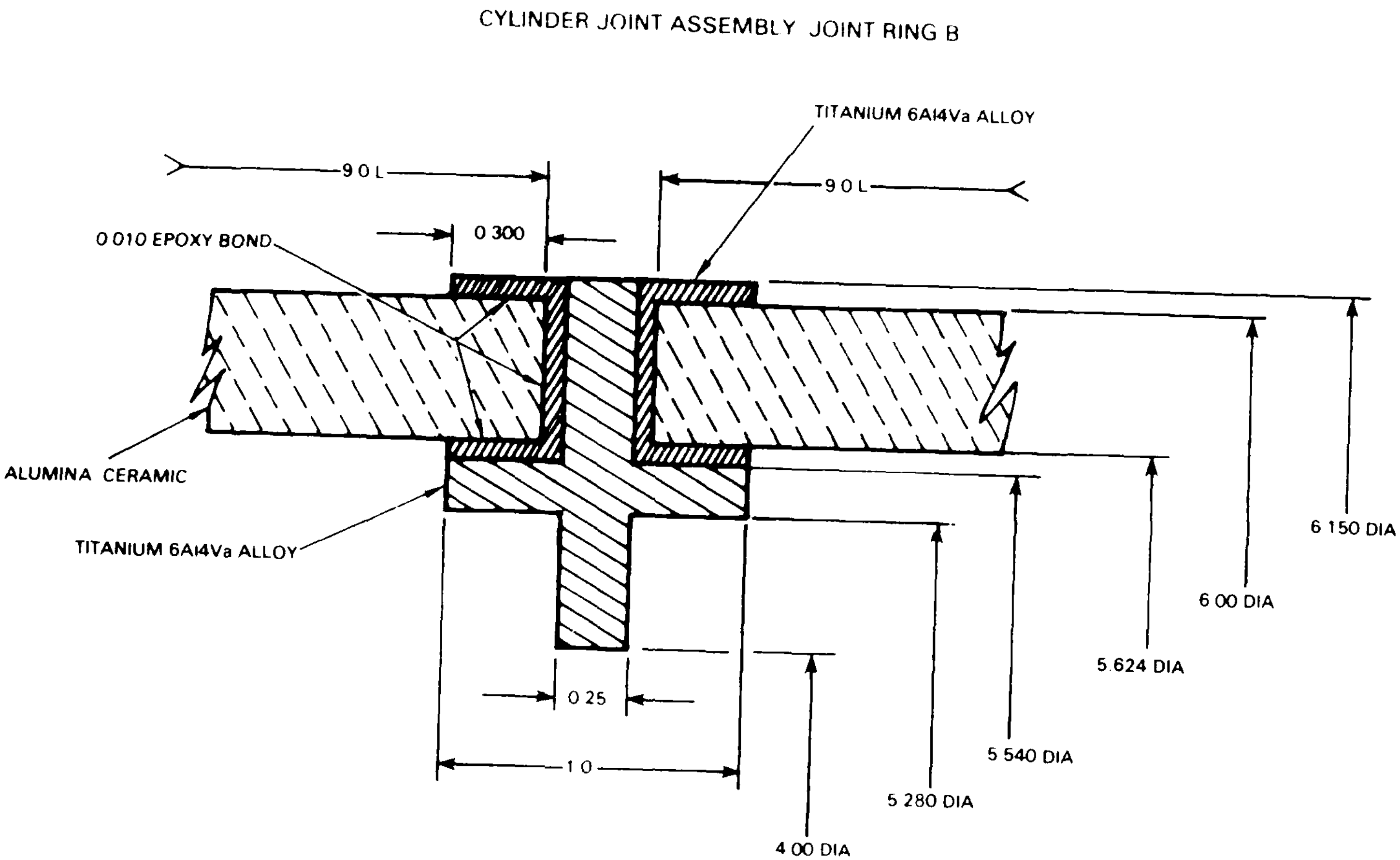

Figure 32. Two Model 1 cylinders joined by joint ring B. Joint ring B is calculated to fail under 10,500 psi external pressure when incorporated into a housing assembly made up of six, or more, Model 1 or Model 2 ceramic cylinders and Figure 21 end closures.

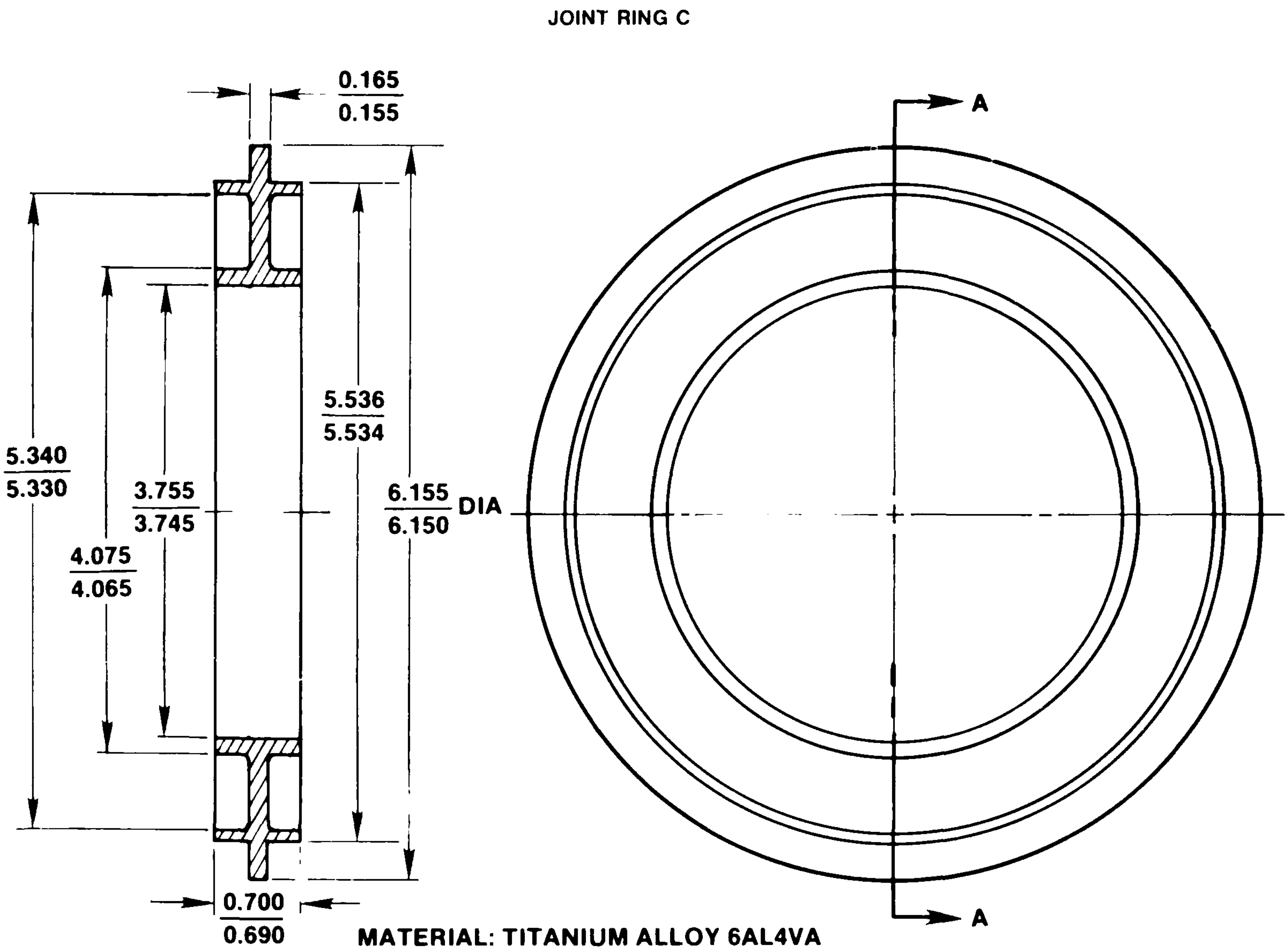

Figure 33. Joint ring C for Model 1 and Model 2 ceramic cylinders. The weight of joint ring C is 359 grams.

CYLINDER JOINT ASSEMBLY JOINT RING C

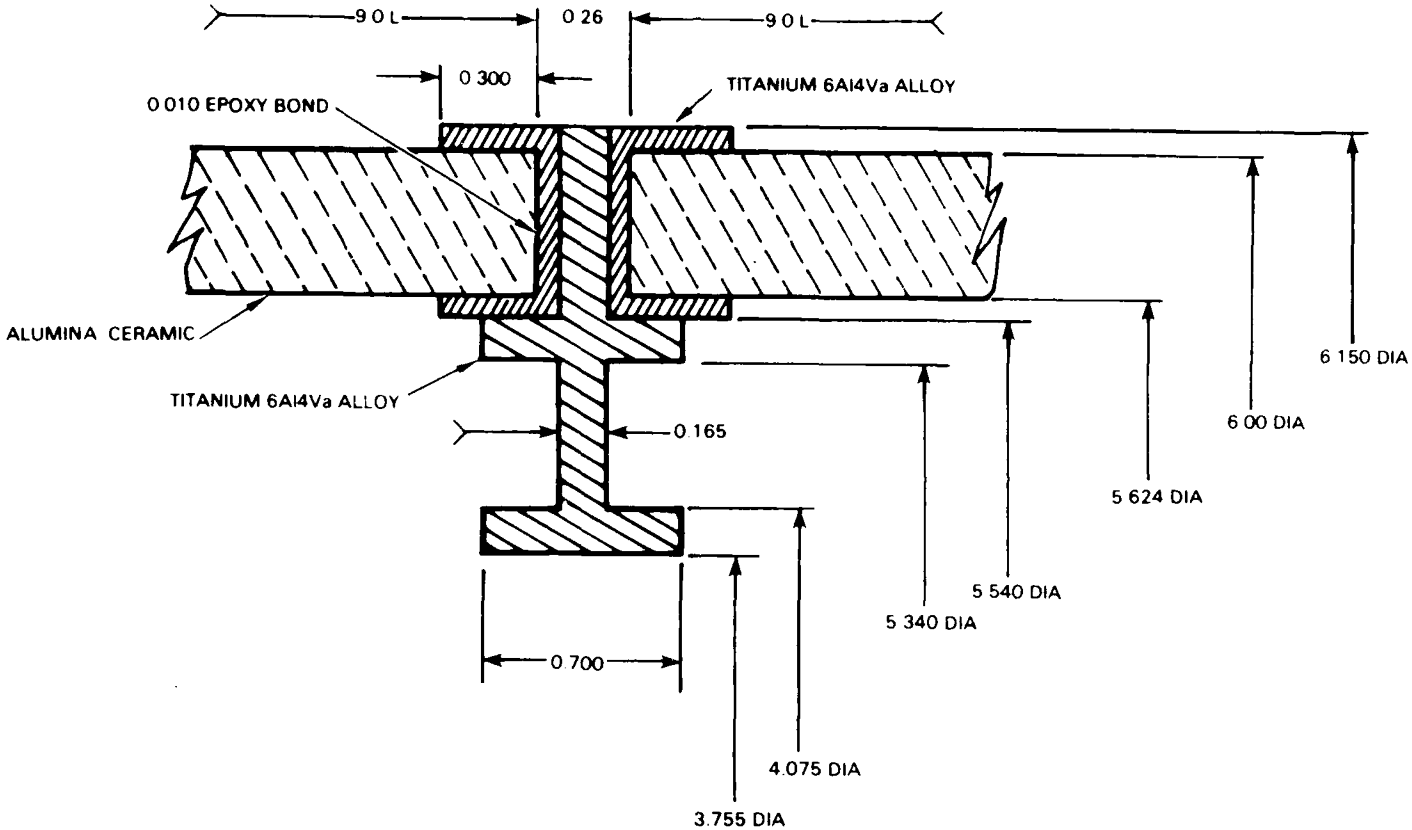

Figure 34. Two Model 1 cylinders joined by joint ring C. This joint ring will fail under 12,500 psi external pressure when incorporated into a housing assembly made up of six, or more, Model 1 or Model 2 cylinders and Figure 21 end closures. The critical pressure of joint ring C matches the critical pressure of the end closures.

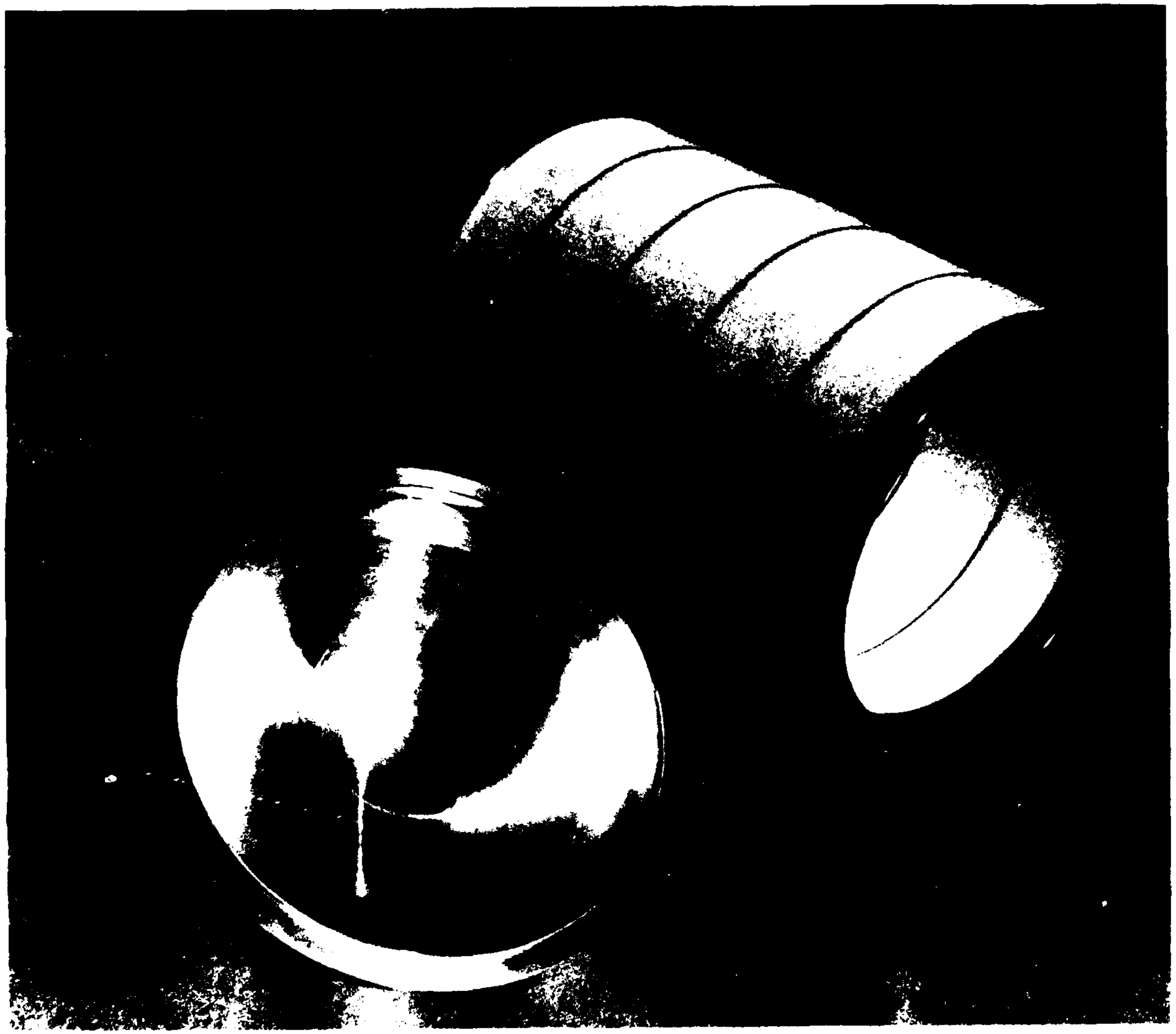

Figure 35. Components of Test Assembly I: one *polylithic Model I* cylinder with end caps and two end closures.

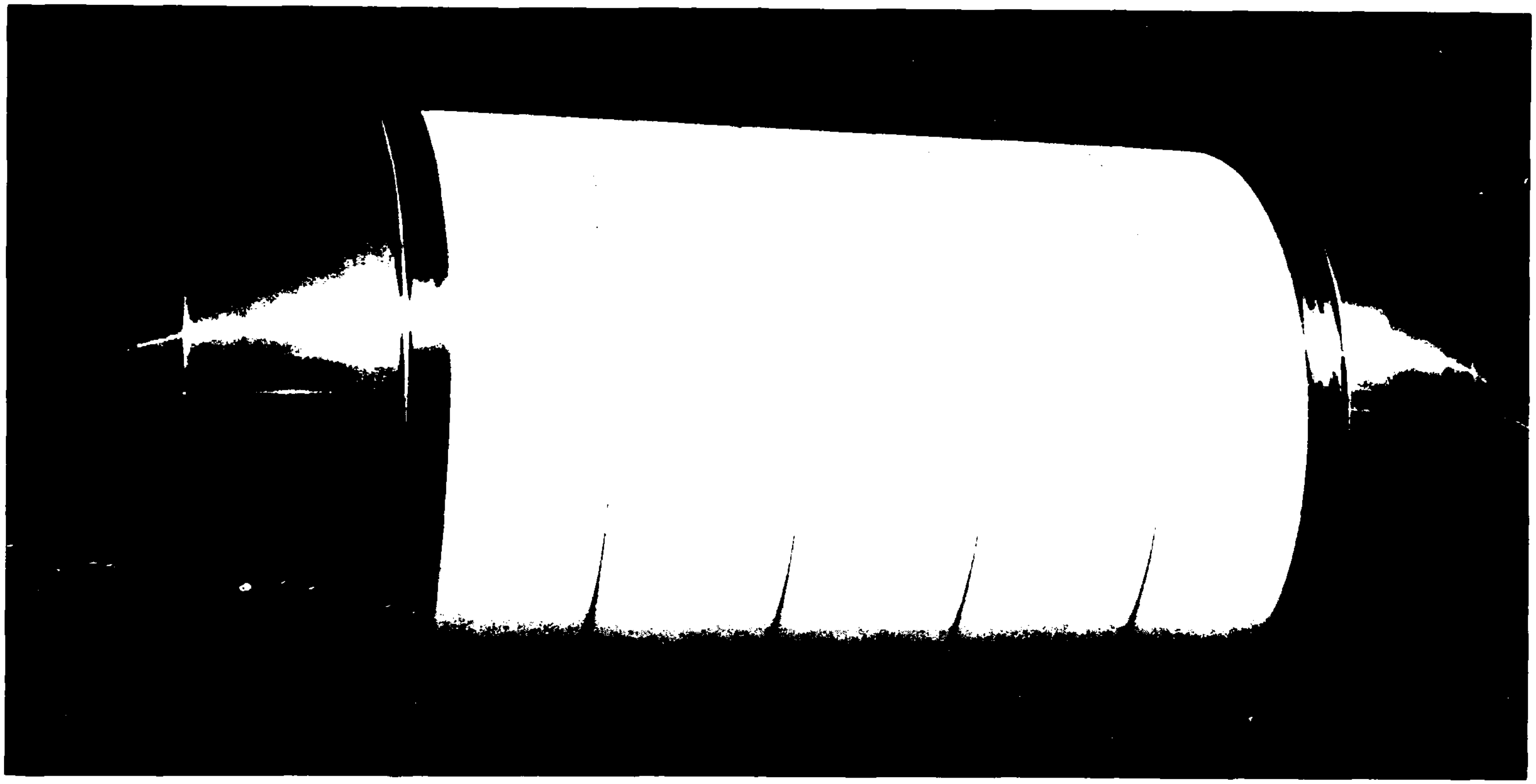

Figure 36. Test Assembly I with end closures in place.

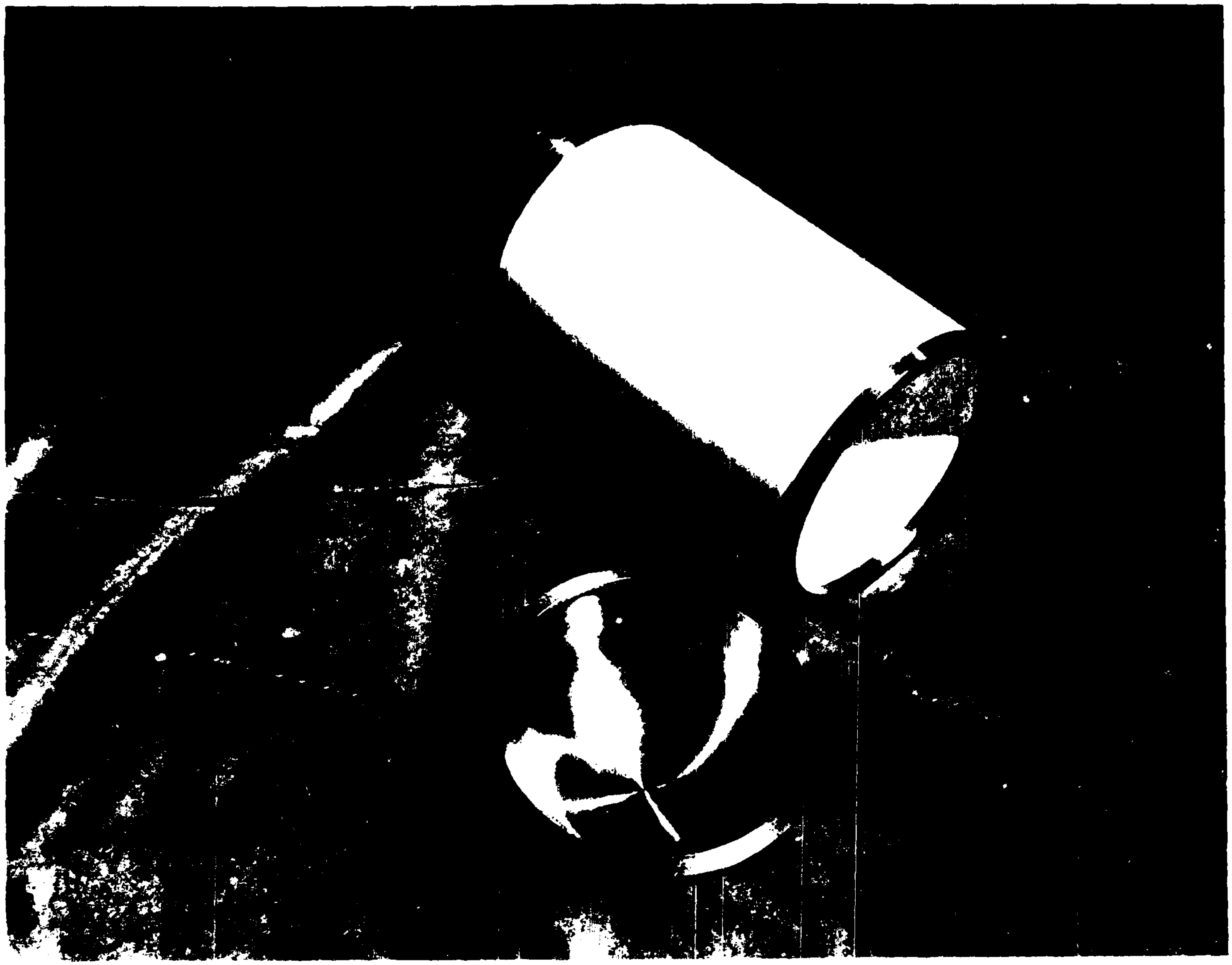

Figure 37. Components of Test Assembly II: one *monolithic Model I* cylinder with end caps and two end closures

Figure 38 Test Assembly II with end closures in place.

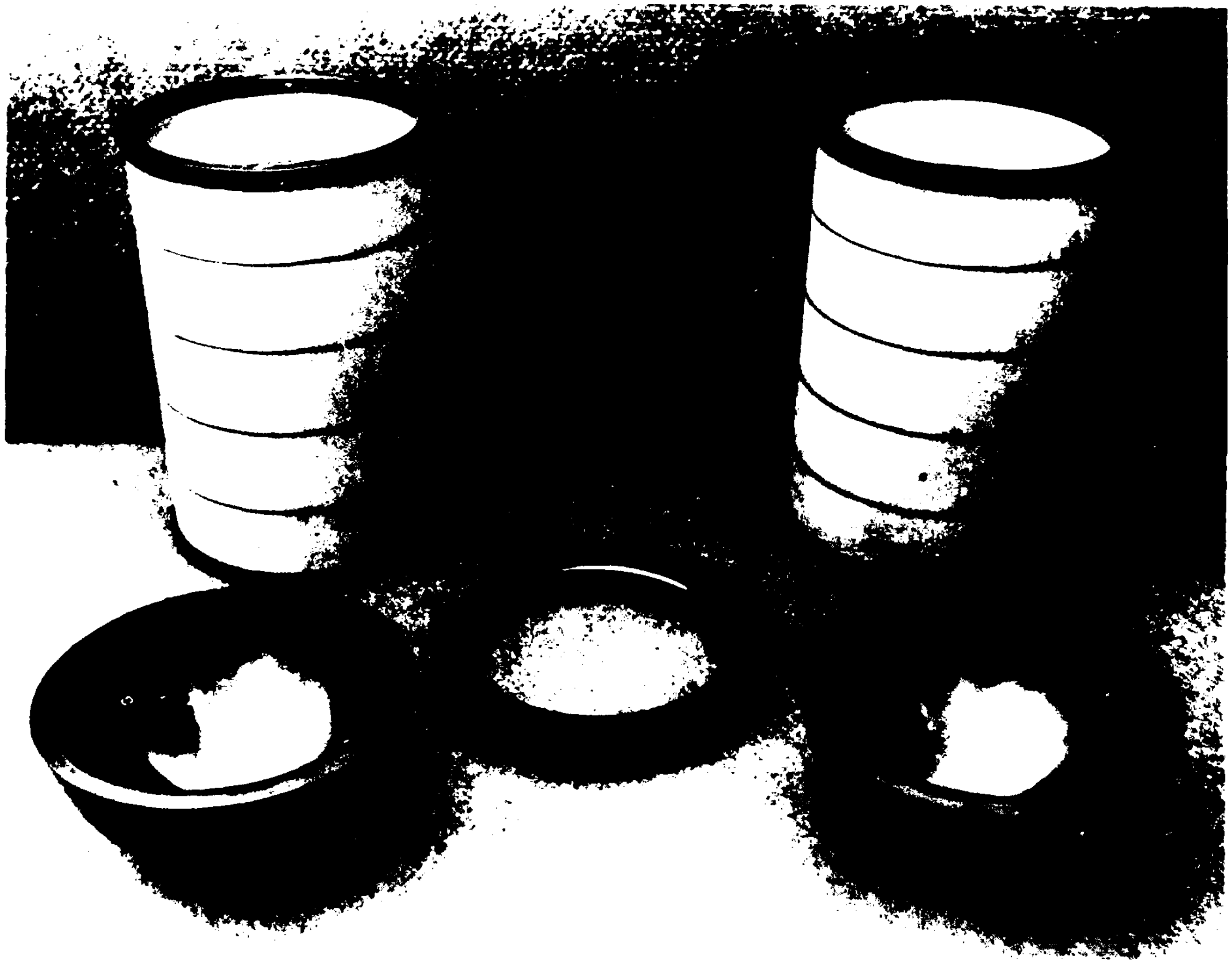

Figure 39. Components of Test Assembly III: two *polylithic* Model 1 cylinders with end caps, one joint ring A, and two end closures.

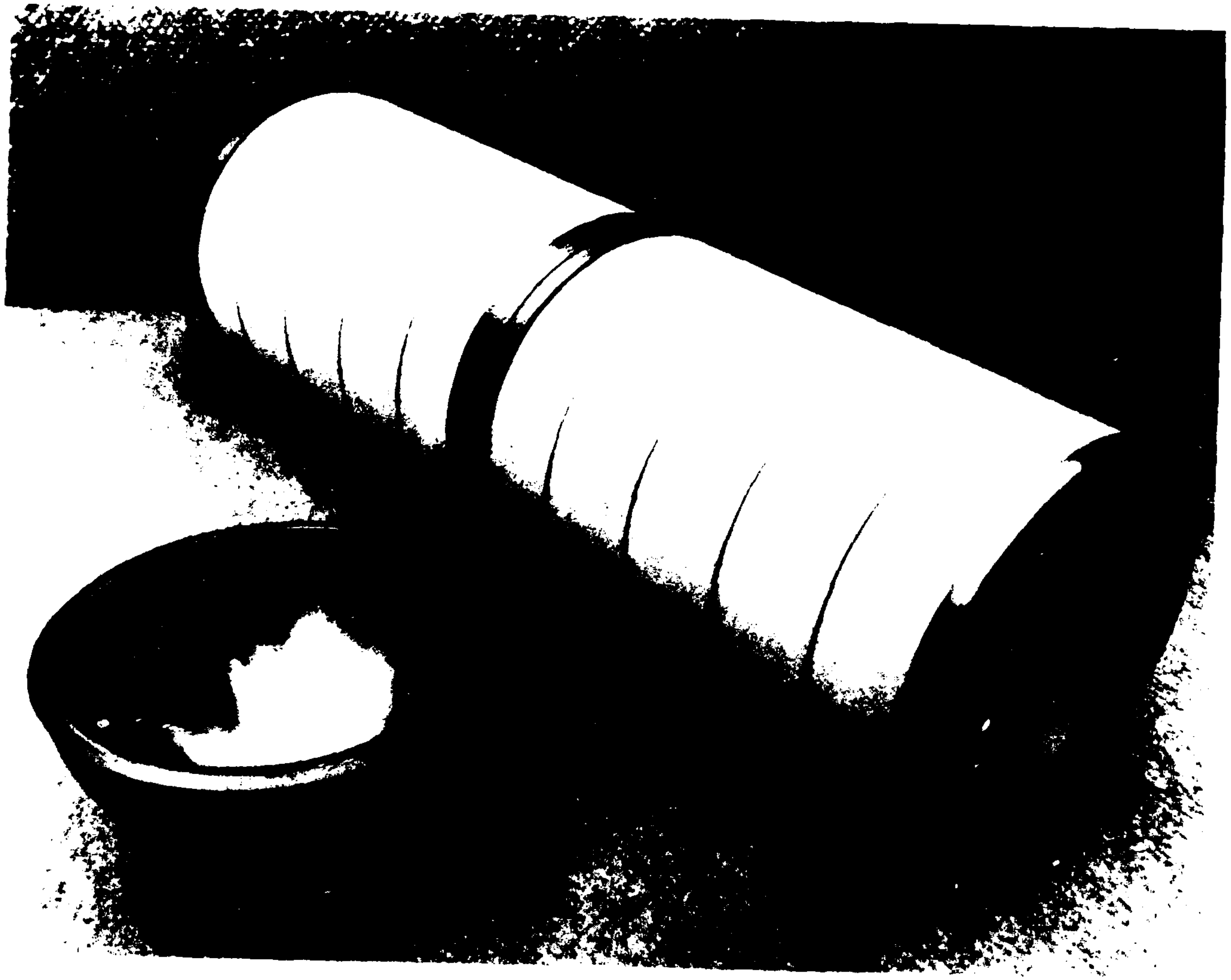

Figure 40. Test Assembly III partially assembled.

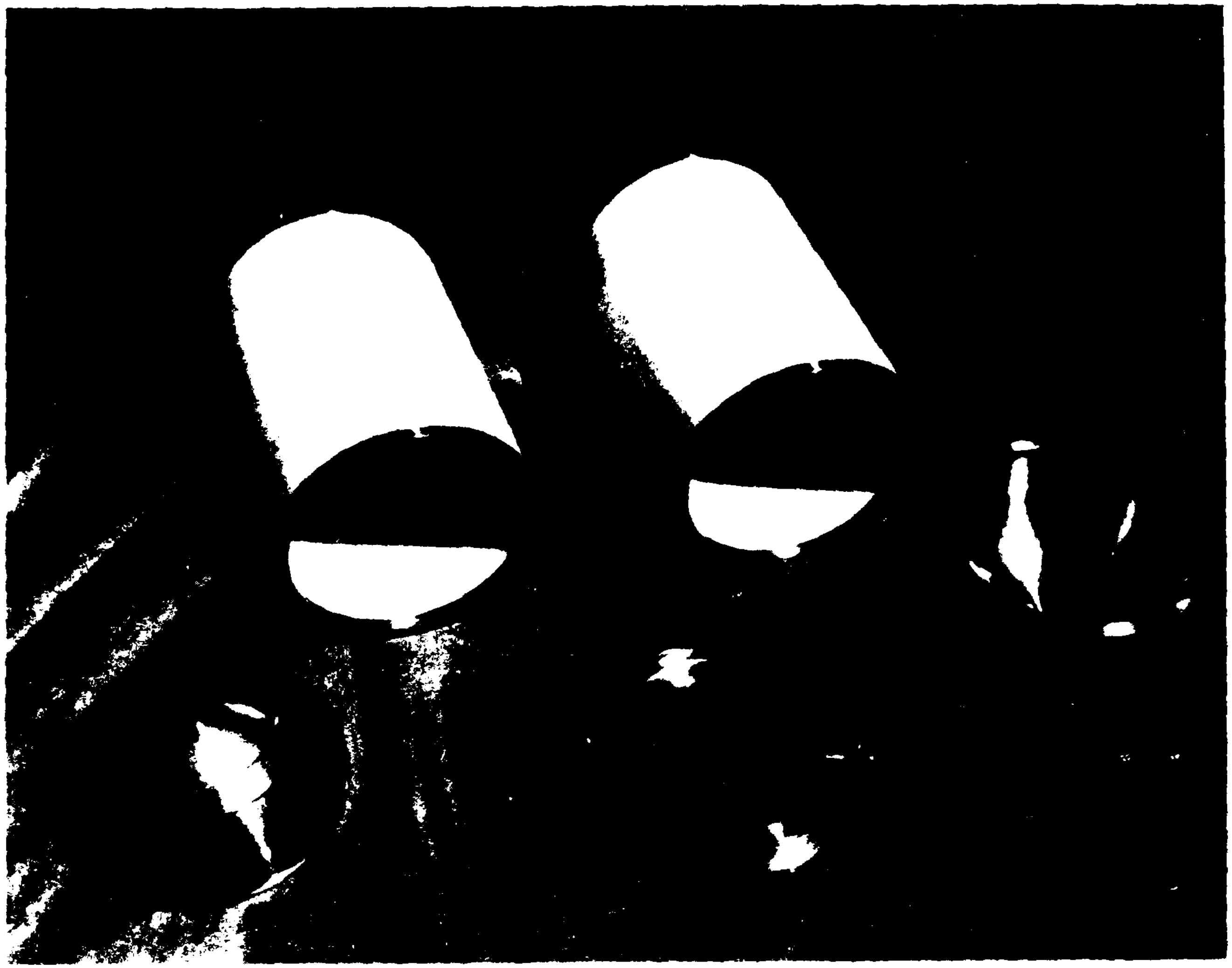

Figure 41. Components of Test Assembly IV: two *monolithic* Model I cylinders with end caps, one joint ring B, and two end closures with penetrations.

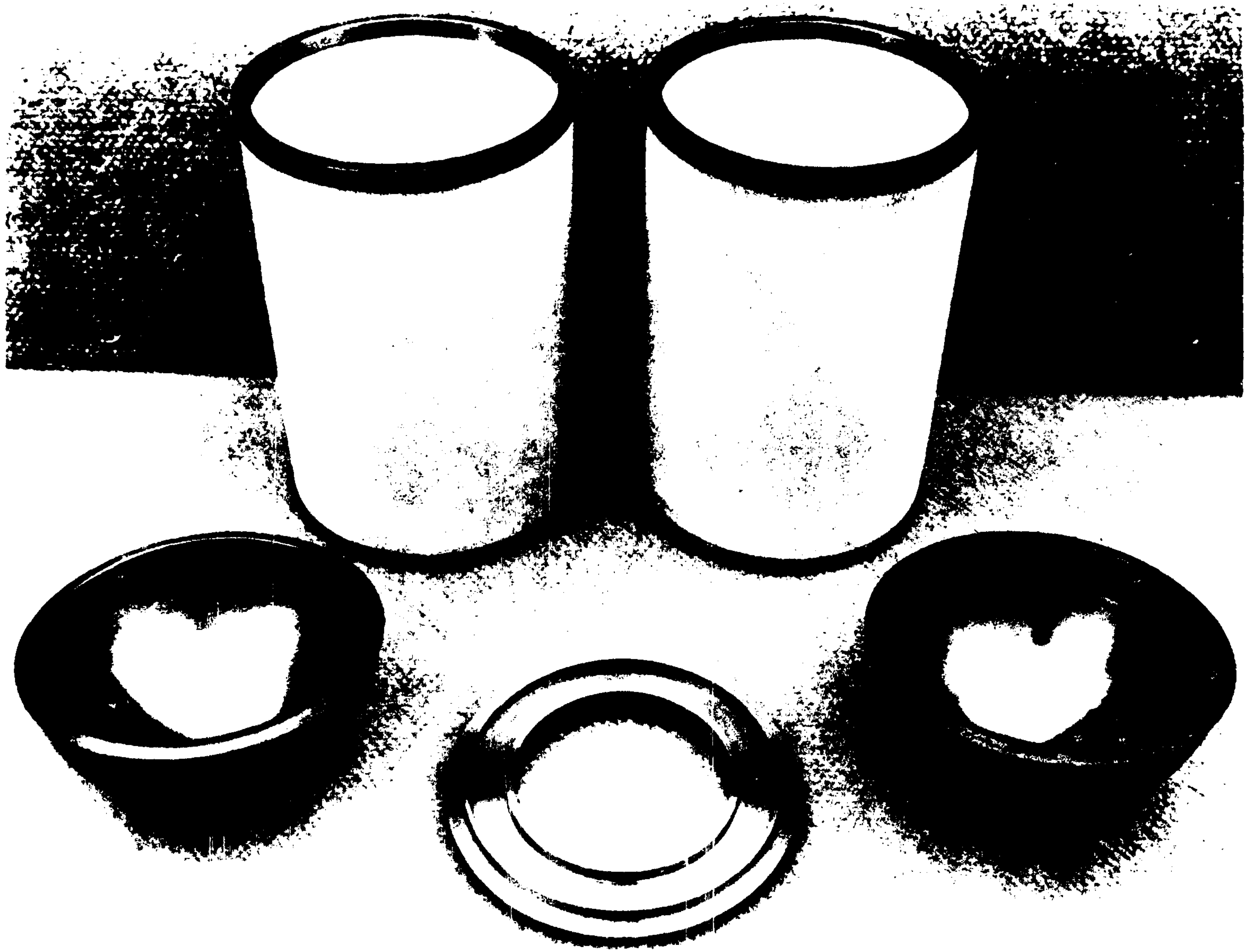

Figure 42. Components of Test Assembly V: two *monolithic* Model 1 cylinders with end caps, one joint ring C, and two end closures with penetrations.

Figure 43. Insertion of a solid plastic plug into interior of the ceramic housing for the reduction of implodable volume during hydrostatic testing. Note the large annular space between the plastic plug and the ceramic cylinder.

Figure 44. Wrapping of vinyl electrical insulation tape around the exterior of the test assemblies. The tape seals all the joints in the assembly against hydrostatic pressure.

Figure 45. Tape wrapped Test Assembly I prior to placement in the pressure vessel.

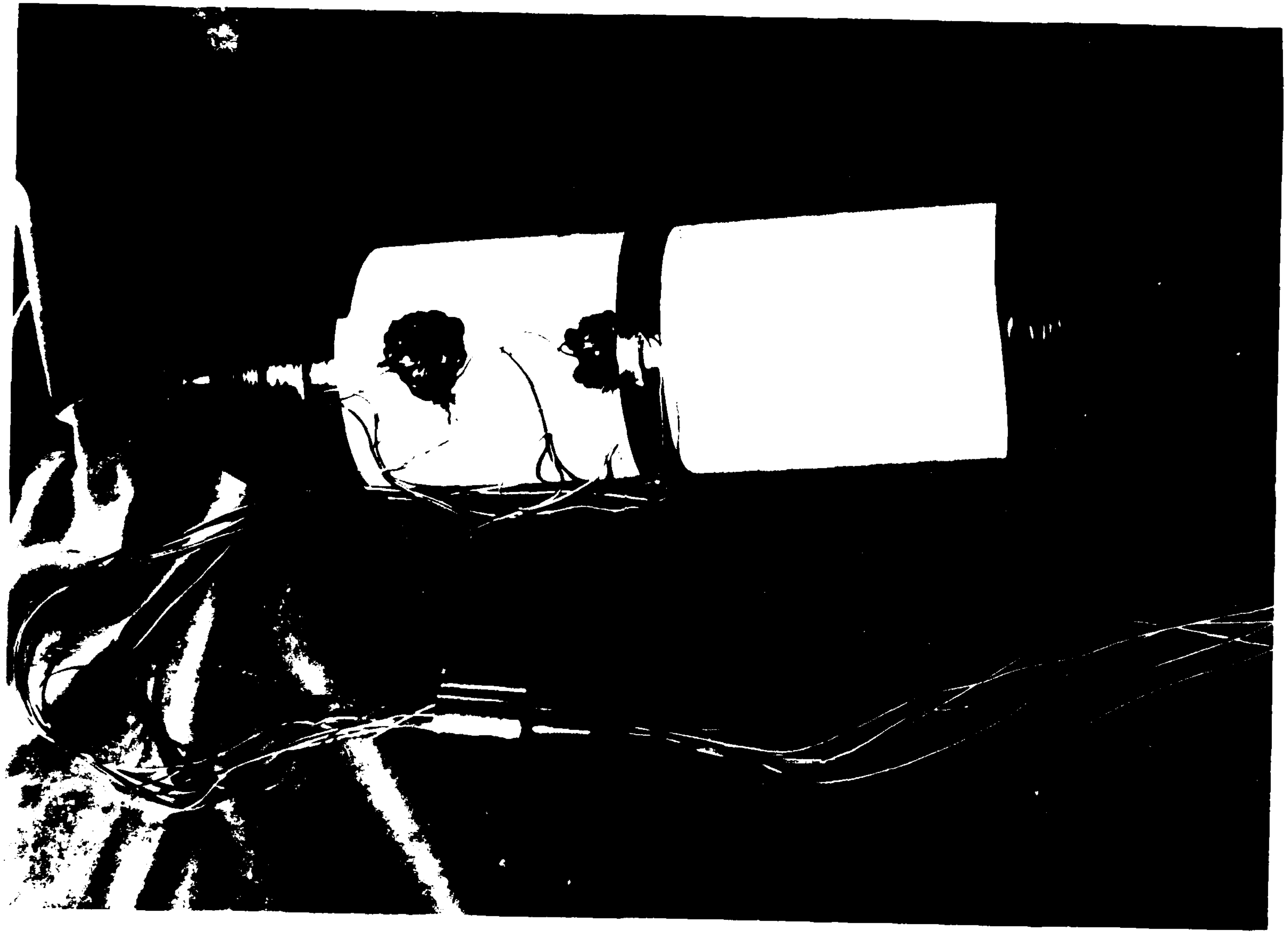

Figure 46. Instrumented Test Assembly IV prior to placement in the pressure vessel. Note the waterproofed gages on the exterior of the test assembly

Figure 47. Instrumented Test Assembly V prior to placement in the pressure vessel. Note the penetrators in the end closure for feedthrough of instrumentation leads from the interior of the housing assembly.

Figure 48. Failed Test Assembly 1. Failure was triggered by implosion of the titanium end closure. Note that the force of implosion fractured the plastic plug.

Figure 49. Closeup of the fractured plastic plug of Figure 48. Note that the impact of the central fragment from the imploded titanium end closure acted like a hammer blow on the tip of the plastic plug, causing it to spall.

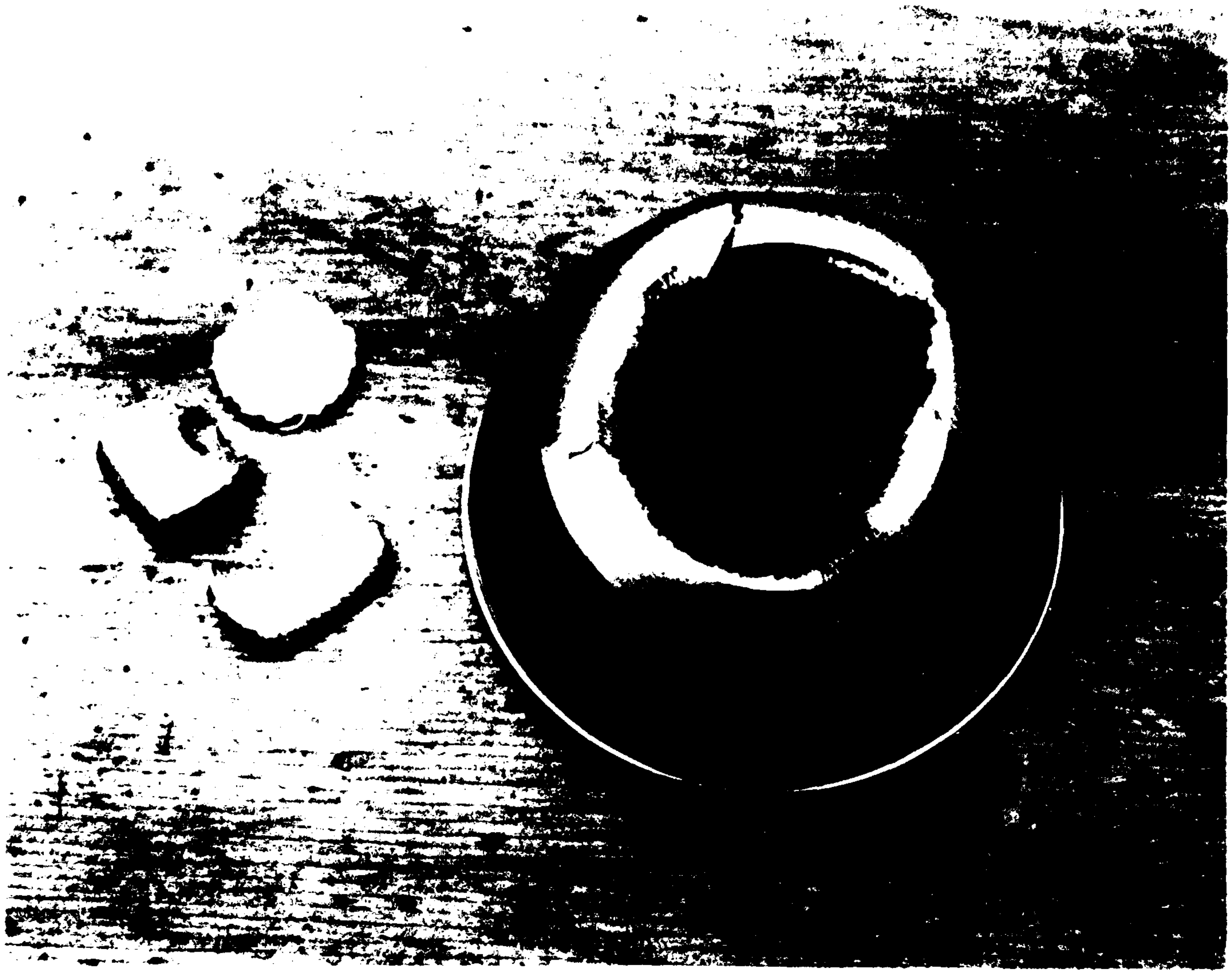

Figure 50. Closeup of the imploded end closure of Figure 48. Note that the implosion is the result of local plastic buckling at the apex of the hemisphere caused by cyclic fatigue of the titanium alloy after 1,000 pressure cycles to 9,000 psi and 150 cycles to 10,000 psi.

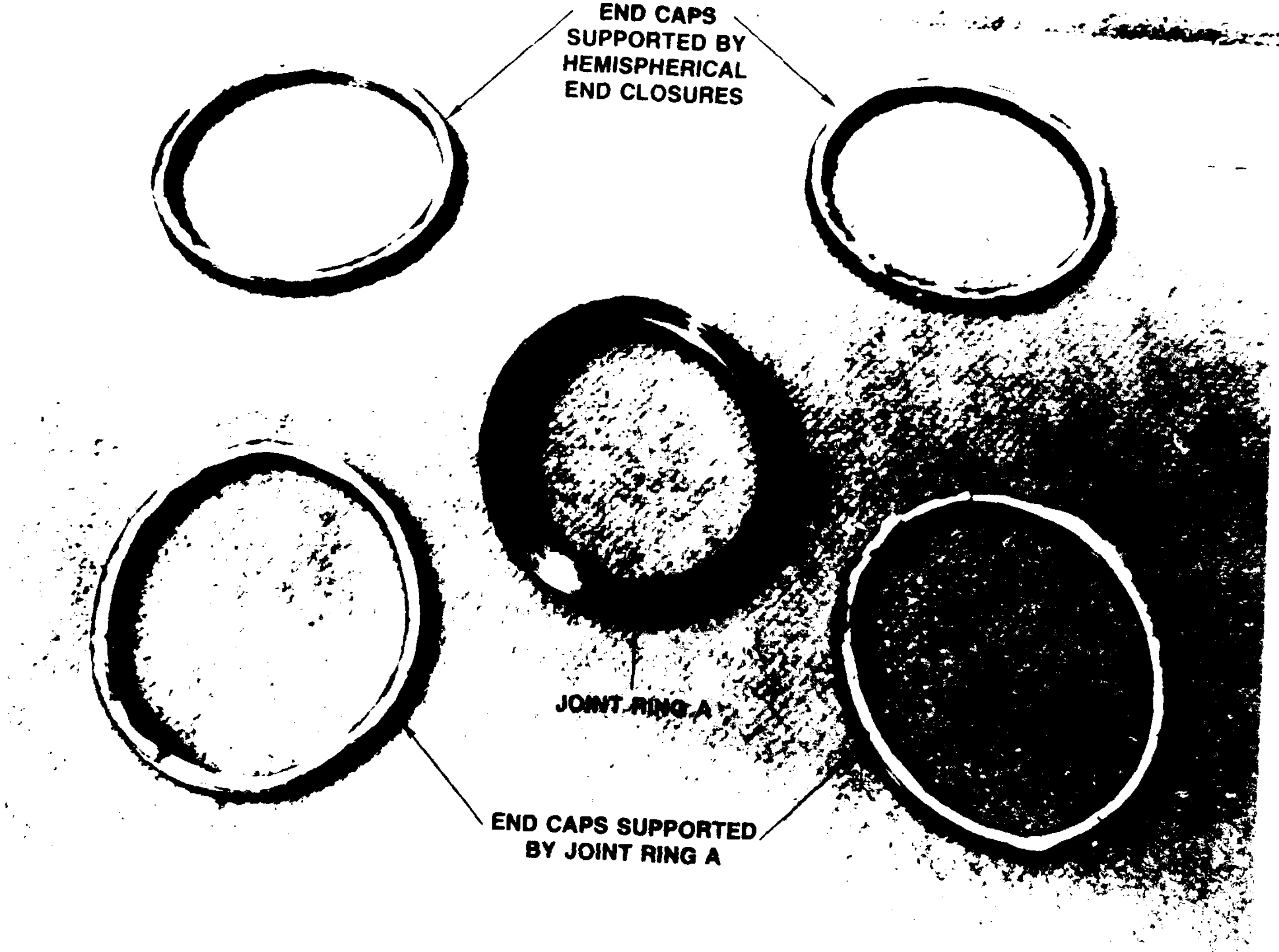

Figure 51 The buckling of joint ring A caused the Model I ceramic cylinders of Test Assembly III to fail at 7,400 psi of external pressure. This finding is based on the observation that only the end caps of the cylinder supported by the joint ring A deformed, while those supported by the end closure did not

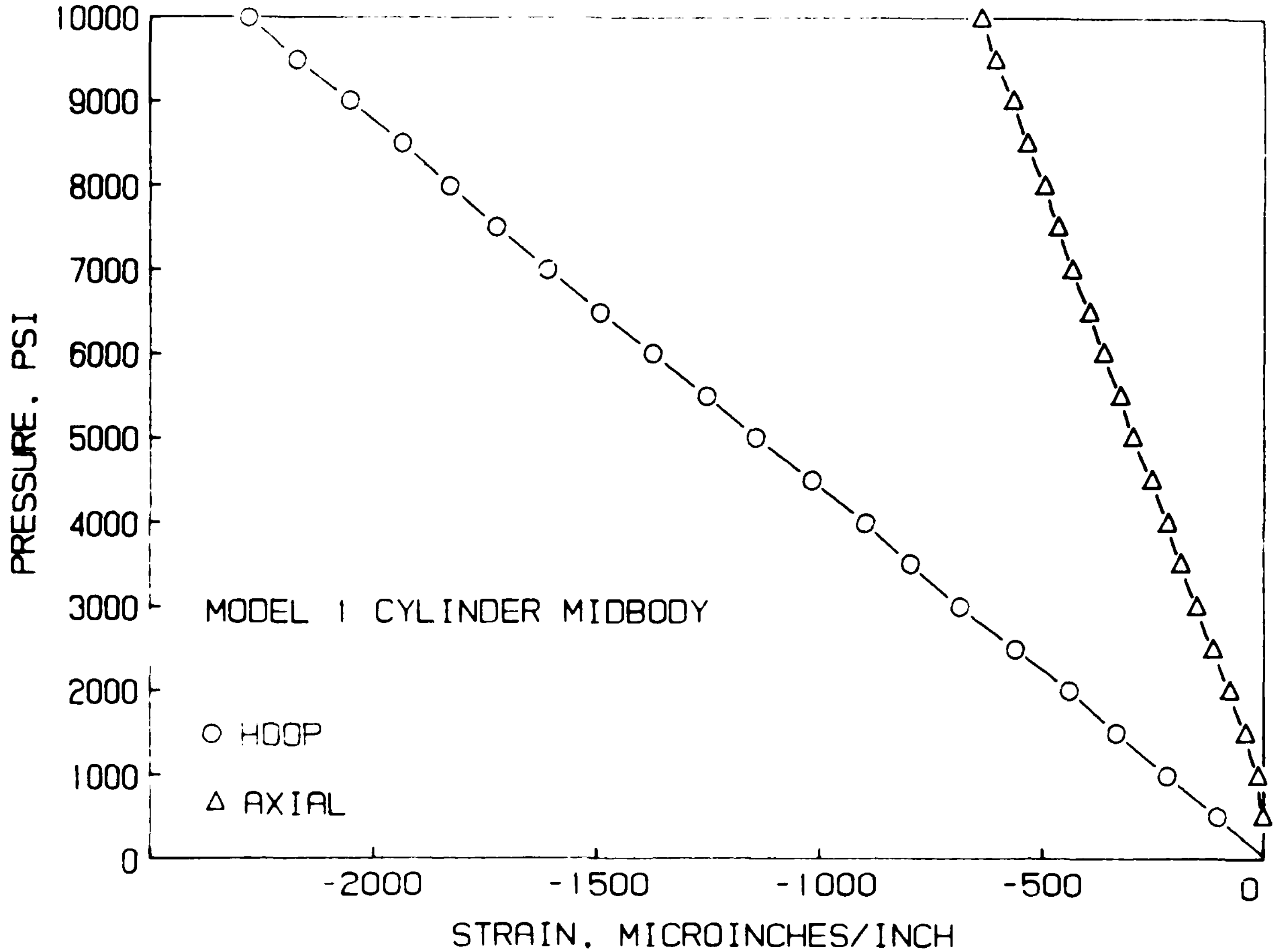

Figure 52. Strain on the *exterior surface* of the Model 1 cylinder *midbay* between an end closure and joint ring B in Test Assembly IV

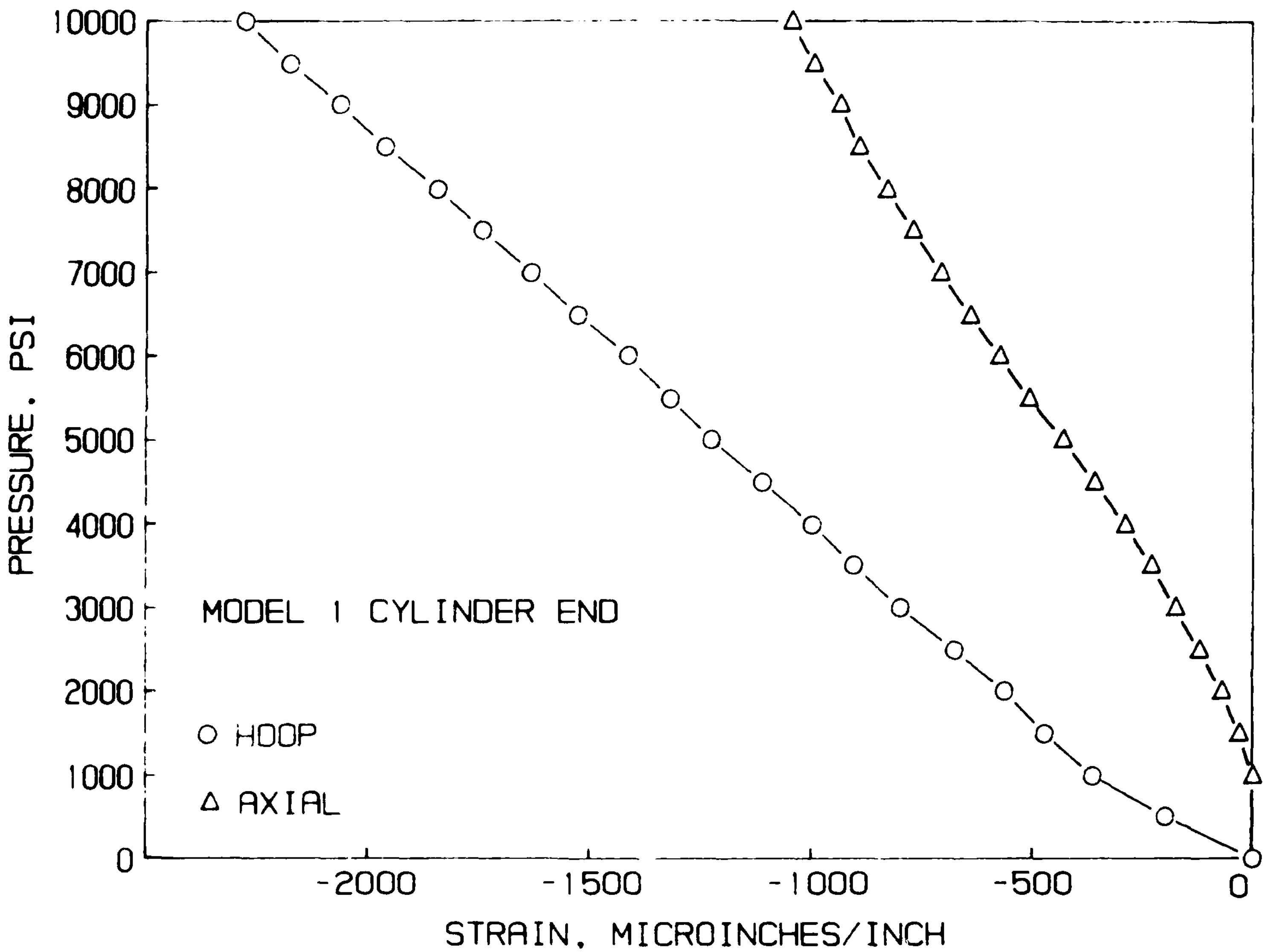

Figure 53. Strain on the *exterior surface* of the Model 1 cylinder *adjacent* to joint ring B in Test Assembly IV.

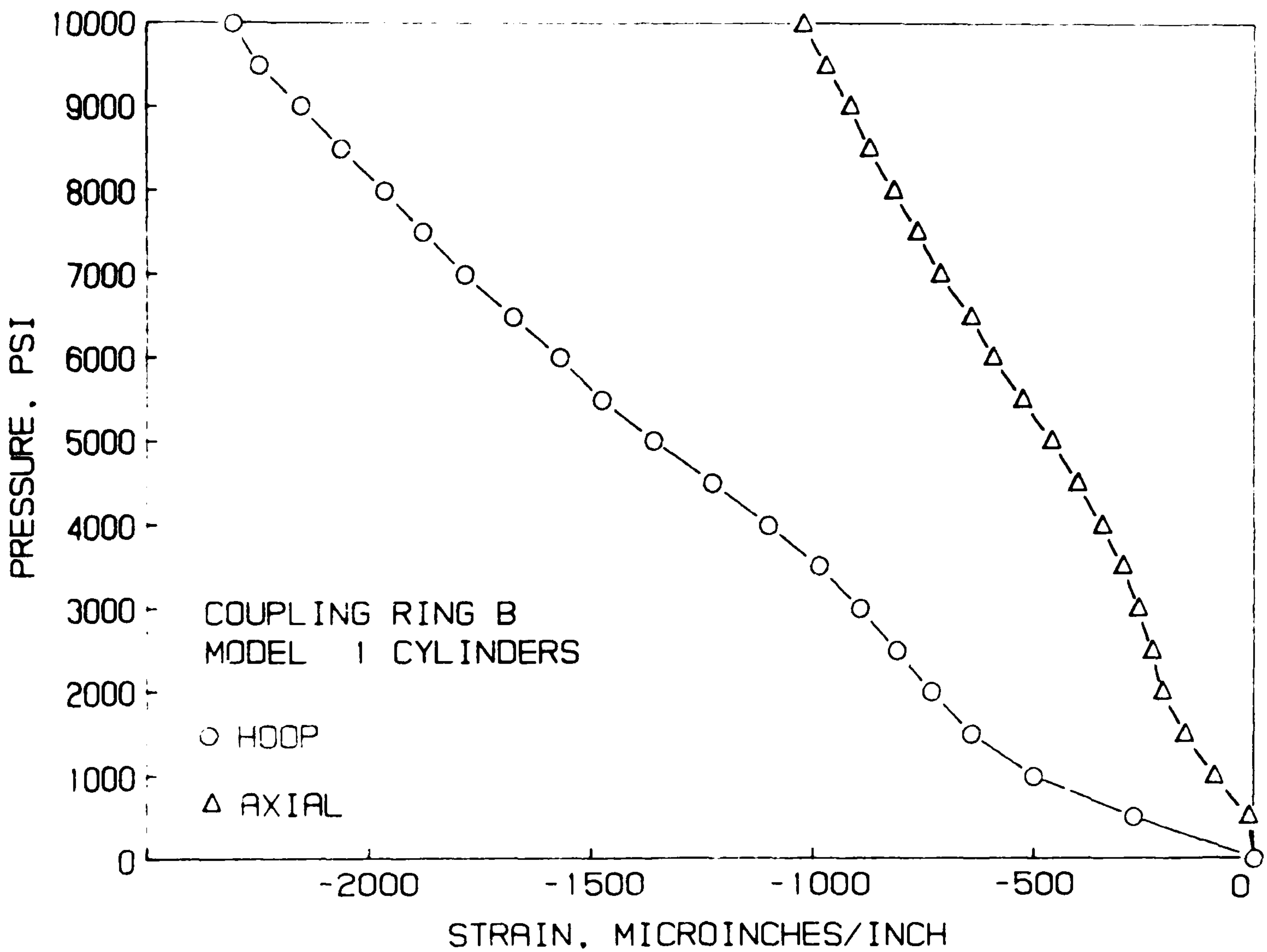

Figure 54. Strains on the *exterior surface* of joint ring B supporting two Model 1 ceramic cylinders in Test Assembly IV

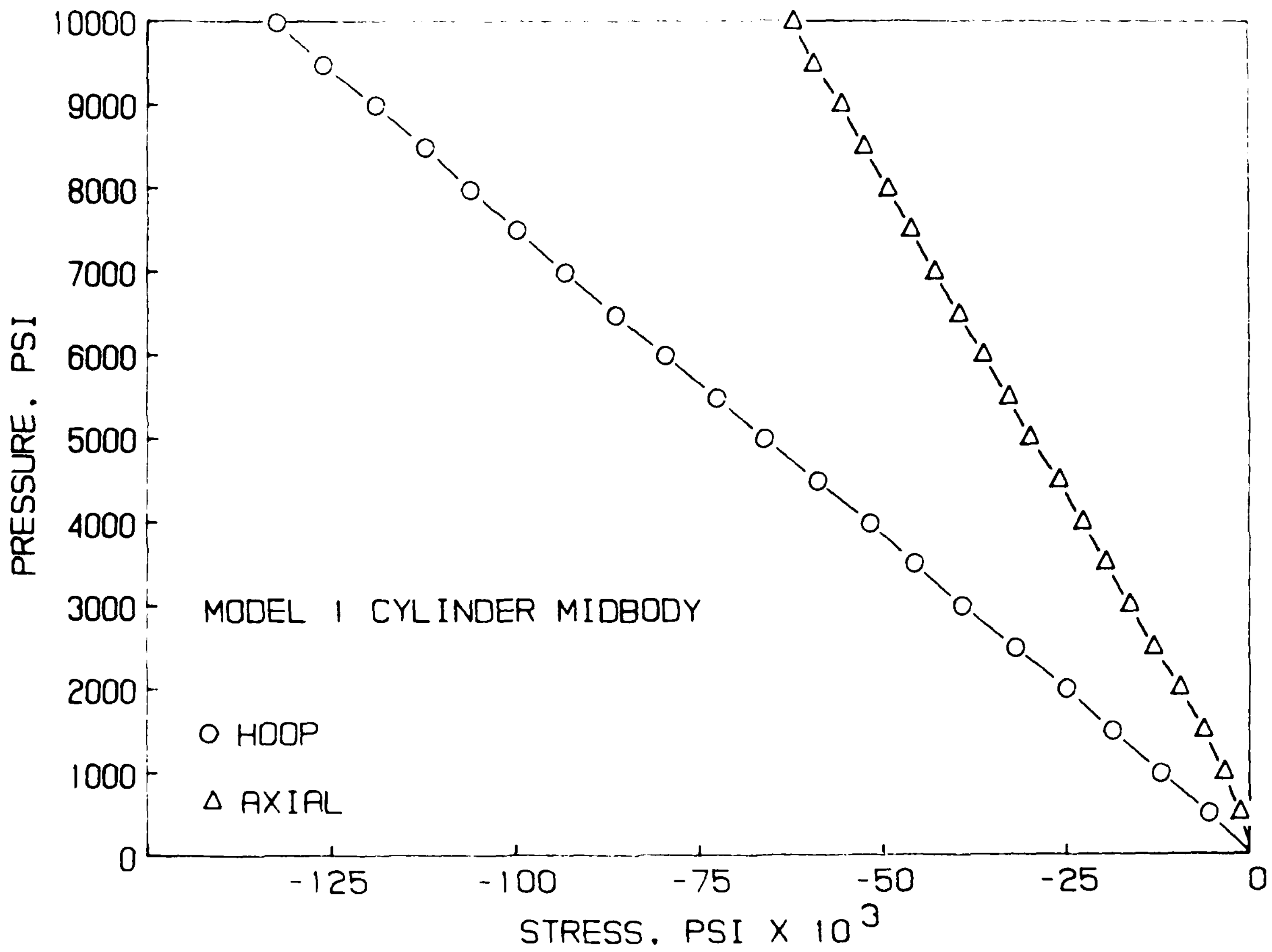

Figure 55. Stresses on the *exterior surface* of the Model I cylinder *midway* between an end closure and joint ring B in Test Assembly IV

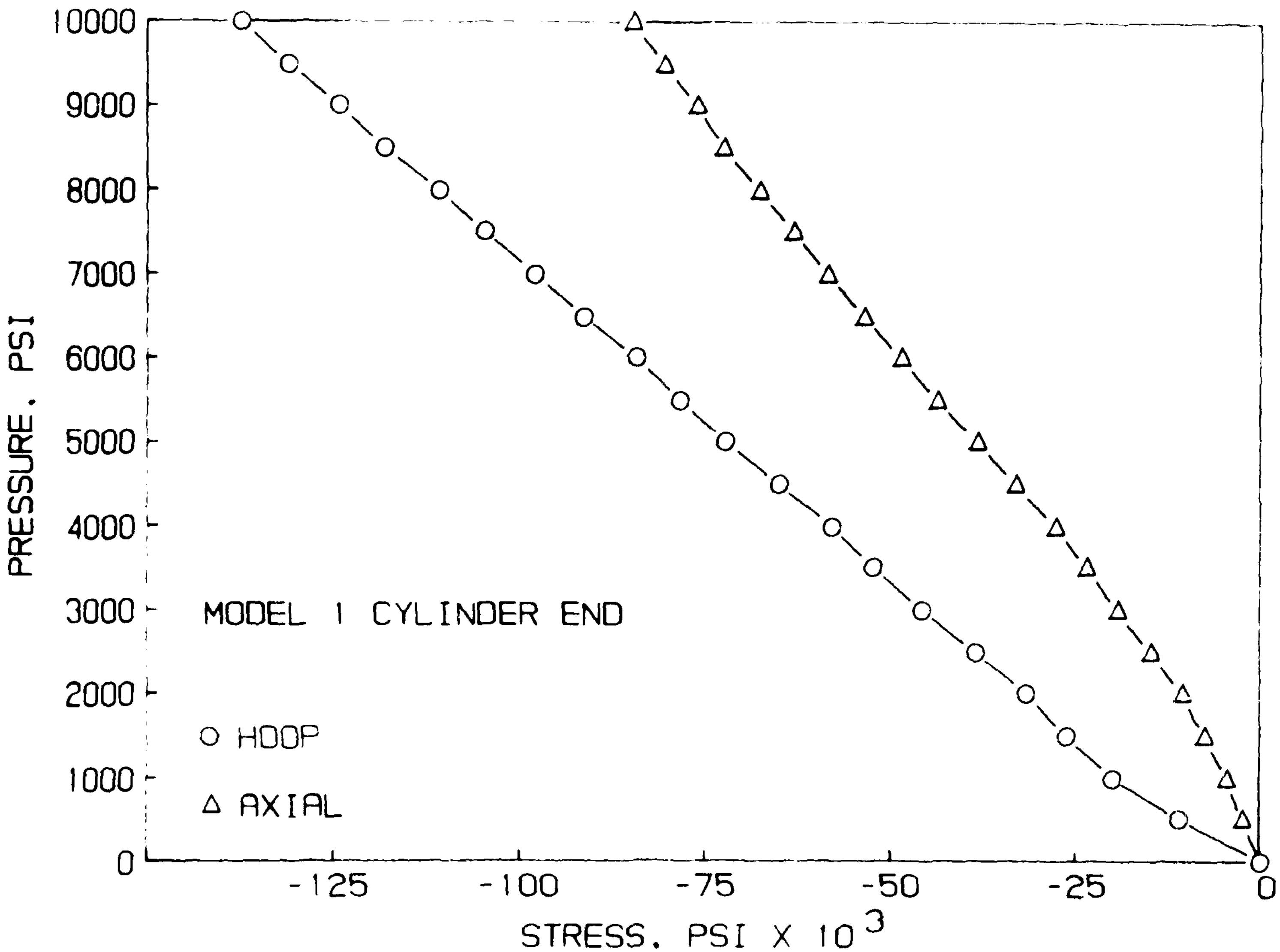

Figure 56. Stresses on the *exterior surface* of the Model 1 cylinder *adjacent* to join ring B in Test Assembly IV.

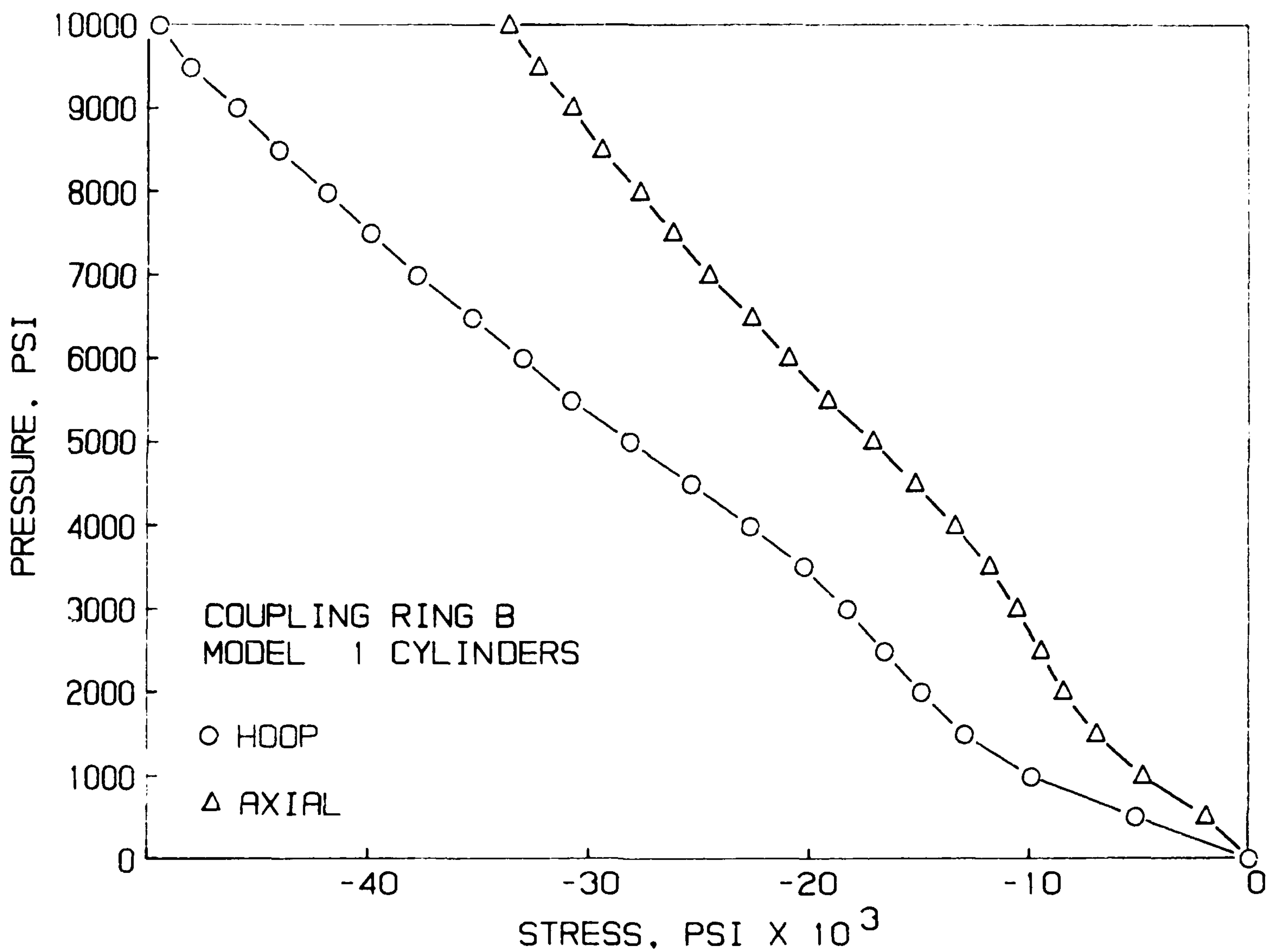

Figure 57. Stresses on the *exterior surface* of joint ring B supporting two Model 1 ceramic cylinders in Test Assembly IV.

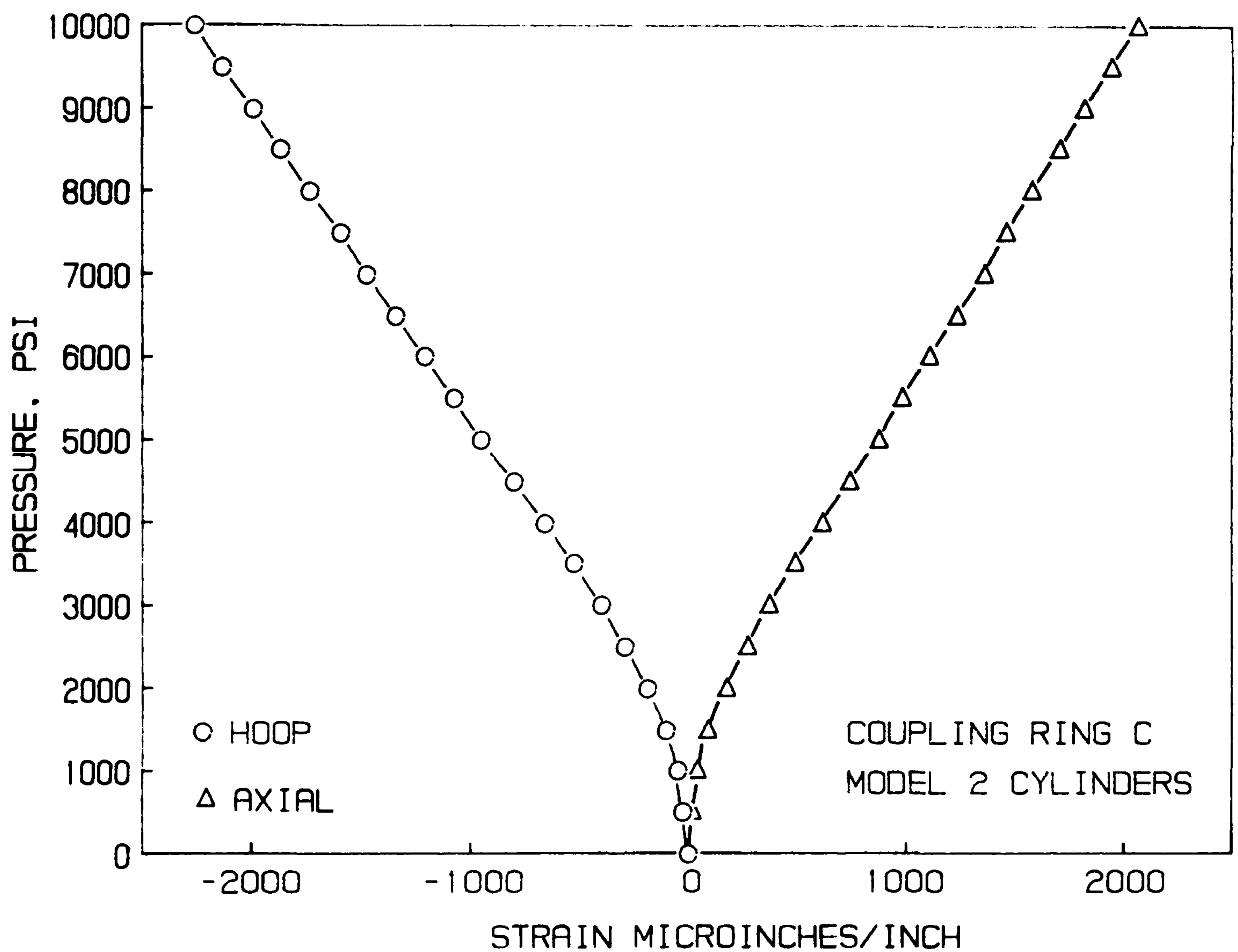

Figure 58. Strain *at the center of the lower flange* on joint ring C (ID of the joint ring) supporting two Model 2 ceramic cylinders in Test Assembly VII.

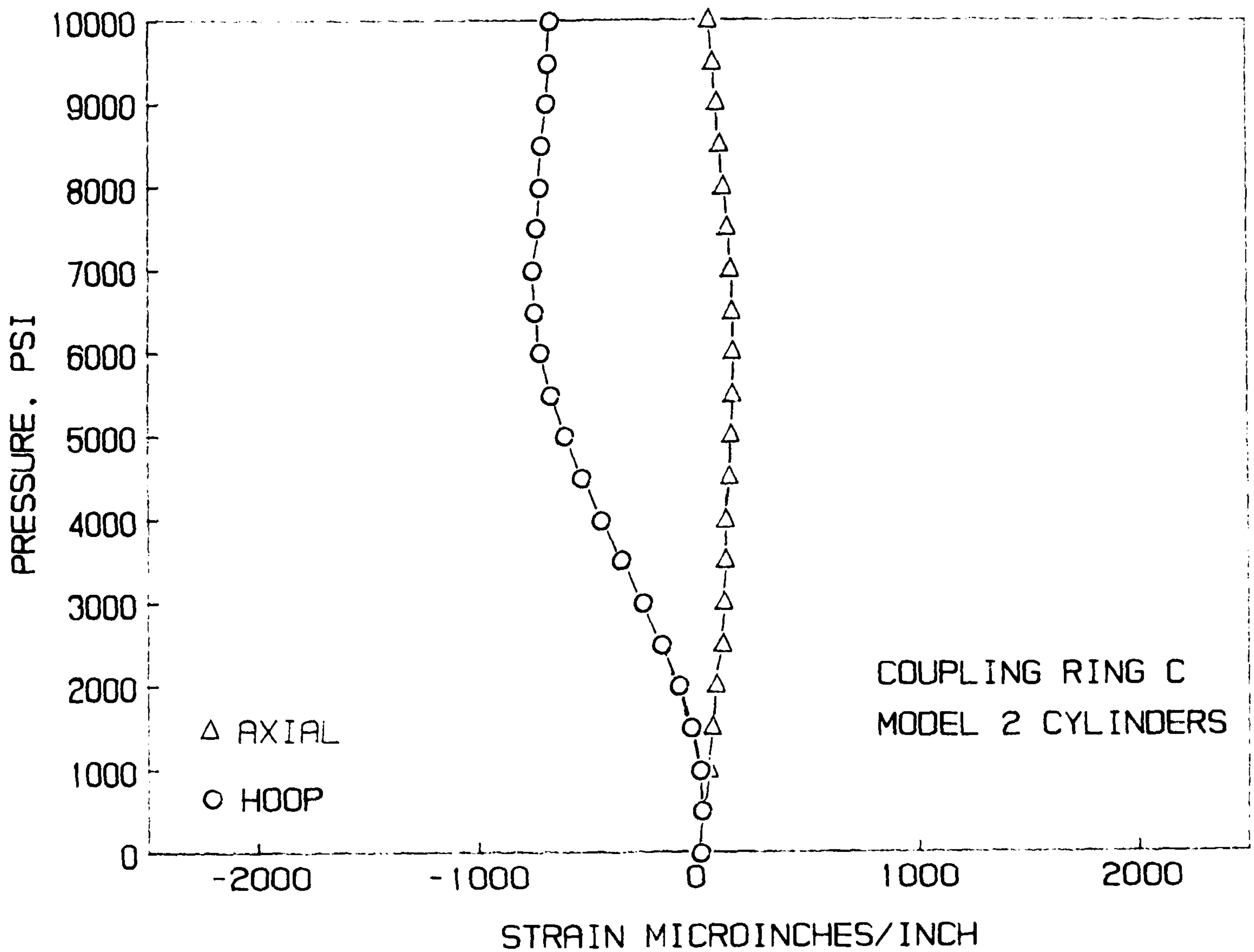

Figure 59. Strain on the *web* of joint ring C supporting two Model 2 ceramic cylinders in Test Assembly VII.

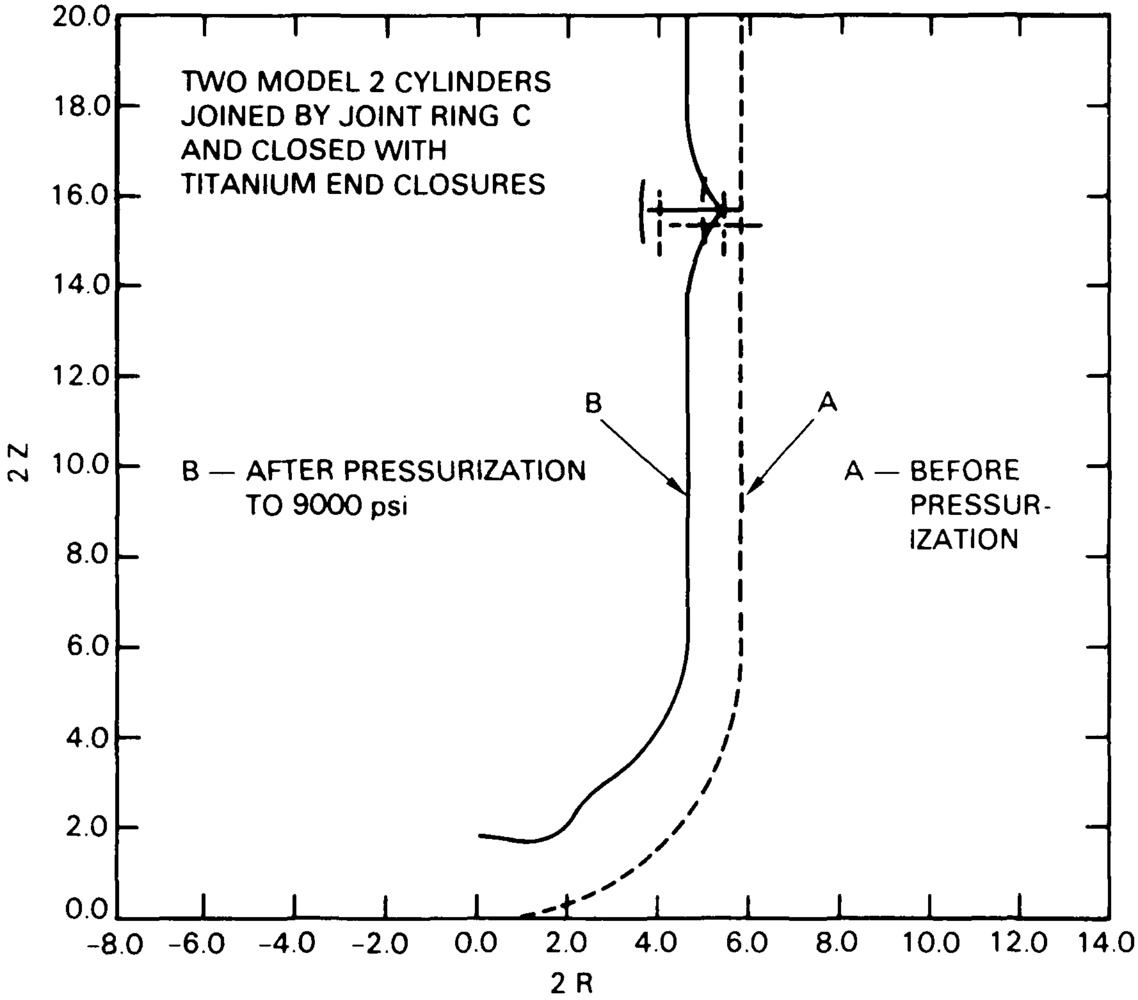

Figure 60. Computer-generated image of radial deflections in Test Assembly VII under hydrostatic loading. Note the bending of the lower flange on joint ring C predicted by BOSOR 4B computer program. The magnitude of stresses generated by bending of the lower flange is shown in Figure 61.

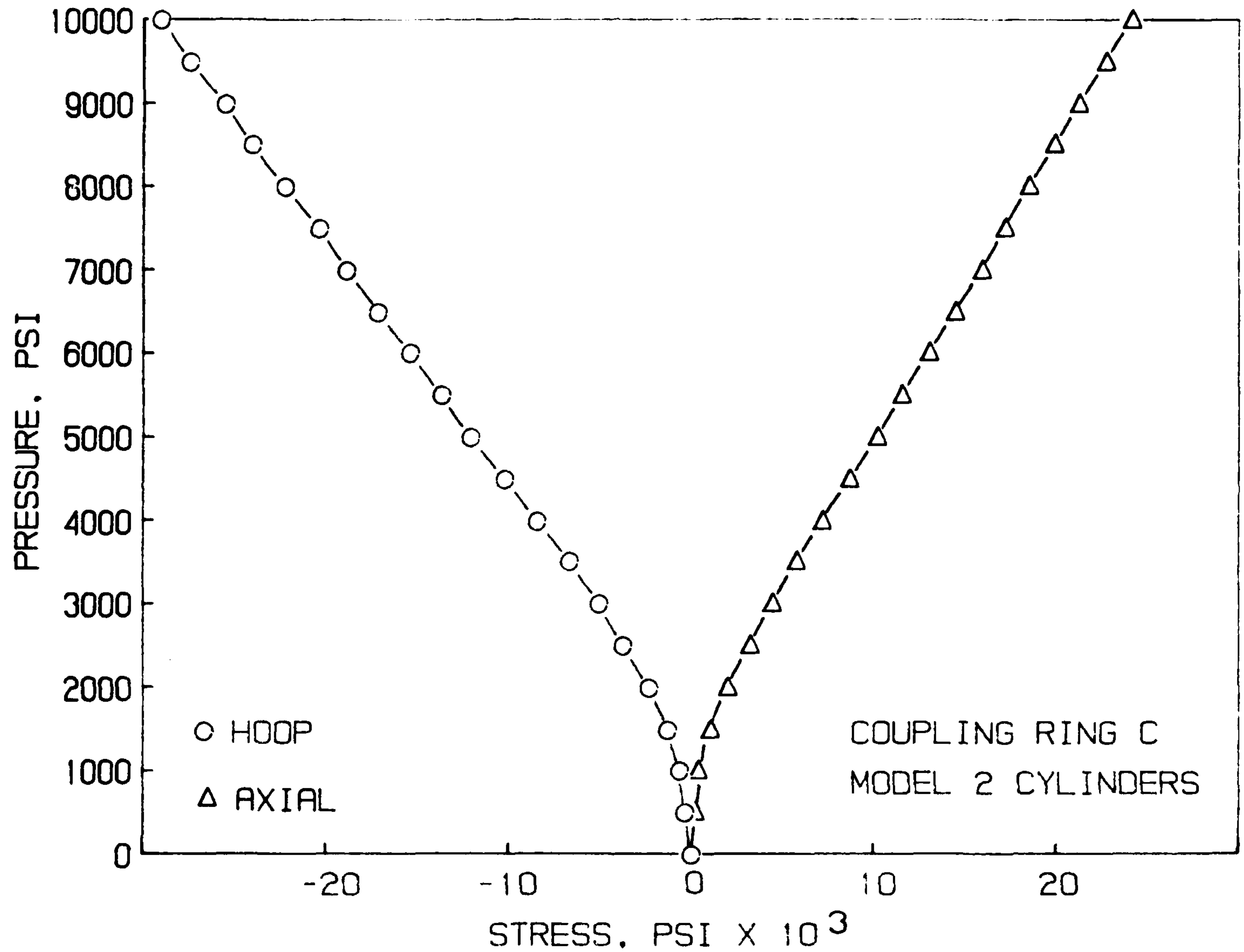

Figure 61. Stresses *at the center of the lower flange* of joint ring C (ID of the joint ring) supporting two Model 2 ceramic cylinders in Test Assembly VII. The presence of positive axial stress confirms the presence of bending on the lower flange predicted by the BOSOR 4B computer program.

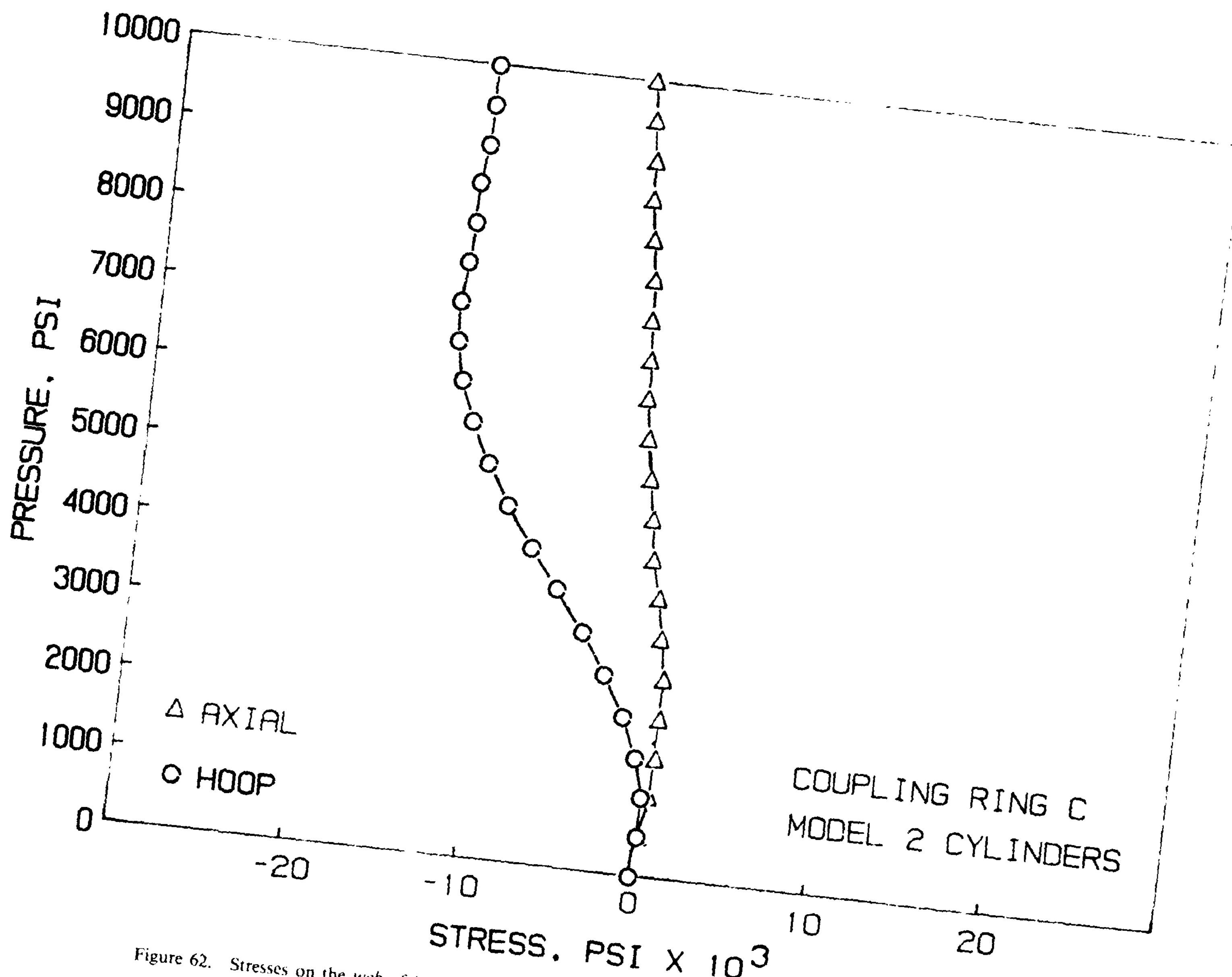

Figure 62. Stresses on the *web* of joint ring C supporting two Model 2 ceramic cylinders in Test Assembly VII.

DATE
FILMED
3 8